# *Glasnik hemičara i tehnologa Bosne i Hercegovine*
# *Bulletin of the Chemists and Technologists of Bosnia and Herzegovina*

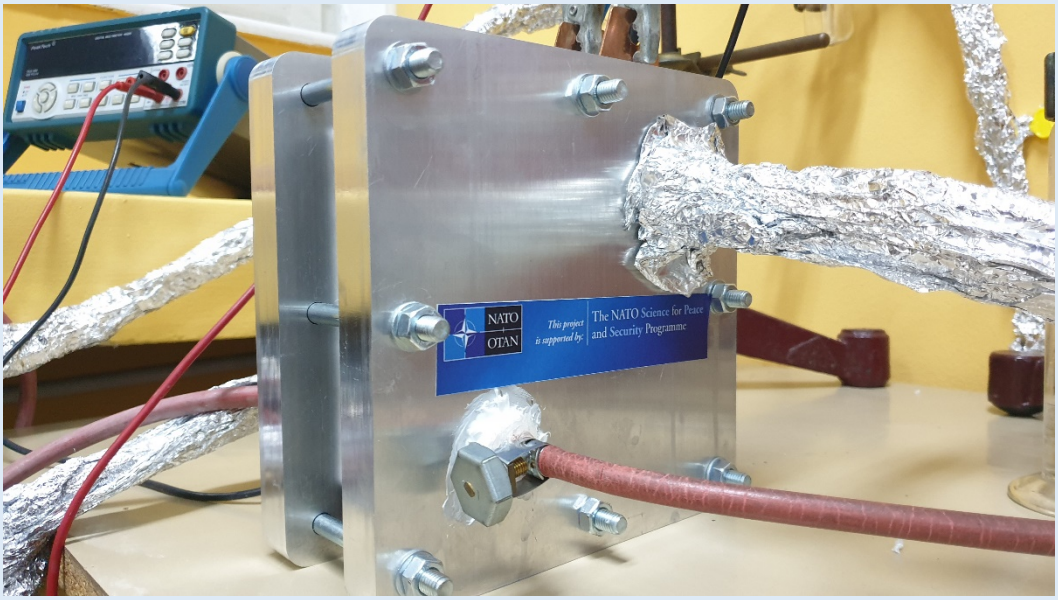


**58**

**June, 2022.**

**Univerzitet u Sarajevu - Prirodno-matematički fakultet, Sarajevo**
**University of Sarajevo - Faculty of Science, Sarajevo**

# *Glasnik hemičara i tehnologa Bosne i Hercegovine*
# *Bulletin of the Chemists and Technologists of Bosnia and Herzegovina*


**58**

**June, 2022.**

**Univerzitet u Sarajevu - Prirodno-matematički fakultet, Sarajevo**
**University of Sarajevo - Faculty of Science, Sarajevo**

Glasnik hemičara i tehnologa Bosne i Hercegovine

*Bulletin of the Chemists and Technologists of Bosnia and Herzegovina*

Print ISSN: 0367-4444
Online ISSN: 2232-7266

Zmaja od Bosne 33-35, BA-Sarajevo
Bosnia and Herzegovina
Phone: +387-33-279-918
Fax: +387-33-649-359
E-mail: glasnik@pmf.unsa.ba
glasnikhtbh@gmail.com

# EDITORIAL BOARD

Faculty of Science Sarajevo
Zmaja od Bosne 33-35, BA-Sarajevo
Bosnia and Herzegovina
Phone: +387-33-279-904 (Administration)
+387-33-279-911 (Executive Editors)
Fax: +387-33-649-359

E-mail: glasnik@pmf.unsa.ba
glasnikhtbh@gmail.com

**Dejan Milošević**
Department of Physics, Faculty of Science, University of Sarajevo, Sarajevo, Bosnia and Herzegovina
**Željko Jaćimović**
Department of Chemical Technology, Faculty of Meallurgy and Technology, University of Montenegro, Podgorica, Montenegro
**Ljudmila Benedik**
Department of Environmental Sciences, "Jožef Stefan" Institute, Ljubljana, Slovenia
**Meliha Zejnilagić-Hajrić**
Department of Chemistry, Faculty of Science, University of Sarajevo, Sarajevo, Bosnia and Herzegovina
**Tidža Muhić-Šarac**
Department of Chemistry, Faculty of Science, University of Sarajevo, Sarajevo, Bosnia and Herzegovina
**Sabina Gojak-Salimović**
Department of Chemistry, Faculty of Science, University of Sarajevo, Sarajevo, Bosnia and Herzegovina
**Ismet Tahirović**
Department of Chemistry, Faculty of Science, University of Sarajevo, Sarajevo, Bosnia and Herzegovina
**Danijela Vidic**
Department of Chemistry, Faculty of Science, University of Sarajevo, Sarajevo, Bosnia and Herzegovina
**Mustafa Memić**
Department of Chemistry, Faculty of Science, University of Sarajevo, Sarajevo, Bosnia and Herzegovina
**Andrea Gambaro**
Department of Environmental Sciences, Informatics and Statistics, University Ca' Foscari of Venice, Venice, Italy
Institute for the Dynamics of Environmental Processes - National Research Council (CNR-IDPA), Venice, Italy
**Dragana Đorđević**
Centre of Chemistry - IChTM, University of Belgrade, Belgrade, Serbia
**Aida Šapčanin**
Department of Natural Sciences in Pharmacy, Faculty of Pharmacy, University of Sarajevo, Sarajevo, Bosnia and Herzegovina
**Jože Kotnik**
Department of Environmental Sciences, "Jožef Stefan" Institute, Ljubljana, Slovenia
**Lucyna Samek**
AGH University of Science and Technology, Faculty of Physics and Applied Computer Science, Krakow, Poland
**Angela Maria Stortini**
Department of Molecular Sciences and Nanosystems, University Ca' Foscari of Venice, Venice, Italy
**Ivan Spanik**
Institute of Analytical Chemistry, Slovak University of Technology, Bratislava, Slovakia
**Mirjana Vojinović Miloradov**
Department of Environmental Engineering, Faculty of Technical Sciences, University of Novi Sad, Novi Sad, Serbia
**Heike Bradl**
Department of Environmental Engineering, University of Applied Sciences Trier, Birkenfeld, Germany
**Lea Kukoč-Modun**
Department of Analytical Chemistry, Faculty of Chemistry and Technology, University of Split, Split, Croatia
**Sanja Ćavar Zeljković**
Centre of the Region Haná for Biotechnological and Agricultural Research, Department of Genetic Resources for Vegetables, Medicinal and Special Plants, Crop Research Institute, Šlechtitelů 29, Olomouc, Czech Republic
Centre of Region Haná for Biotechnological and Agricultural Research, Czech Advanced Technology and Research Institute, Palacky University, Šlechtitelů 27, Olomouc, Czech Republic
**Igor Jerković**
Department of Organic Chemisty, Faculty of Chemistry and Technology, University of Split, Split,Croatia
**Roderick W. Bates**
Division of Chemistry and Biological Chemistry, School of Physical and Mathematical Sciences, Nanyang Technlogical University, Singapore, Singapore
**Safija Herenda**
Department of Chemistry, Faculty of Science, University of Sarajevo, Sarajevo, Bosnia and Herzegovina
**Muna Abu-Dalo**
Department of Chemistry, Jordan University of Science and Technology, Irbid, Jordan

The journal is published semiannual, and full text version of the papers published are available free of cost at http://www.pmf.unsa.ba/hemija/glasnik.

Bulletin of the Chemists and Technologists has been licensed for indexing in:

*Emerging Sources Citation Index* (Web of Science, Clarivate Analytics)

*CAPlus* (Chemical Abstracts Plus):

*Academic Search Complete* (EBSCO)

Glasnik hemičara i tehnologa Bosne i Hercegovine

*Bulletin of the Chemists and Technologists of Bosnia and Herzegovina*

**2022**
Issue 58

Print ISSN: 0367-4444
Online ISSN: 2232-7266

# CONTENT



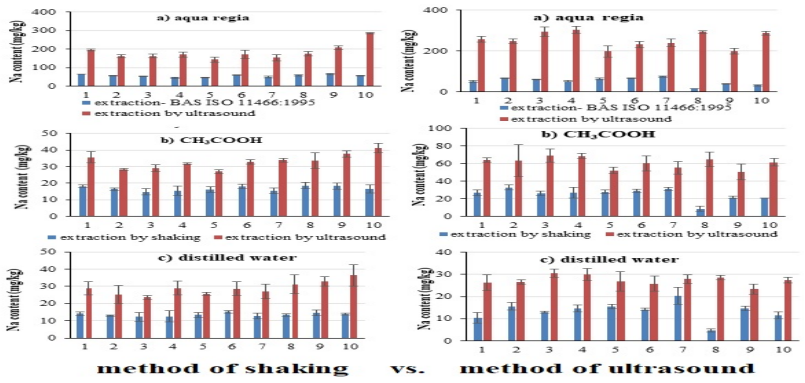

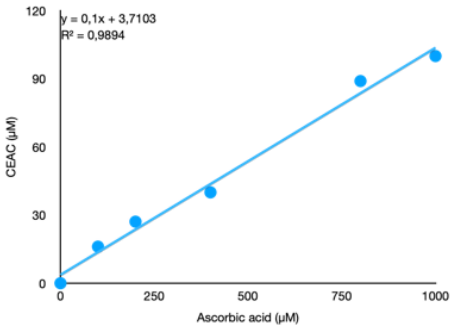




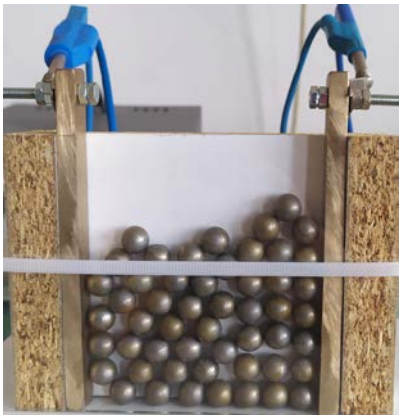



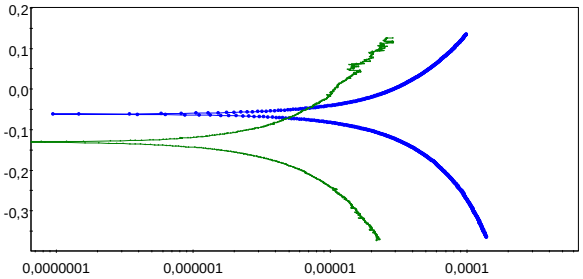

## Editorial

Achieving the objective of climate neutrality in EU by 2050. will not be possible without deep decarbonization of industry, transport and energy sectors. Decarbonization of hydrogen production holds the central place in these efforts as it can be used as high energy value fuel (in combustion engines or fuel cells) for transport and domestic use, but also for electrical grid stabilization and full utilization of solar and wind power. Furthermore, production of hydrogen solely for Haber-Bosch process uses 1 % of the world's energy production, with the 1.4 % share of total CO2 emissions.

Hydrogen produced by electrochemical water splitting using solar, wind or nuclear energy has zero carbon footprint. However, efficiency of this process, as well as the overall efficiency of electrochemical hydrogen cycle (electrochemical production, electrochemical compression, electrochemical utilization) significantly depends on the thermodynamics and kinetics of fundamental electrochemical processes at the electrode/electrolyte interface. Consequently, rational design of affordable and scalable materials with excellent electrocatalytic performance (activity, stability and selectivity) towards the hydrogen evolution, hydrogen oxidation, oxygen evolution and oxygen reduction reactions has never been more important and appreciated. Current research approaches absoultely rely on the knowledge of fundamental catalytic and electrochemical processes combined with quantum mechanics and computational methods, which enables rational planing of experimental work.

Although Bosnia and Herzegovina is not yet part of the European Union, its geographic position and existing industry dictates the need for prompt investments in research and development for transition to hydrogen-based green technologies. University of Sarajevo – Faculty of Science is currently the only academic/research institution in Bosnia and Herzegovina with active research projects dealing with (electro)catalysts for hydrogen economy.
Project Optimizing Fuel Cell Catalyst Stability upon Integration with Reforming, funded by NATO Science for Peace programme and realized in colaboration with National Institute of Chemistry from Ljubljana and University of Belgrade – Faculty of Physical Chemistry, addresses stability of new Pt/modified graphene and nonPt/modified graphene composites for PEM-FC. Beside scientific outputs of the project, development of the real system (PEM fuel cell) has been done in colaboration with the project end user Center for Advanced Technologies Sarajevo.

Also, first investments in green hydrogen production are starting to formalize, as private company HEET d.o.o. from Rama-Prozor is setting up the first green hydrogen production plant in Bosnia and Herzegovina, based on PEM electrolyzer supplied by solar energy.

These first steps are important because Bosnia and Herzegovina will soon be at the decarbonization or isolation crossroad, as there is still no strategy necessary for smooth connection to already well established European activities.

**Editors**

Glasnik hemičara i tehnologa Bosne i Hercegovine

Bulletin of the Chemists and Technologists of Bosnia and Herzegovina

2022

58

Original Scientific Article

Print ISSN: 0367-4444
Online ISSN: 2232-7266

DOI: https://doi.org/10.35666/2232-7266.2021.58.01

UDC: 547.56:634.233.002.2

1-6

# Phenolic content and bioactivity of two sour cherry cultivars and their products

**Kazazic, M., Mehic, E., Djapo-Lavic, M.**

*Dzemal Bijedic University of Mostar, Faculty of Education, Department of Chemistry, Univerzitetski kampus bb, Mostar, Bosnia and Herzegovina*

**Article info**
Received: 16/06/2021
Accepted: 12/04/2022

**Keywords:**
Sour Cherry
Polyphenols
Anthocyanins
Antioxidant Activity
Bioactive Compounds

***Corresponding author:**
**Maja Kazazić**
E-mail: maja.kazazic@unmo.ba
Phone: 00-387-36-514-207

**Abstract:** Bioactive compounds are produced as secondary metabolites in plants. Positive correlation between presence of bioactive compounds and health benefits of plants have been reported in many studies. Sour cherry contains high content of bioactive compounds, mostly polyphenols and anthocyanins. They are mostly consumed in fresh state, but are also used to produce jam, jelly, marmalade, juice, and syrup. Aim of this study was to evaluate total phenolic content, anthocyanins, as well as the antioxidant activity in two sour cherry cultivars and their products, jams and juice, prepared using traditional recipes. Total phenolic content was determined using Folin-Ciocalteu method and antioxidant activity was assessed using ABTS radical cation decolorization assay. pH-Differential method was used to determine anthocyanin content. Marasca cultivar had higher content of phenols, anthocyanins and antioxidant activity than Oblačinska cultivar. Processing of sour cherries had a greater impact on the reduction of anthocyanin content but did not have significant effect on antioxidant activity.

## INTRODUCTION

Fruits are natural sources of bioactive phytochemicals that are produced in plants as secondary metabolites. Numerous studies have shown the protective effect and positive influence of fruit consumption on human health (Jakobek Šeruga, Medvidović-Kosanović, et al., 2007; Shashirekha, Mallikarjuna, and Rajarathnam 2015). Beneficial effects of fruit have been attributed to the presence of the bioactive compounds. Sour cherries (Prunus cerasus L.) are rich in bioactive compounds, and they contain high levels of phenolic compounds and anthocyanins (Khoo, Clausen, Pedersen et al., 2011; Serradilla, Fotirić Akšić, Manganaris et al., 2017). Several studies have demonstrated that sour cherries contain significant levels of anthocyanins that have strong antioxidant and anti-inflammatory activity with a real impact on human health (Khoo et al., 2011; Blando, Gerardi and Nicoletti 2004; He and Giusti 2009; Levaj, Dragović-Uzelac, Delonga et al., 2010). It has been shown that consumption of sweet or sour cherries may reduce the risk of cancer, inflammatory diseases including arthritis, and muscle soreness, (Prvulović, Popović, Malenčić et al., 2012) cardiovascular diseases, osteoporosis as well neurodegenerative diseases and diabetes mellitus (Kim and Padilla-Zakour, 2004; Viljevac Vuletić, Dugalić, Mihaljević et al., 2017).

Sour cherry is mostly used to produce jam, jelly, stewed fruit, marmalade, and syrup in the food industry (Corts, Rodrigues, Ortiz Marcide et al., 2008). The production of cherries in the continental part of Bosnia and Herzegovina is mainly related to the cultivation of the Oblačinska cultivar, which is the most demanded variety because of its high quality (Mitić, Obradović, Kostić et al., 2012) and high anthocyanin content. In Herzegovina, due to different climates, Maraska is the most grown sour cherry cultivar. The sour cherry Marasca is a rich source of organic and inorganic bioactive compounds (Pedisić, Levaj, Dragović-Uzelac et al., 2007). Marasca had higher polyphenolic content and higher antioxidant activity compared to other sour cherry cultivars. Both cultivars showed industrial potential for processing that can be used in the production of various functional beverages (Repajić, Bursać Kovačević, Putnik. et al., 2015).

The aim of this study was to evaluate fresh samples, jams and juices of two different sour cherry cultivars, Oblačinska and Marasca regarding the amount of total phenolic content, anthocyanins and antioxidant activity.

## MATERIALS AND METHODS

*Chemicals*

Compound 2,2´ - azino-bis (3-ethylbenzthiazoline-6-sulfonic acid) (ABTS) was purchased from Sigma-Aldrich (Germany) and 6-hydroxy-2,5,7,8-tetramethylchroman-2-carboxylic acid (Trolox) from Across organics (USA). Potassium chloride was purchased from Lach:ner (Czech Republic). All other chemicals were purchased from Semikem (BiH).

*Cherry samples*

Fruits of two sour cherry (Prunus cerasus L.) cultivars Oblačinska and Marasca were collected in May 2019, in the area of Mostar, Bosnia and Herzegovina. Immediately after harvesting, samples were frozen at -20oC until analysis. All fruits were harvested at the optimum maturity stage for the technology of jam and juice production.

*Jam preparation*

To prepare jams 350 g of fruits and 120 g of sugar were mixed and stirred until boiling. Fruits were cooked under atmospheric pressure for 20 minutes. Jams were prepared in three series and filled into hot glass jars. They were allowed to cool at room temperature and stored in dark until analysis. Jams were analyzed within one week.

*Juice preparation*

Juices were prepared in three series by mixing 300 g of fruits, 100 g of sugar and 200 mL of water and cooked for 15 minutes. Juices were filtrated after they were cooked and filled into hot glass bottles. Samples were stored in dark at room temperature and analyzed within one week.

*Extraction procedure*

The amount of 200 g of frozen sour cherries from each cultivar was homogenized using a food blender. 1 g of homogenized sample was extracted with 10 mL of acidified methanol (1% HCl) for 60 min at 200 rpm at room temperature using an orbital shaker (Agitador orbital, Optic Ivymen System). All samples were analyzed the same day when they were prepared. Jams were extracted using the same procedure.

*Determination of total phenolic (TF) content*

Total phenolic content was determined with the Folin-Ciocalteu colorimetric method described by Singleton, Orthofer, and Lamuela-Raventos (1999) and as previously described by Kazazic, Djapo and Ademovic (2016). Standard curve of gallic acid was used for the evaluation of results. For sample measurement, 100 µL of the extract was added to 5 mL (1/10 dilution) of Folin Ciocalteu phenol reagent and 900 µL of distilled water. After 5 min, 4 mL of 15% sodium carbonate (Na2CO3) was added. Following the incubation at room temperature for 120 minutes the absorbance at 765 nm was measured.

Data are presented as average values of three measurements for each sample (R2=0.998 for fresh samples, R2=0.999 for juices and R2=0.999 for jams).

The content of TF was expressed as mg of gallic equivalent (GAE) per 100 g of fruits fresh weight (FW) for fresh samples and jams. For juices the content of TF was expressed as mg of gallic equivalent (GAE) per L of juice.

*Determination of total anthocyanin (TA) content*

Total anthocyanin content was determined using the pH-differential method (Zhishen, Mengcheng and Jianming 1999). Two solutions of fruit samples were prepared, one with 0.5 mL of extracts in 2 mL of potassium chloride buffer (0.025 M, pH 1.0) and other with 0.5 mL of extracts in 2 mL of sodium acetate buffer (0.4 M, pH 4.5). The absorbance was measured at both 510 nm and 700 nm with a spectrophotometer (Genesys 20 thermo spectronic) after 20 min. The total anthocyanin content is expressed as mg of cyanidin-3-glucoside equivalent (CGE) per 100 g of fruits fresh weight (FW) for fresh samples and jams. For juices the content of anthocyanin was expressed as mg of cyanidin-3-glucoside equivalent (CGE) per L of juice.

*Determination of antioxidant activity (AA) using the ABTS method*

Determination of the antioxidant activity with ABTS• (Re, Pellegrini, Proteggente et al., 1999) was done as described in work by Kazazic et al. (2016). ABTS cation radical (ABTS•) was made by dissolving 19.5 mg of ABTS and 3.3 mg of potassium persulfate in 7 mL of distilled water and allowing free radical generationin the dark at room temperature for 12-16 h. Then ABTS radical solution was diluted in ethanol to an absorbance of 0.70 ± 0.02 at 734 nm. Then 40 µL of the sample was mixed with 4 mL of diluted ABTS radical solution in the cuvette and absorbance was measured at 734 nm after 6 minutes. All the solutions were prepared on the same day of the experiment. The results were expressed as mmol of Trolox (TE) equivalent per kilogram for fresh samples and jams, and as mmol of Trolox (TE) equivalent per L in juices (R2=0.9942 for fresh samples, R2=0.9939 for juices and R2=0.9947 for jams).

*Statistical analysis*

All measurements are expressed as mean ± standard deviations. The statistical differences are considered significant at $p < 0.05$. All the analyses were done in triplicates.

## RESULTS AND DISCUSSION

Quantitative content of investigated bioactive compounds (total phenols and total anthocyanins) and antioxidant activity in fresh sour cherries, jams and juices are presented in Tables 1, 2 and 3.

**Table 1**: The content of total phenols (TF), total anthocyanins (TA) and antioxidant activity (AA) by ABTS method in sour cherries

| Cultivar | TF, mg GA/100 g FW | TA, mg CGE/100g FW | AA, mmol TE/kg FW |
|---|---|---|---|
| **Marasca** | 340.80±23.23$^{b}$ | 79.7±0.35$^{b}$ | 29.03±1.49$^{b}$ |
| **Oblačinska** | 235.81±68.10$^{a}$ | 65.3±0.76$^{a}$ | 23.66±0.96$^{a}$ |

*Values with different letters in the same column are significantly different at p<0.05

**Table 2:** The content of total phenols (TF), total anthocyanins (TA) and antioxidant activity (AA) using ABTS method in sour cherries jams

| Cultivar | TF, mg GA/100 g FW | TA, mg CGE/100g FW | AA, mmol TE/kg FW |
|---|---|---|---|
| **Marasca** | 366.34±29.78$^{b}$ | 32.26±2.52$^{b}$ | 28.90±1.80$^{b}$ |
| **Oblačinska** | 306.67±12.57$^{a}$ | 21.10±1.85$^{a}$ | 23.71±2.20$^{a}$ |

*Values with different letters in the same column are significantly different at p<0.05

**Table 3:** The content of total phenols (TF), total anthocyanins (TA) and antioxidant activity (AA) determined by ABTS method in sour cherries juice

| Cultivar | TF, mg GA/L FW | TA, mg CGE/L FW | AA, mmol TE/L FW |
|---|---|---|---|
| **Marasca** | 514.48±83.70$^{b}$ | 48.78±3.28$^{b}$ | 42.03±0.25$^{b}$ |
| **Oblačinska** | 365.59±15.17$^{a}$ | 34.77±0.95$^{a}$ | 30.55±0.07$^{a}$ |

*Values with different letters in the same column are significantly different at p<0.05

The total phenolic content in the sour cherries was 235.81 mg (GA)/100 g FW in the Oblačinska cultivar and lower than reported by Khoo et al. (2011), and Mitić et al. (2012). Sour cherry Marasca fruit had higher total phenolic content (340.80 mg (GA)/100 g FW) than Oblačinska which is in accordance with Viljevac Vuletić et.al. (2017). Čoga, Jurkić, Zeman et al. (2017) reported values for total phenolic content in Marasca fresh fruits from 391.4 mg (GA)/100 g to 691.7 mg (GA)/100 g. Variation of total phenolic content in Marasca cultivar was due to significant difference in chemical composition for fruits of Marasca cultivar depending on climatic conditions (Čoga et al., 2017).

For jam samples total phenolic content was 306.67 mg (GA)/100 g FW for the Oblačinska cultivar and 366.34 mg (GA)/100 g FW for the Marasca cultivar which is in accordance with values reported by Kim and Padilla-Zakour (2004). Levaj et al. (2010) pointed that sour cherry Marasca fruits and jams contained the higher level of phenolic compounds than sour cherry Oblačinska which is similar to our results. The study by Poiana, Moigradean, Dogaru et al. (2011) showed that changes in total phenolic compounds in sour cherries were less pronounced compared to strawberry and cherries during thermal processing and storage. Vukoja, Pichler and Kopjar (2019) pointed that jams with a higher concentration of added sugar have a higher concentration of total phenols, comparable to the results of our study.

The total phenolic content in juices ranged from 365.59 mg (GA)/L FW for the Oblačinska cultivar and 514.48 mg (GA)/L FW for the Marasca cultivar.

The concentration of total anthocyanins in sour cherries was 65.3±0.76 mg CGE/100 g FW for the Oblačinska cultivar and 79.7±0.35 mg CGE/100 g FW for the Marasca cultivar. These results are in accordance with the anthocyanin content determined by Blando et al. (2004) (27.8 - 80.4 mg (CGE)/100 g FW). Viljevac Vuletić et al. (2017) investigated the impact of season, location, and cultivar influence on bioactive compounds of sour cherries and reported that total anthocyanin content was higher in Marasca cultivar compared to Oblačinska. Anthocyanin concentrations reported by Vijevac Vuletić et al. (2017) were higher than anthocyanin concentrations in this study due to the difference in extraction method used. Anthocyanins are vacuola pigments and ultrasound extraction which was used by Viljevac Vuletić et al. (2017) enhances transfer from the sample to the solvent improving the extraction of anthocyanins (Rodrigues, Fernandes, Sosua de Brito et al., 2015).
Total anthocyanin content in jam samples ranged from 21.10±1.85 mg (CGE)/100 g FW for Oblačinska cultivar and 32.26±2.52 mg (CGE)/100 g FW for Marasca cultivar. Anthocyanin losses are probably due to complex formation with other compounds during jam processing, namely sugars and degradation products of ascorbic acid (Bursać Kovačević, Levaj and Dragović-Uzelac 2009).

Antioxidant activity depends on the method of extraction and method used for their determination. The ABTS assay was performed to assess the antioxidant activity of sour cherries and their products jams and juices. ABTS is not found naturally, so there is possible criticism that the assay is not directly relevant to any biological function. Model of synthetic radicals has been used frequently in many laboratories around the world for screening and routine determination even though they are not directly related to food. Yet these methods are used to determine the antioxidant activity in most studies due to their simplicity, low cost and repeatability (Milić et al., 2021; Sokol-Letowska et al., 2020; Miguel-Chávez, 2017). ABTS assay can be used to determine the antioxidant capacity of numerous compounds, namely carotenoids, phenolic, and plasma (Re et al., 1999). Antioxidant activity of compounds with redox potential that is lower than that of ABTS can be determined using this assay. Since phenols have redox potential lower than ABTS, this radical is used to determine the antioxidant activity of these molecules (Miguel-Chávez, 2017). The antioxidant activity in the

Marasca cultivar was 29.03±1.49 mmol (TE)/kg which is lower than reported by Dragovic-Uzelac, Levaj, Bursać et al. (2007) (45.36±3.05 mmol TE/kg FW). In Oblačinska cultivar antioxidant activity was found to be 23.66±0.96 mmol (TE)/kg.

Juices and jams represent a noticeable source of antioxidants despite processing. It has been previously reported that the inclusion of sugar and industrial processing of sour cherry does not significantly impact their antioxidant capacity (Kirakosyan, Seymour, Urcuyo Llanes et al., 2009). Anthocyanin losses are compensated by the formation of Maillard products that can contribute to the antioxidant properties (Vukoja et al., 2019).

The correlation between antioxidant activity and total polyphenol content was statistically significant ($r = 0.906$, $p < 0.01$), whereas the correlation between antioxidant activity and total anthocyanin content was non-significant ($r = 0.212$, $p > 0.05$). This can be explained by the high content of melatonin (a phenolic substance), which is a strong antioxidant, in the sour cherry juice (Burkhardt, Tan, Manchester et al., 2001; Reiter, Tan, Leon et al., 2005).

## CONCLUSIONS

In conclusion, the content of total phenols and antioxidant activity were well preserved after processing in the final products of sour cherry. The treatment process had a greater impact on the reduction of the anthocyanin content but did not have a significant effect on the reduction of the content of total phenols and antioxidant activity. Results showed that juices and jams possess noticeable content of bioactive compounds with antioxidant activity in the diet.
The obtained results also showed that there are significant differences in the content of investigated bioactive compounds among selected sour cherry varieties in the Herzegovina region. Further investigations are needed to investigate polyphenolic compounds profile and effects of processing of Marasca and Oblačinska sour cherries.

## REFERENCES

Blando, F., Gerardi, C., Nicoletti, I. (2004). Sour Cherry (Prunus cerasus L) Anthocyanins as Ingredients for Functional Foods. Journal of Biomedicine and Biotechnology, 5, 253-258.

Burkhardt, S., Tan, D. X., Manchester, L. C., Hardeland, R., Reiter, R. J. (2001). Detection and Quantification of the Antioxidant Melatonin in Montmorency and Balaton Tart Cherries (Prunus cerasus). Journal of Agricultural and Food Chemistry, 49, 4898-4902.

Bursać Kovačević, D., Levaj, B., Dragović-Uzelac, V. (2009). Free radical scavenging activity and phenolic content in strawberry fruit and jam. Agriculturae Conspectus Scientificus, 74(3), 155-159.

Corts, R. M., Rodrigues, L. C., Ortiz Marcide, J. M., Sanches, R. P. (2008). Characterization of sour (Prunus cerasus L.) and sweet cherry (Prunus avium L.) varieties with five isozyme systems. The Revista Brasileira de Fruticultura, 30, 154-158.

Čoga, L., Jurkić, V., Zeman, S., Jurkić, A., Slunjski, S. (2017). Chemical composition of sour cherry cv. Marasca fruit in climatic two different years. Glasnik Zaštite Bilja, 40 (5), 6-13.

Dragović-Uzelac, V., Levaj, B., Bursać, D., Pedišić, S., Radojčić, I., Biško, A. (2007). Total Phenolics and Antioxidant Capacity Assays of Selected Fruits. Agriculturae Conspectus Scientificus, 72(4), 279-284.

He, J., Giusti, M. (2009). Anthocyanins: Natural Colorants with Health-Promoting Properties. Annual Review of Food Science and Technology, 1, 163-178.

Jakobek, L., Šeruga, M., Medvidović-Kosanović, M., Novak, I. (2007). Anthocyanin content and antioxidant activity of various red fruit juices. Deutsche Lebensmittel-Rundschau, 103, 58-64.

Kazazic, M., Djapo M., Ademovic, E. (2016). Antioxidant activity of water extracts of some medicinal plants from Herzegovina region. International journal of pure and applied bioscience, 4 (2), 85-90.

Khoo, G.M., Clausen, M.R., Pedersen, B.H., Larsen, E. (2011). Bioactivity and total phenolic content of 34 sour cherry cultivars, Journal of Food Composition and Analysis, 24, 772–776.

Kirakosyan, A., Seymour, E. M., Urcuyo Llanes, D. E., Kaufman, P. B., Bolling, S. F. (2009). Chemical profile and antioxidant capacities of tart cherry products. Food Chemistry, 115(1), 20-25.

Kim, D. O., Padilla-Zakour, O. I. (2004). Jam Processing Effect on Phenolics and Antioxidant Capacity in Anthocyanin-rich Fruits: Cherry, Plum, and Raspberry. International Journal of Food Science, 69 (9), 395-400.

Levaj, B., Dragović-Uzelac, V., Delonga, K., Kovačević Ganić, K., Banović, M., Bursać Kovačević, D. (2010). Polyphenols and Volatiles in Fruits of Two Sour Cherry Cultivars, Some Berry Fruits and Their Jams. Food Technology and Biotechnology, 48 (4), 538–547.

Miguel-Chávez, R.S. (2017). Phenolic antioxidant capacity: a review of the state of the art. In: Soto Hernandez, M., Palma Tenango, M., Garcia Mateos, M.R. (Eds), Phenolic compounds biological activity. (pp. 59-74). IntechOpen.

Milić, A., Daničić, T., Tepić Horecki, A., Šumić, Z., Bursać Kovačević, D., Putnik, P., Pavlić, B. (2021). Maximizing Contents of Phytochemicals Obtained from Dried Sour Cherries by Ultrasound-Assisted Extraction. Separations, 8(9), 155.

Mitić, N. M., Obradović, V. M., Kostić, A. D., Micić, J. R., Pecev, T. E. (2012). Polyphenol Content and Antioxidant Activity of Sour Cherries from Serbia. Chemical Industry & Chemical Engineering Quarterly, 18(1), 53-62.

Pedisić, S., Levaj, B., Dragović-Uzelac, V., Kos, K. (2007). Physicochemical Composition, Phenolic Content and Antioxidant Activity of Sour Cherry cv. Marasca During Ripening. Agriculturae Conspectus Scientificus, 72 (4), 295-300.

Poiana, M. A., Moigradean, D., Dogaru, D., Mateescu, C., Raba, D., Gergen, I. (2011). Processing and storage impact on the antioxidant properties and color quality of some low sugar fruit jams. Romanian Biotechnological Letters, 16 (5), 6504-6512.

Prvulović, D., Popović, M., Malenčić, Dj., Ljubojević, M., Barać, G., Ognjanov, V. (2012). Phenolic content and antioxidant capacity of sweet and sour cherries. Studia Universitatis Babes-Bolyai Chemia, 57 (4), 175-181.

Re, R., Pellegrini, N., Proteggente, A., Pannala, A., Yang, M., Rice-Evans, C. (1999). Antioxidant activity applying an improved ABTS radical cation decolorization assay. Free Radical Biology & Medicine, 26 (9-10), 1231-1237.

Reiter, R. J., Tan, D. X., Leon, J., Kilic, U., Kilic, E. (2005). When Melatonin Gets on Your Nerves: Its Beneficial Actionsin Experimental Models of Stroke. Experimental Biology and Medicine, 230(2), 104-117.

Repajić, M., Bursać Kovačević, D., Putnik, P., Dragović-Uzelac, V., Kušt, J., Čošoć, Z., Levaj, B. (2015). Influence of Cultivar and Industrial Processing on Polyphenols in Concentrated Sour Cherry (Prunus cerasus L.) Juice. Food Technology and Biotechnology, 53(2), 215-222.

Rodrigues, S., Fernandes, F. A. N., Sosua de Brito, E., Sousa, A. D., Narain, N. (2015). Ultrasound extraction of phenolics and anthocyanins from jabuticaba peel. Industrial Crops and Products, 69, 400-407.

Serradilla, M. J., Fotirić Akšić, M., Manganaris, G. A., Ercisli, S., Gonzalez-Gomez, D., Valero, D. (2017). Fruit Chemistry, Nutritional Benefits and Social Aspects of Cherries. In: Quero-Garcia, J., Iezzoni, A., Pulawska, J., Lang G. (Eds), Cherries: botany, production and uses. (pp. 420-441). CABI.

Shashirekha, M.N., Mallikarjuna, S.E., Rajarathnam, S. (2015). Status of bioactive compounds in foods, with focus on fruits and vegetables. Critical Reviews in Food Science and Nutrition, 55 (10),1324-39.

Singleton, V. L., Orthofer, R., Lamuela-Raventos, R. M. (1999). Analysis of total phenols and other oxidation substrates and antioxidants by means of folin-ciocalteu reagent. Methods in Enzymology, 299, 152-178.

Sokół-Łętowska, A., Kucharska, A. Z., Hodun, G., Gołba, M. (2020). Chemical composition of 21 cultivars of sour cherry (Prunus cerasus) fruit cultivated in Poland. Molecules, 25(19), 4587.

Viljevac Vuletić, M., Dugalić, K., Mihaljević, I., Tomaš, V., Vuković, D., Zdunić, Z., Puškar, B., Jurković, Z. (2017). Season, location and cultivar influence on bioactive compounds of sour cherry fruits. Plant, Soil and Environment, 63 (9), 389–395.

Vukoja, J., Pichler, A., Kopjar, M. (2019). Stability of anthocyanins, phenolics and color of tart cherry jams. Foods, 8, 255.

Zhishen, J., Mengcheng, T., Jianming W. (1999). The determination of flavonoid contents in mulberry and their scavenging effects on superoxide radicals. Food Chemistry, 64 (4), 555-559.

**Summary/Sažetak**

Bioaktivne supstance su sekundarni metaboliti proizvedeni u biljkama. Mnoge studije zabilježile su direktnu povezanost između prisustva bioaktivnih supstanci i pozitivnih efekata biljaka na zdravlje. Višnje imaju visok sadržaj bioaktivnih supstanci, uglavnom polifenola i antocijanina. Najčešće se konzumiraju u svježem stanju, ali se koriste za proizvodnju džema, želea, marmalade, sokova i sirupa. Cilj ovog istaživanja bio je utvrditi ukupni sadržaj fenola, antocijanina i antioksidativne aktivnosti dvije sorte višanja, te njihovih proizvoda, džemova i sokova, pripremljenih po tradicionalnoj recepturi. Ukupni sadržaj fenola određen je metodom Folin-Ciocalteu. Za određivanje antioksidativne aktivnosti korišten je ABTS test obezbojenja radikalnih spojeva. Sadržaj antocijanina određen je primjenom pH diferencijalne metode. Sorta Marasca imala je veći sadržaj fenola, antocijanina i antioksidativnu aktivnost u poređenju sa sortom Oblačinska. Procesiranje višanja imalo je veći utjecaj na smanjenje sadržaja antocijana, ali nije imala značajan utjecaj na antioksidativnu aktivnost.

Glasnik hemičara i tehnologa Bosne i Hercegovine

Bulletin of the Chemists and Technologists of Bosnia and Herzegovina

2022

58

Print ISSN: 0367-4444
Online ISSN: 2232-7266

Original Scientific Article
DOI: https://doi.org/10.35666/2232-7266.2022.58.02
UDC: 543.067.2[627.41:666.327]

7-18

# Extractability of sodium ions from soil

**Sulejmanović J.[a*], Jurković J.[b], Ajanović T.[a], Selović A.[a], Nuhanović M.[a], Ajanović A.[c], Kovo K.[b], Durić L.[b], Botonjić M.[b]**

[a]*University of Sarajevo-Faculty of Science, Zmaja od Bosne 33-35, Sarajevo, Bosnia and Herzegovina*

[b]*University of Sarajevo-Faculty of Agriculture and Food Science, Zmaja od Bosne 8, Sarajevo, Bosnia and Herzegovina*

[c]*University of Sarajevo-Faculty of Veterinary, Zmaja od Bosne 90, 71000 Sarajevo, Bosnia and Herzegovina*

**Article info**
Received: 04/10/2021
Accepted: 18/01/2022

**Keywords:**
Soil
Sodium
Ultrasound
Green Solvents

***Corresponding author:**
**Jasmina Sulejmanović**
E-mail:
jasmina_sulejmanovic@yahoo.com
Phone: +387 33 279 882

**Abstract:** In this study, soil samples from two selected locations: "A" (alluvial soil) and "B" (clay loam) were analyzed. Chemical analysis of soil samples included determination of soil pH and soil suspension conductivity. Two different extraction methods were applied: shaking and ultrasound method for extraction of sodium ions from soil with three solvents (aqua regia, 5% $CH_3COOH$ and distilled water). The values of pseudo-total (extracted with aqua regia) and bioavailable Na content (extracted with 5% $CH_3COOH$ and distilled water) in the soil sample "A" were in the range of 46.35-66.55 mg Na/kg; 14.77-18.59 mg Na/kg and 12.58-15.20 mg Na/kg of soil, respectively, by applying shaking method. By the same method, in the case of soil sample "B" the ranges were 17.15-75.66 mg Na/kg; 20.87-32.80 mg Na/kg and 4.62-20.33 mg Na/kg of soil, for the extraction by aqua regia, 5% $CH_3COOH$ and distilled water, respectively. Ultrasonic extraction in all cases gained higher results compared to the shaking method. In general, the application of ultrasound shows a positive effect on the extractability of $Na^+$ ions from soil samples.

## INTRODUCTION

Sodium is found in the soil and plants as monovalent and belongs to the group of nutrients (Lutgens and Tarbuck, 2003). It has the role of electrolyte, due to its high content in the protoplasm, it affects its hydration - it is important in the regulation of water content. The availability of metals to plants, as well as the migration of metals to deeper soil layers, largely depends on the fractions in which the metals are found in the soil. The metal fractions in the soil are exchangeable ions, carbonates, Fe and Mn oxides, organic and residual fractions (Liang, Wang, Gao et al., 2014, Slukovskaya, Kremenetskaya, Drogobuzhskaya et al., 2020). The distribution of metals between different forms in which they can be found in the soil is controlled by both physic and chemical processes and time intervals (Acosta, Jansen, Kalbitz et al., 2011). Therefore, it is possible that individual metals in the soil occur in several different chemical forms depending on the type of metal and physicochemical properties of soil (Tessier, Campbell, Bisson et al., 1979; Kotoky, Bora, Baruah et al., 2003; Du, Xue, Liu et al., 2008; Cui and Du, 2011). The decomposition of the soil primary minerals of Feldspar releases sodium, which for the most part immediately binds to the adsorption complex of the soil. This reduces the mobility and risk of leaching from the soil, except in sandy soils. If the adsorption complex contains more than 15% $Na^+$ ions, the soil is classified as alkaline soils (multivalent cations are most strongly bound to the adsorption complex, with the exception of $H^+$ ion, due to its smaller diameter it has a higher binding strength). Cations of lower retention (retention power on the adsorption complex) are the easiest to desorb, and Na+ ion has the weakest retention, primarily due to the large hydration membrane. When NaCl content in the soil exceeds 0.5%, the problem of salinity occurs (Kanber and Unlu, 2010). Salinity, in the form of NaCl, is one of

the main abiotic stresses that reduces plant growth and development (Maathuis, Ahmad and Patishtan et al., 2014). Some metals can bind more strongly to the solid phases of the soil, resulting in poorer desorption. Therefore, in metals that have a high affinity for binding to the solid phase, the efficiency of its removal is lower than in other metals. Today, salinity is one of the most important factors threatening the sustainability of irrigated agriculture. Salinity reduces the productivity if not brought under control (Kanber and Unlu 2010). Furthermore, excessive amounts of sodium ruin the physical structure of the soil. The root development is also affected due to the aggregate's fragmentation causing a decline in water and air permeability (Karadağ, Eren, Çetinkaya et al., 2015). For the experimental part of this work, two different soil samples were taken from the surface layer (up to 20 cm depth) marked as: soil "A" (alluvial soil) and soil "B" (clay loam). The bioavailable sodium content of the soil was determined by extraction with selected green solvents ($H_2O$ and 5% $CH_3COOH$) using two methods of extraction: ultrasound and shaking. The obtained results were compared with the pseudo-total content of sodium in each soil, which was determined according to BAS ISO 11466: 1995 (E). Sodium content was determined by atomic emission spectrometry. The obtained results enabled the evaluation of the efficiency of the applied extraction methods.

## EXPERIMENTAL

*Reagents and solutions*

All used reagents were of analytical grade. $CaCl_2x2H_2O$, p.a., HCl, 36% p.a., $HNO_3$, 65% p.a., and $CH_3COOH$, 96% p.a. were obtained by Semikem, Sarajevo. Standard Na solution (Certi PUR 1000 mg/ L), and KNO3, 2000 mg/L were obtained by Merck, Darmstadt. Working solutions were prepared by diluting Na standard solution.

*Analysis*

The analysis included the following experimental steps: sampling of two different soil samples (marked as soil "A" and soil "B") and dividing them into 10 subsamples with two parallels (A1-A10 and B1-B10); determination of the moisture content (%) in soil samples; preparation of soil suspension in water and in $CaCl_2x2H_2O$ to determine pH and conductivity. Sodium extraction from the soil samples referred as pseudo-total sodium content was performed by the method BAS ISO 11466:1995 (E). Furthermore, sodium extraction from the soil samples was tested by the extraction of soils in distilled water and 5% acetic acid by ultrasound and shaking to determine the effectiveness of the tested methods and solvents.

*Soil type, sampling and preparation of soil samples*

Soil samples analyzed for sodium content were sampled from two locations in Bosnia and Herzegovina and marked as: soil sample A and soil sample B. The soil sample A belongs to the type of alluvial soil, due to the river nearby, while soil itself belongs to the category of clayey sand. The soil was fertilized with burnt manure, while the crops in the previous vegetation were: real grains (barley, wheat, oats and spelled), and vegetables (tomato, watermelon, parsnips and peas). The soil sample B belongs to the type of clay loam. The classification of analyzed soils was performed by the Institute for pedology, agrochemistry and melioration, Sarajevo, Bosnia and Herzegovina. For fertilization of this type of soil in the previous vegetation, beef manure was used, while the crops in the previous vegetation were: potatoes (which were additionally fertilized with artificial fertilizer NPK formulation 15:15:15) and tomatoes (which are additionally fertilized with sheep manure and artificial fertilizer NPK with a formulation of 7:20:30).

From both locations, 10 kg of each soil samples were taken from the surface layer of the soil (depth up to 20 cm), with a plastic spatula from the arable layer. The samples were cleaned of pieces of organic origin and stones, air-dried and stored in 2 L polyethylene bags. Afterwards, air-dry soil samples were ground in a porcelain mortar and sieved through a 2 mm sieve to eliminate all impurities. To minimize the humidity impact on the method, precision samples were dried at 105°C to the constant weight.

*Determination of active soil reaction, substitution acidity and electrical conductivity*

Determination of active (pH in water) and substitution acidity (pH in calcium chloride dihydrate solution) in soil samples (A and B) was performed according to the method of BAS ISO 10390:2006. The pH of the soil is potentiometrically determined from the soil-water suspension in a ratio of 1:5, giving information on the active acidity of the soil, while measuring the pH of the soil suspension in 0.01 mol/L $CaCl_2x2H_2O$ solution indicates the value of the soil substitution acidity. For determining the specific conductivity of the soil which is a consequence of the presence of free ions, i.e. soluble salts in the soil, the same aqueous suspension of soil is taken as for determining the pH.

*Determination of the pseudo-total amount of sodium in soil samples*

From the prepared soil samples, 20 parallels weighing 3 g (±0.1 mg) were transferred to balloons with a ground neck and a flat bottom of 250 mL. 21 mL of HCl and 7 mL of $HNO_3$ were added to the samples. Solvent soil samples were placed in a digester and digestion was performed for 16 hours at room temperature and then continued at 108°C for 2 hours. The samples were then cooled and filtered into a 100 mL volumetric flask over quantitative filter paper, marked with corresponding labels and filled to the mark with 0.5% $HNO_3$. The resulting solutions were used to determine the pseudo-total Na content by atomic spectrometer Varian AA240FS in emission mode.

*Determination of water-soluble and exchangeable soil fraction*

From the prepared soil samples, 20 parallels weighing 10 g (±0.1 mg) were transferred to polyethylene bottles with the corresponding label. 50 mL of distilled water was added to the samples to determine the water-soluble

forms of Na from the soil. Sample vials were placed in a shaker by shaking the samples at room temperature for 2 hours at 180 rpm. The samples were then filtered into a 100 mL volumetric flask over quantitative filter paper and diluted to the mark with distilled water. The obtained filtrates were immediately tested for Na content by the AES method. At the same time, 20 more parallels were prepared in the same manner, only by replacing distilled water with 5% $CH_3COOH$ acid in order to determine the exchangeable soil fraction. To suppress ionization, potassium nitrate solution with a potassium concentration of 2000 μg/mL was added to each sample as well as to each blank probe.

*Ultrasonic extraction of sodium from a soil sample*

From the prepared soil samples, 20 parallels weighing 3 g (±0.1 mg) were weighed. 21 mL of HCl and 7 mL of $HNO_3$ were then added to the weighed samples, according to the BAS ISO 11466:1995 (E). The samples were then placed in an ultrasonic bath with a frequency of 37 kHz, for 2 hours. The contents of the vessels were then filtered through filter paper (blue tape) into 100 mL volumetric vessels and filled up with distilled water. The obtained filtrates were used to determine Na content by AES-flame technique. Furthermore, 20 parallels weighing 10 g (±0.1 mg) and 3 g (±0.1 mg) were weighed in the same way to determine the effect of ultrasound on the efficiency of $Na^+$ ion extractability in the case when distilled water and 5% acetic acid were used as solvent, respectively. The samples were therefore poured with 50 mL of distilled water and 50 mL of 5% $CH_3COOH$, respectively, and placed in an ultrasonic bath for 2 hours at 37 kHz. The contents of the vials were filtered through quantitative filter paper into 100 mL volumetric vessels and made up to the defined volume with distilled water. The obtained filtrates were used to determine the Na content by the AES method.

The calculation of the metal content in the soil was done according to the formula (Eq.1):

$$(\text{mg Na})/(\text{kg soil}) = (c \cdot V \cdot f)/m \cdot 100 \qquad \text{Eq. 1}$$

where:
c (mg/L) - metal concentration,
V (L) - solution volume;
m (g) - mass of air-dry soil sample;
f- dilution factor.

## RESULTS AND DISCCUSSION

*Moisture content of soil samples*

The moisture content in a total of 20 analyzed samples was determined gravimetrically based on weight loss by drying the samples at a temperature of 105°C to constant weight. The obtained results are given in Table 1. The mean value of moisture content in the soil samples "A" is 15.34% and 12.41% for soil samples "B".

**Table 1:** Moisture content in soil samples (%)

| Sample A | Sample B |
|---|---|
| A1=11.34 % | B1=11.95 % |
| A2=16.28 % | B2=12.67 % |
| A3=17.47 % | B3=12.98 % |
| A4=15.03 % | B4=10.17 % |
| A5=17.22 % | B5=10.24 % |
| A6=14.24 % | B6=14.17 % |
| A7=15.83 % | B7=11.65 % |
| A8=17.91 % | B8=12.98 % |
| A9=17.63 % | B9=13.11 % |
| A10=10.40 % | B10=14.13 % |

*Active and substitutional soil acidity and electrical conductivity of soil samples*

pH is an important indicator of soil quality, plays a significant role in many soil processes such as solubility and availability of plant nutrients, microbial activity and degradation of organic matter in the soil, sorption of contaminants and various physicochemical processes involved in the biogeochemical cycle (Sintorini, Widyatmoko, Sinaga et al., 2021). The results of pH values determined in the suspensions of soil with water (active acidity) and with 0.01 mol/L $CaCl_2x2H_2O$ (substitution acidity) for soil samples "A" and "B" were presented in Table 2, as well as the values of electrical conductivity in suspension with distilled water.

**Table 2**: The result of pH value and electrical conductivity of soil samples.

| "A" | | | | "B" | | | |
|---|---|---|---|---|---|---|---|
| Samples | pH ($H_2O$) | pH $CaCl_2$ x $2H_2O$ | Conductivity (μS/cm) | Samples | pH ($H_2O$) | pH $CaCl_2$ x $2H_2O$ | Conductivity (μS/cm) |
| A1 | 6.02 | 5.08 | 231 | B1 | 6.71 | 6.10 | 1068 |
| A2 | 6.11 | 5.11 | 263 | B2 | 7.46 | 6.60 | 626 |
| A3 | 6.13 | 5.34 | 270 | B3 | 6.74 | 6.09 | 598 |
| A4 | 7.61 | 6.86 | 492 | B4 | 5.89 | 4.90 | 187 |
| A5 | 6.29 | 5.33 | 300 | B5 | 5.85 | 4.96 | 289 |
| A6 | 6.85 | 6.14 | 617 | B6 | 6.99 | 6.25 | 600 |
| A7 | 6.06 | 6.03 | 452 | B7 | 6.95 | 6.21 | 466 |
| A8 | 6.76 | 6.02 | 362 | B8 | 6.56 | 5.94 | 501 |
| A9 | 7.00 | 6.25 | 333 | B9 | 6.96 | 6.23 | 658 |
| A10 | 6.15 | 5.63 | 323 | B10 | 6.97 | 6.11 | 685 |
| Min | 6.02 | 5.08 | 231 | Min | 5.85 | 4.90 | 187 |
| Max | 7.61 | 6.86 | 617 | Max | 7.46 | 6.60 | 1068 |
| *Avg. | 6.50 | 5.78 | 364 | *Avg. | 6.71 | 5.94 | 568 |
| **SD value | 0.58 | 0.62 | 133 | **SD value | 0.55 | 0.60 | 275 |

*Avg= Average value; **SD value- standard deviation

The obtained average pH value (6.50; 6.71) of the analyzed soil samples determined in water from the soil samples "A" and "B", respectively, shows that analyzed soils belong to the class of neutral and slightly acidic soils (Sirsat, Cernadas, Fernández-Delgado et al., 2017). Nevertheless, the difference in the pH value of different soil samples from the same plot is also due to the inhomogeneous distribution of the fertilizer used to fertilize the investigated plot.

Regarding the value of the substitution acidity (5.78), which represents the exchange of ions from the adsorption complex of the soil (Minasny, McBratney, Brough et al., 2011), with cations from the neutral salt (K$_2$Cl$_2$, Ca$^{2+}$), the difference between soil pH and pH ($CaCl_2x2H_2O$) with a value of 0.72 indicates moderate soil fertility. The same could be concluded with regard to the average value of the conductivity of soil samples "A", which is 364 µS/cm. It can be related to soil depletion because a large number of crops have been sown in previous vegetation. The average substitution acidity for soil samples "B" is 5.94. According to the value of ΔpH for pH ($H_2O$) and pH ($CaCl_2x2H_2O$) which is 0.77, the given soil is richer in exchangeable ions than the soil from the "A" location, which is additionally confirmed by the higher average conductivity value (Chen and Ma, 2016) in the given samples (568 µS/cm).

The determination of such soil properties, can refer to the influence of metal mobility (Šapčanin, Čakal, Jaćimović et al., 2017).

*Sodium concentrations extracted by various extraction agents - method of shaking*

Sodium concentrations measured after soil extraction from "A" by various extraction agents ranged from 12.29-66.55 mg Na/kg of soil (Figure 1(a) and Table 3). As can be seen, the highest results were obtained using aqua regia as an extraction agent. Aqua regia dissolves most metals, except those that are tightly bound in silicate soil minerals. Therefore, the content of Na extraction agent is referred to as pseudo-total content (Sungur, Soylak and Ozcan, 2014).

The values of the pseudo-total Na content in the specified soil sample "A" are in the range from 46.35-66.55 mg Na/kg of soil, where the values of standard deviations are ≤3.88 mg Na/kg soil. In the case of soil samples "B", the values of Na content are in the range 17.15-75.66 mg Na/kg soil with standard deviations ≤3.81 mg Na/kg of soil. It is necessary to know the concentration of sodium in the soil because Na participates in the total ion exchange and is a useful indicator of soil fertility.

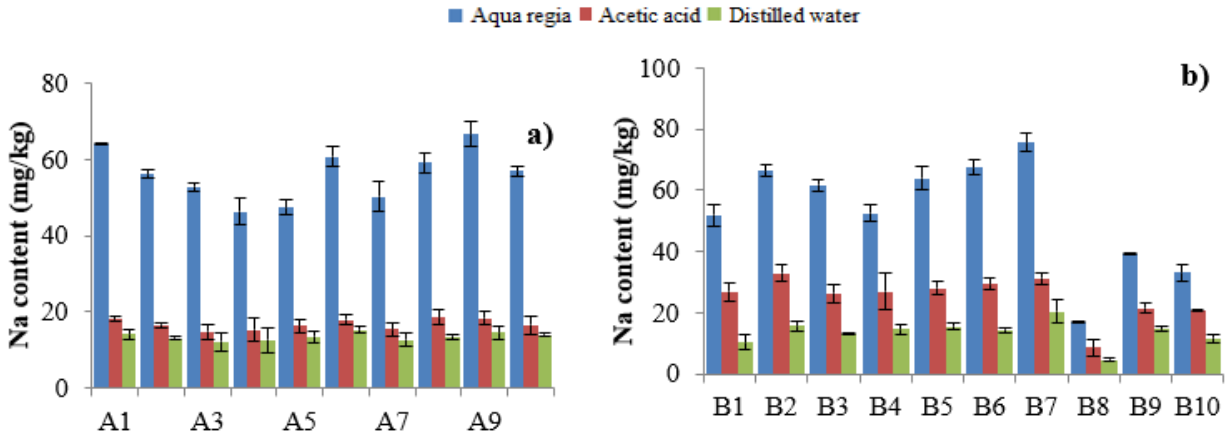


**Figure 1:** Comparative results of Na concentration (mg Na/kg of soil) in soil samples obtained using three different extraction agents assisted by the method of shaking for samples "A" (a) and "B" (b).

In contrast to the pseudo-total Na content, the bioavailable forms of sodium are determined using green solvents (5% $CH_3COOH$ acid and distilled $H_2O$) and represent the values of Na that will be potentially available in the real conditions (Dočekalová, Kovaříková, Dočekal et al., 2012). With 5% $CH_3COOH$, the content of Na in the soil were in the range of 14.77-18.59 mg Na/kg of soil (±≤2.95 mg Na/kg of soil) and 20.87-32.80 mg Na/kg of soil, if samples B8.1 and B8.2 are excluded (±≤6.01 mg Na/kg of soil) for the samples of "A" and "B" location, respectively (Figure 1(b) and Table 4). Slightly higher results were obtained with 5% $CH_3COOH$, approximately by 15-22% and 46% higher results for samples "A" and "B", respectively, compared to the results obtained by extraction with distilled water. In comparison to the values of the pseudo-total Na content in the soil samples, 5% $CH_3COOH$ could extract on average about 34% and 49% $Na^+$ ions in relation to its pseudo-total value from samples "A" and "B", respectively. These results showed that the analyzed soils by chemical structure consists of easily available organic and inorganic forms in which the $Na^+$ ion is present.

In the case of distilled water as an extraction agent, the obtained Na values referred to the mobile fraction of sodium (Minkina, Motuzova, Mandzhieva et al., 2013; Slukovskaya, Kremenetskaya, Drogobuzhskaya et al., 2020) were in the range of 12.58-15.20 mg Na/kg of soil (±3.29 mg Na/kg of soil) and 4.62-20.33 mg Na/kg of soil (±3.86 mg Na/kg of soil) for soil samples "A" and "B", respectively.

According to the obtained results up to 25% of Na content could be extracted with distilled water from its pseudo-total content of the soil samples. Since the values of Na in the soil samples "A" obtained with acetic acid were not significantly higher compared to the use of distilled water (about 9%), there are not many weakly bound $Na^+$ ions to inorganic sites (carbonates).

Furthermore, relatively low values of standard deviations in all three cases indicated good Na homogeneity in the examined soils. In addition, obtained values with 5% $CH_3COOH$ were higher about 54% compared to the results obtained by extraction with distilled water from the "B" which is due to a higher proportion of loosely bound Na+ ions for inorganic sites (carbonates).

**Table 3:** Mean values of the soil samples "A" for all three extraction agents used - shaking method

| Samples | ISO (mg/kg) | $CH_3COOH$ (mg/kg) | $H_2O$ (mg/kg) |
|---|---|---|---|
| A 1.1; A | 63.96±0.10 | 18.21±0.83 | 14.10±1.26 |
| A 2.1; A | 56.19±1.18 | 16.47±0.70 | 13.14±0.39 |
| A 3.1; A | 52.76±1.18 | 14.77±1.85 | 12.29±2.40 |
| A 4.1; A | 46.35±3.36 | 15.37±2.95 | 12.58±3.29 |
| A 5.1; A | 47.42±2.13 | 16.30±1.62 | 13.45±1.49 |
| A 6.1; A | 60.73±2.51 | 17.93±1.33 | 15.20±0.84 |
| A 7.1; A | 50.18±3.88 | 15.47±1.82 | 12.71±1.71 |
| A 8.1; A | 59.06±2.75 | 18.59±1.87 | 13.52±0.74 |
| A 9.1; A | 66.55±3.34 | 18.38±1.89 | 14.55±1.61 |
| A 10.1; A | 56.85±1.25 | 16.49±2.44 | 14.06±0.52 |

**Table 4**: Mean values of the soil samples "B" for all three extraction agents used - shaking method

| Samples | ISO (mg/kg) | $CH_3COOH$ (mg/kg) | $H_2O$ (mg/kg) |
|---|---|---|---|
| B 1.1; B | 51.83±3.47 | 26.91±2.96 | 10.36±2.32 |
| B 2.1; B | 66.32±1.74 | 32.80±2.76 | 15.58±1.68 |
| B 3.1; B | 61.32±1.85 | 26.21±2.82 | 13.05±0.46 |
| B 4.1; B | 52.50±2.89 | 26.79±6.01 | 14.58±1.50 |
| B 5.1; B | 63.93±3.81 | 27.90±2.28 | 15.44±1.05 |
| B 6.1; B | 67.37±2.44 | 29.39±1.76 | 14.21±0.59 |
| B 7.1; B | 75.66±3.21 | 31.09±1.83 | 20.33±3.86 |
| B 8.1; B | 17.15±0.17 | 8.55±2.65 | 4.62±0.74 |
| B 9.1; B | 39.39±0.30 | 21.52±1.70 | 14.72±1.02 |
| B 10.1; B | 33.01±2.76 | 20.87±0.30 | 11.55±1.44 |

Comparing the values of Na content in the soil suspensions from "A" and "B" location in the case of distilled and acetic acid as an extraction agent, it is obvious that the soil from "B" location is richer in available forms of Na. This is in accordance with the fact that beef manure was used to fertilize the soil of the "B" location in the previous vegetation, and the number of sown crops was more modest compared to the soil from "A" location. Therefore, the soil from the "B" location remained richer in terms of available forms of Na, which can be extracted quite well with the green solvents used (distilled water and 5% $CH_3COOH$). Table 3 and 4 shows overall results of all 10 samples of the tested soil from the "A" and "B", respectively, for all three extraction agents used.

*Sodium concentrations extracted by various extraction agents - ultrasonic extraction*

Determination of Na concentration in the soil from "A" and "B" locations was also performed by applying ultrasound to soil extraction with three selected solvents (aqua regia, 5% $CH_3COOH$ and distilled water). The application of ultrasound was primarily aimed at controlling the pseudo-total Na content from the soil, and for 18 hours it can be extracted only by applying ultrasound to the same solvents for 2 hours. The obtained results are presented in Figure 2 as well as in Table 5 and 6.

The highest results (Figure 2a and 2b) were obtained with aqua regia, followed by 5% $CH_3COOH$ and distilled water, which is the same trend as in the case of shaking extraction. However, it can be noticed that significantly higher concentrations of Na were obtained by ultrasound in the tested soil, for all samples, and the difference is especially significant when aqua regia is used as a solvent.

Furthermore, using ultrasound to extract Na from soil samples with 5% $CH_3COOH$ and distilled water, it could be seen that the results for samples "A" were almost similar and close, regardless of the solvent. In the case of soil samples "B", the Na content using 5% $CH_3COOH$ and distilled water is more significant, due to the fact that there are more available forms of Na+ ion, as well as the fact that the soil was less sown. According to the presented results, with distilled water it is possible to extract 17%, while with 5% $CH_3COOH$ only 22% of its pseudo-total content in the soil from the "A" location, which is in the range of 153.3-285.6 mg/kg soil. The maximum standard deviations are 22.98, 4.79 and 6.28 mg/kg in the case of using aqua regia, 5% $CH_3COOH$ and distilled water, respectively.

Regarding the results of extractions of soil samples "B", the following intervals for sodium content are recorded, as follows: from 198.5-303.2 mg/kg; from 50.53-68.99 mg/kg and from 23.31-30.64 mg/kg when aqua regia, 5% $CH_3COOH$ and distilled water were used as extraction agent, respectively. In relation to the pseudo-total sodium content in the mentioned soil, 26% can be extracted with 5% acetic acid and 13% with distilled water. The maximum standard deviations are 27.56, 18.34 and 4.43 mg/kg for extraction carried out with aqua region, 5% $CH_3COOH$ and distilled water, respectively.

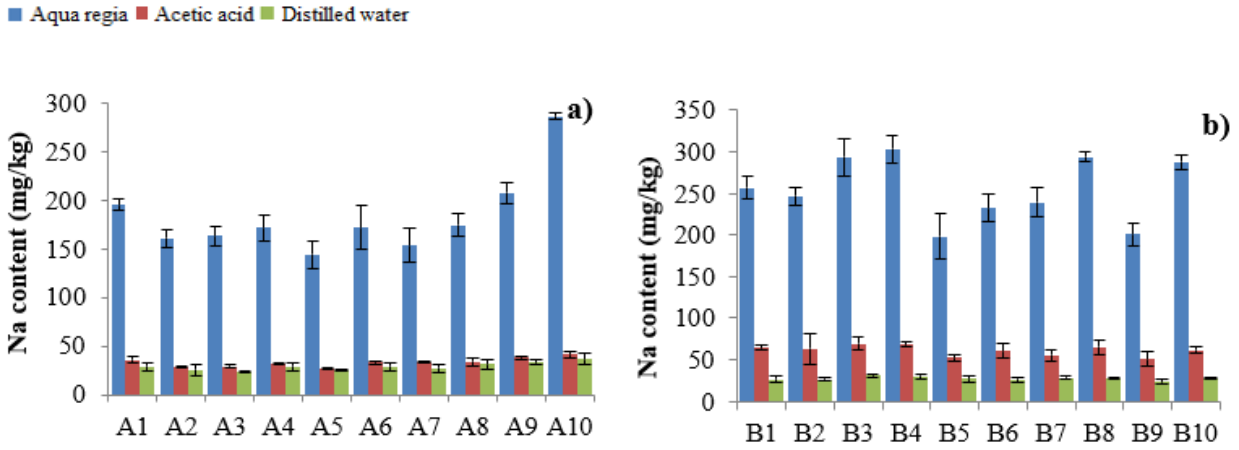


**Figure 2**: Comparative results of Na concentration (mg Na/kg of soil) in soil samples obtained using three different extraction agents assisted by the method of ultrasound for samples "A" (a) and "B" (b).

**Table 5:** Mean values of the soil samples "A" for all three extraction means used - application of the ultrasound method

| Samples | ISO (mg/kg) | $CH_3COOH$ (mg/kg) | $H_2O$ (mg/kg) |
|---|---|---|---|
| A 1.1; A 1.2 | 195.1±5.5 | 35.64±3.35 | 28.79±3.83 |
| A 2.1; A 2.2 | 160.4±8.4 | 28.27±0.69 | 25.18±5.19 |
| A 3.1; A 3.2 | 163.1±9.8 | 29.02±2.02 | 23.58±1.04 |
| A 4.1; A 4.2 | 171.2±13.2 | 31.68±0.66 | 29.01±4.09 |
| A 5.1; A 5.2 | 143.8±14.5 | 27.05±1.05 | 25.51±0.82 |
| A 6.1; A 6.2 | 171.7±23.0 | 32.80±1.27 | 28.62±4.10 |
| A 7.1; A 7.2 | 153.3±17.1 | 33.90±1.13 | 27.07±4.05 |
| A 8.1; A 8.2 | 174.3±11.7 | 33.57±4.79 | 31.19±5.34 |
| A 9.1; A 9.2 | 207.3±11.1 | 37.64±2.00 | 32.86±2.66 |
| A 10.1; A | 285.6±3.4 | 41.14±2.75 | 36.43±6.28 |

**Table 6:** Mean values of the soil samples "B" for all three extraction means used - application of the ultrasound method

| Samples | ISO (mg/kg) | $CH_3COOH$ (mg/kg) | $H_2O$ (mg/kg) |
|---|---|---|---|
| B 1.1; B 1.2 | 256.6±13.4 | 64.36±2.54 | 26.30±3.48 |
| B 2.1; B 2.2 | 247.2±22.4 | 63,33±18.34 | 26.55±1.10 |
| B 3.1; B 3.2 | 294.1±22.4 | 68.99±7.57 | 30.64±1.86 |
| B 4.1; B 4.2 | 303.2±17.2 | 68.59±4.18 | 30.00±2.76 |
| B 5.1; B 5.2 | 198.5±27.6 | 52.21±3.71 | 26.75±4.43 |
| B 6.1; B 6.2 | 232.0±16.3 | 60.41±8.47 | 25.75±3.43 |
| B 7.1; B 7.2 | 239.4±18.4 | 55.35±7.10 | 27.86±2.00 |
| B 8.1; B 8.2 | 294.2±6.2 | 64.30±8.36 | 28.54±0.94 |
| B 9.1; B 9.2 | 200.6±13.9 | 50.51±9.13 | 23.31±2.40 |
| B 10.1; B | 287.6±9.5 | 61.54±4.20 | 27.52±1.28 |

In the studies published on ultrasonic assisted extraction of metals, some controversial results on the behavior of metals during extraction have been reported. In the work of Väisänen and co-workers (2001) ultrasound-assisted extraction method and the method by reflux with aqua regia resulted in almost equal Ag, As, Cd, Cu, and Pb concentrations in soil.

Ultrasonic treatment can also cause the release of lower amounts of metal such as Ni in the exchangeable metal soil fraction in comparison to the conventional procedure. These results are probably due to the re-adsorption of metals on the surface of soil during the extraction step, which is enhanced by the application of ultrasound (Leśniewska, Krymska, Świerad et al., 2016). However, acid type and the concentration in the liquid extractant seems to be one of the most critical parameters affecting ultrasound leaching (Güngör and Elik, 2007) as well as the length of time and power used in sonication (Davidson and Delevoye, 2001).

*Correlation analysis of sodium content determined by different extraction agents*

*a) method of shaking*

To determine the correlation of Na content from soil samples of "A" and "B" locations with different extraction agents applying the shaking method the conclusion was made from the mean value of two parallels for all 10 subsamples of each of the tested soil. In all samples, the results of Na content in the soil obtained by extraction with 5% $CH_3COOH$ compared to the extraction with the aqua regia are significantly lower on average 70% for soil samples "A" and 50% for soil samples "B" (Table 3 and 4).

However, taking into account the comparative analysis for aqua regia and 5% $CH_3COOH$ (Figure 3a), there is a statistically very significant correlation, $r^2$=0.83 for the soil from "A" and $r^2$=0.94 for the soil from "B" location.

The obtained correlation values for both soil types indicate a high degree of correlation of numerical indicators of $Na^+$ ion content in the examined soil with different extraction agents, i.e. the increase in available forms of sodium is directly related to the increase in pseudo-total Na content in the soil. The relationship between the Na content in the soil and its water-soluble forms (extraction in distilled water) in relation to its pseudo-total content in is presented in Figure 3b. As in the previous case, the results of soil extraction with distilled water are significantly lower, on average 75% lower in the case of soil samples "A", than the results of soil extraction by aqua regia with a statistically slightly lower, but very significant positive correlation ($r^2$=0.74). The same interpretation can be considered for soil samples "B", where a statistically significant positive correlation was confirmed ($r^2$=0.83). Furthermore, due to similar results using 5% $CH_3COOH$ and distilled water for both soil samples a correlation analysis was performed for these two solvents to exclude an experimental error.

The obtained correlation analysis is shown in Figure 3c. Although the results of extraction with distilled water are slightly lower compared to the results of extraction with 5% $CH_3COOH$, a statistically very significant positive correlation was found for the soil samples "A" and "B" of $r^2$=0.80 and $r^2$=0.83, respectively, which excluded the experimental error. These data suggests that the tested soil has a chemical composition whose available forms of sodium are mostly used, so the increase in Na content with 5% $CH_3COOH$ is only about 20% higher for soil from "A" location. However, in terms of soil results from the "B" location, a slightly more positive effect of acetic acid on $Na^+$ ion extraction was observed since the obtained values were on average 50% higher compared to the extraction of the same soil with distilled water. This is in accordance with the fact that the soil examined from the "A" location was sampled after the soil was used for sowing, so it is poorer in the available forms of the determined metal.

*b) method of ultrasound*

The correlation analysis for the method of ultrasound and different extraction agents was carried out in the same way as by applying the shaking method of soil samples. The obtained correlation graphs are shown in Figure 4. Although the values of extractions along the aqua regia are 5.5 and 6 times higher for soil samples "A" and "B", respectively, compared to the results when 5% $CH_3COOH$ is used, in both cases a statistically significant positive correlation was obtained ($r^2$=0.87 soil "A" and $r^2$=0.90 soil "B").

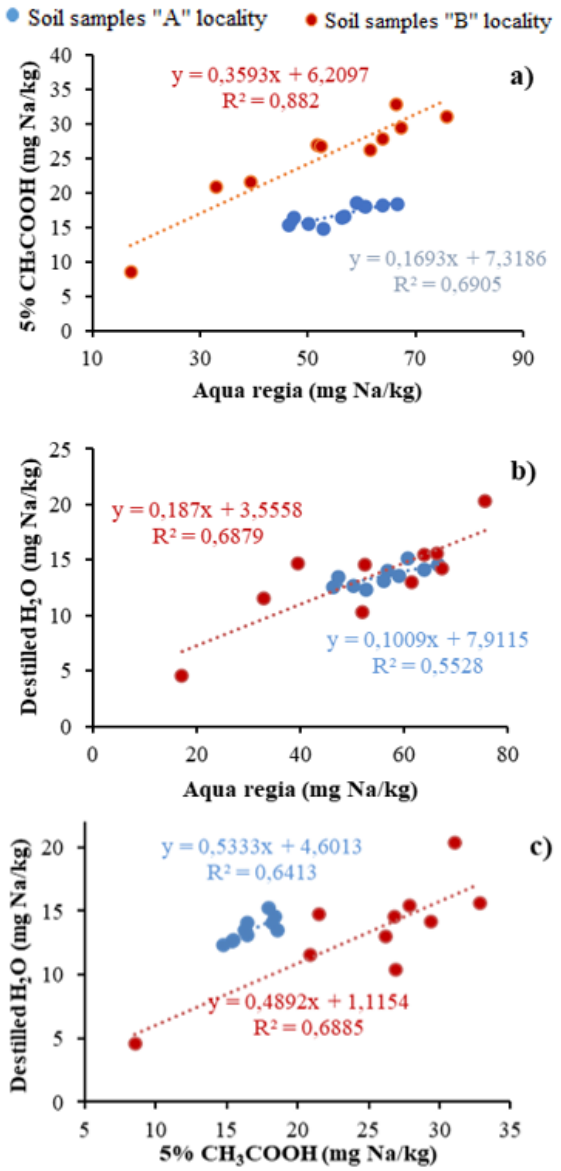


**Figure 3**: Correlation analysis of Na content (mg/kg of soil) obtained by extraction with aqua regia and 5% $CH_3COOH$ (3a); aqua regia and distilled water (3b); 5% $CH_3COOH$ and distilled water (3c) by shaking method.

According to the results shown in Figure 4a and 4b, it can be concluded that a significant positive statistical correlation was obtained, with $r^2$=0.86 for soil samples "A" and $r^2$=0.81 for soil samples "B". Since the results with $CH_3COOH$ and distilled $H_2O$ obtained by ultrasonic extraction do not differ significantly, a correlation analysis was applied and the results were shown in Figure 4c.

For soil samples of "A" location, with 5% $CH_3COOH$, on average, up to 13% higher results were obtained, which is up to 4.25 mg Na/kg of soil. However, in terms of correlation analysis, a significant positive statistical correlation can be stated since $r^2$=0.91, thereby rejecting an experimental error. Additionally, 5% acetic acid is not a strong enough extraction agent that even with ultrasonic waves is not able to significantly extract the more strongly bound forms in which sodium occurs.

Contrary wise 5% $CH_3COOH$ extracted on average 55% more sodium regarding to the distilled water as solvent from the samples of "B" location. However, in terms of correlation analysis, a slightly lower but still significant positive correlation was obtained with $r^2$=0.74.

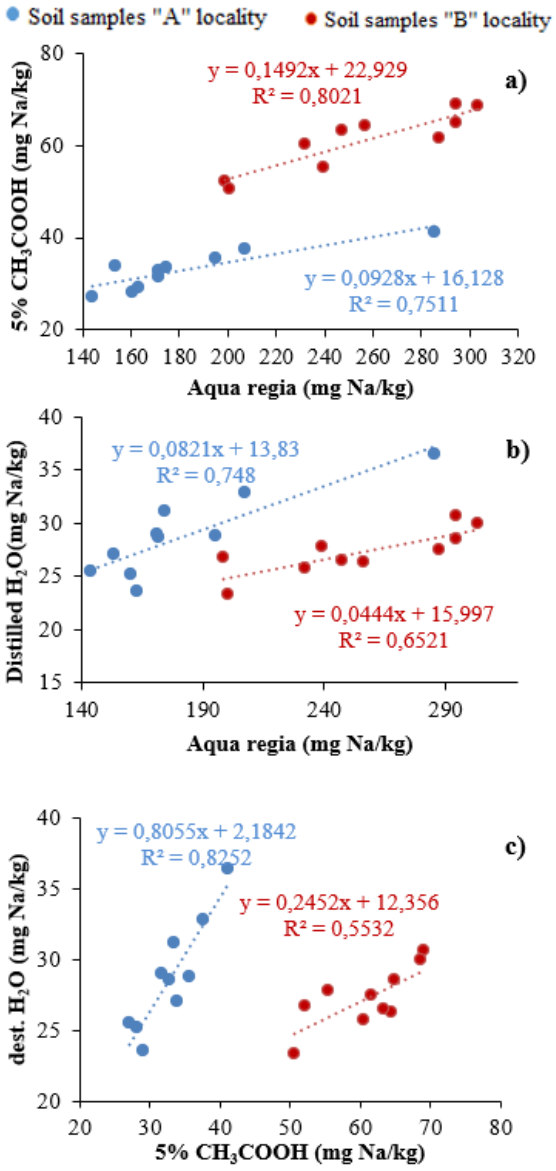


**Figure 4:** Correlation analysis of Na content (mg/kg of soil) obtained by extraction with aqua region and 5% $CH_3COOH$ (4a); aqua regia and distilled water (4b) 5% $CH_3COOH$ and distilled water (4c) by ultrasound method

From all the above, it can be concluded that the increase in the value of water-soluble forms of Na+ ion as well as its forms soluble in slightly acidic conditions, such as 5% $CH_3COOH$ is directly related to the increase of its pseudo-total content in soil. Also, a positive effect of 5% $CH_3COOH$ as a green solvent can be noted, as well as the influence of ultrasound on the extractability of $Na^+$ ions from the soil.

As reported by Chen and Ma (2001), the amount of trace element extracted by common digestion methods might depend on the element analyzed, its origin (anthropogenic or natural), soil properties and element mass fraction.

Comparison of sodium content obtained by different extraction methods

Figures 5-6 present comparative results of Na content in soil from the "A" and "B" location obtained with aqua regia, 5% $CH_3COOH$ and distilled water, using two extraction methods (shaking method and ultrasonic extraction). The extraction with aqua regia in the first case was performed according to the procedure BAS ISO 11466:1995, and not with shaking. The results are given as the mean of two determinations with a standard deviation of repeatability.

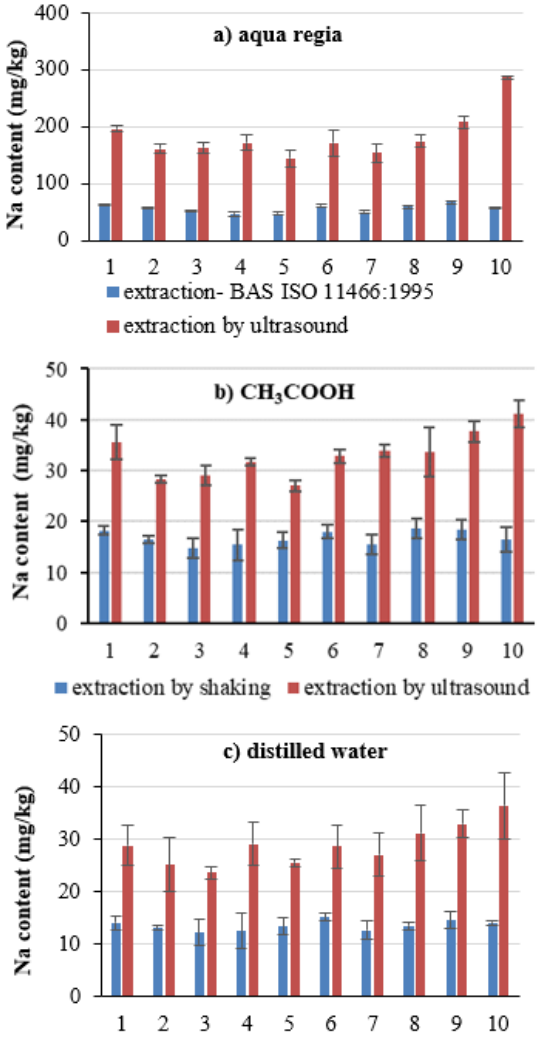


**Figure 5.** Comparative presentation of Na content (mg/kg of soil) obtained according to BAS ISO 11466: 1995 (or shaking method) and ultrasonic extraction with aqua regia (a); $CH_3COOH$ (b) and distilled water (c) for soil from the soil samples of "A" location.

The efficiency of ultrasound extraction was evaluated by comparing the results obtained using the ultrasonic method with the results of the standard BAS ISO method shown in Figure 5. Analyzing the obtained results, a positive effect of ultrasound on the extractability of $Na^+$ ions from soil samples can be found since the obtained results are on average 3 times higher (from 143.78 to 285.63 mgNa/kg of soil) than when extraction is performed without the use of ultrasound (from 46.35 to 66.55 mg Na/kg of soil). Also, an important factor is the duration of extraction, which using the BAS ISO method

without ultrasound lasted a full 18 hours, while using the same extraction agents with ultrasound, the extraction lasted only 2 hours. These data, therefore, favors the use of ultrasound to extract $Na_+$ ions from soil samples, as significantly higher results were achieved in a shorter time, and the use of ultrasound is considered a non-destructive method of sample preparation.

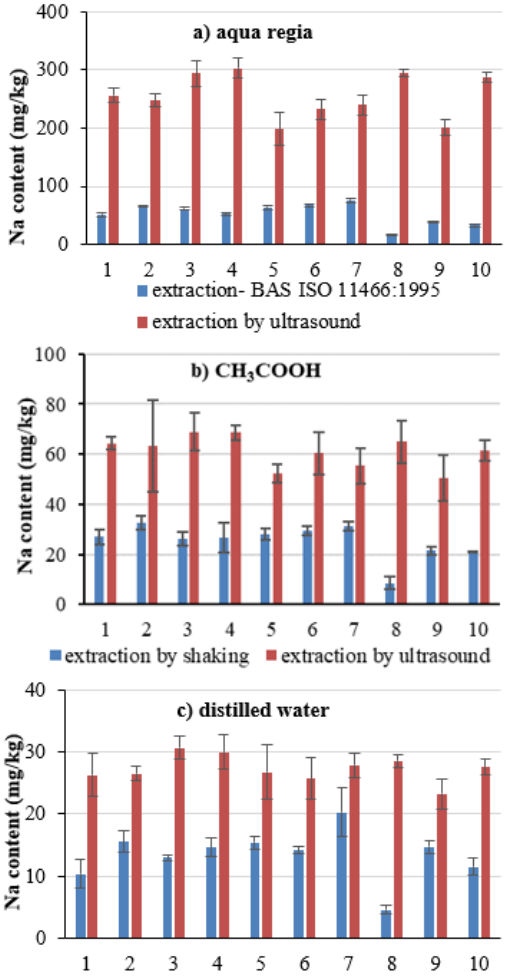


**Figure 6**: Comparative presentation of Na content (mg/kg of soil) obtained according to BAS ISO 11466: 1995 (or shaking method) and ultrasonic extraction with aqua regia (a); $CH_3COOH$ (b) and distilled water (c) for soil from the soil samples of "B" location.

Regarding soil samples "B" (Figure 6), where a higher proportion of soluble forms of Na was previously found, the application of ultrasound was more effective with the use of aqua regia, with the ultrasound/BAS ISO extractability ratio being 6 times higher on average.
According to the results, the ratio of Na content by shaking/ultrasound method with 5% $CH_3COOH$ as an extraction agent is 2, i.e. 3 times higher with ultrasound for soil from "A", i.e. "B" location, respectively. Furthermore, the ratio of Na content by the method of shaking/ultrasound with distilled water as extraction agent was 2, i.e. 2.5 times higher with ultrasound for soil from the location "A", i.e. "B" respectively.

Ultrasound can significantly improve the extraction efficiency mainly due to the effects caused by the cavitation phenomenon (Stanišić et al., 2011, Diehl et al., 2018), which is confirmed by this study. Since insufficient data could be found in the literature for the solubility of sodium ions from soil samples by ultrasonic methods, these results were very significant.

## CONCLUSION

The soil sample "A" belongs to the type of alluvial soil and was fertilized with burnt manure, while soil sample "B" belongs to the type of clay loam fertilized with beef manure. According to the average pH value in distilled water, the analyzed soil samples ("A" and "B") were classified as neutral and weakly acidic soils, while pH in $CaCl_2x2H_2O$ and electrical conductivity show more exchangeable ions for soil samples "B". Up to 25 % and 26% can be extracted with distilled water, while up to 34 % and 49% with 5 % $CH_3COOH$ by shaking samples in relation to the values of its pseudo-total content from soil samples "A" and "B", respectively. An increase in the value of water-soluble and available forms of sodium was found with an increase in the value of the pseudo-total sodium content in the soil, whereby correlation coefficients $r^2 \geq 0.74$ were obtained for all comparison models. Ultrasound yielded significantly higher Na concentrations for both analyzed soils compared to the shaking method, and the difference is especially significant when aqua regia is used as a solvent. Extraction with aqua regia and ultrasound gave results on average 3 times higher than when extraction is performed without the use of ultrasound for "A" soil samples and on average 6 times higher for soil samples "B". The content ratio of the ultrasonic/shaking method with 5% $CH_3COOH$ as extraction agent is 2 or 3 times higher for soil samples "A", i.e. "B", respectively.

In the case of distilled water as an extraction agent, the effect of ultrasound gave 2 and 2.5-times higher results for soil samples "A" and "B", respectively, compared to the method of shaking. In general, the application of ultrasound shows a positive effect on the extractability of $Na^+$ ions from soil samples "A" and "B" using green solvents (distilled water, 5% $CH_3COOH$) but also with the use of a strong extraction agent such as aqua regia. Therefore, the use of ultrasound is preferred in order to improve the extractability of $Na^+$ ions from soil samples, and, in addition, due to the fact that the use of ultrasound is considered a non-destructive method of sample preparation.

## REFERENCES

Acosta, J. A., Jansen, B., Kalbitz, K., Faz, A. and Martínez-Martínez, S. (2011). Salinity increases mobility of heavy metals in soils. Chemosphere, 85(8), 1318-1324.

BAS ISO 11466: 1995 (E). Soil quality — Extraction of trace elements soluble in aqua regia

BAS ISO 10390:2006 Soil quality — Determination of pH

Chen, M. and Ma, L. Q. (2001). Comparison of three aqua regia digestion methods for twenty Florida soils. Soil science society of America Journal, 65(2), 491-499.

Cui, Y. and Du, X. (2011). Soil heavy-metal speciation and wheat phytotoxicity in the vicinity of an abandoned lead–zinc mine in Shangyu City, eastern China. Environmental Earth Sciences, 62(2), 257-264.

Davidson, C. M. and Delevoye, G. (2001). Effect of ultrasonic agitation on the release of copper, iron, manganese and zinc from soil and sediment using the BCR three-stage sequential extraction. Journal of Environmental Monitoring, 3(4), 398-403.

Dočekalová H., Kovaříková V., Dočekal B. (2012). Mobility and bioaccessibility of trace metals in soils assessed by conventional extraction procedures and passive diffusive samplers. Chemical Speciation & Bioavailability 24(4), 261-5.

Du, P., Xue, N., Liu, L. and Li, F. (2008). Distribution of Cd, Pb, Zn and Cu and their chemical speciations in soils from a peri-smelter area in northeast China. Environmental geology, 55(1), 205-213.

Güngör, H. and Elik, A. D. İ. L. (2007). Comparison of ultrasound-assisted leaching with conventional and acid bomb digestion for determination of metals in sediment samples. Microchemical Journal, 86(1), 65-70.

Kanber, R., Unlu, M. (2010). Tarımda su ve toprak tuzluluğu. Cukurova Universitesi, Adana, Turkey.

Karadağ S., Eren E., Çetinkaya E., Özen S., Deveci S. (2016). Optimization of sodium extraction from soil by using a central composite design (CCD) and determination of soil sodium content by ion selective electrodes. Eurasian Journal of Soil Science, 5 (2), 89-96.

Kotoky, P., Bora, B. J., Baruah, N. K., Baruah, J., Baruah, P. and Borah, G. C. (2003). Chemical fractionation of heavy metals in soils around oil installations, Assam. Chemical Speciation & Bioavailability, 15(4), 115-126.

Leśniewska, B., Krymska, M., Świerad, E., Wiater, J. and Godlewska-Żyłkiewicz, B. (2016). An ultrasound-assisted procedure for fast screening of mobile fractions of Cd, Pb and Ni in soil. Insight into method optimization and validation. Environmental Science and Pollution Research, 23(24), 25093-25104.

Liang, S. X., Wang, X., Li, Z., Gao, N. and Sun, H. (2014). Fractionation of heavy metals in contaminated soils surrounding non-ferrous metals smelting area in the North China Plain. Chemical Speciation & Bioavailability, 26(1), 59-64.

Lutgens F. K., Tarbuck E. J. 2003. Foundations of earth science. Pearson, New Jersey.

Lutgens, F.K. and Tarbuck, E. J., 2011. Foundations of earth science. Upper Saddle River, Pearson, New Jersey.

Maathuis, F. J., Ahmad, I. and Patishtan, J. (2014). Regulation of Na+ fluxes in plants. Frontiers in plant science, 5, 467.

Minasny, B., McBratney, A. B., Brough, D. M. and Jacquier, D. (2011). Models relating soil pH measurements in water and calcium chloride that incorporate electrolyte concentration. European Journal of Soil Science, 62(5), 728-732.

Minkina T. M., Motuzova G. V., Mandzhieva S. S., Nazarenko O. G., Burachevskaya M. V., Antonenko E. M. (2013). Fractional and group composition of the Mn, Cr, Ni, and Cd compounds in the soils of technogenic landscapes in the impact zone of the Novocherkassk Power Station. The European Journal of Soil Science 46, 375–385.

Raymond A. W., Okieimen F. E. (2011). Heavy Metals in Contaminated Soils: A Review of Sources, Chemistry, Risks and Best Available Strategies for Remediation", International Scholarly Research Notices, Article ID 402647, 20

Sapčanin, A., Cakal, M., Jacimovic, Z. Pehlic, E., Gordanet J. (2017). Soil pollution fingerprints of children playgrounds in Sarajevo city, Bosnia and Herzegovina. Environ Science and Pollution Research 24, 10949–10954

Slukovskaya M. V., Kremenetskaya I. P., Drogobuzhskaya S. V, Novikov A. I. (2020). Sequential Extraction of Potentially Toxic Metals: Alteration of Method for Cu-Ni Polluted Peat Soil of Industrial Barren. Toxics, 8(2), 39.

Sintorini M. M., Widyatmoko H., Sinaga E. and Aliyah N. (2021). Effect of pH on metal mobility in the soil. The 5th International Seminar on Sustainable Urban Development, IOP Conf. Series: Earth and Environmental Science 737, 012071.

Sirsat M. S, Cernadas E., Fernández-Delgado M., Khan R. (2017). Classification of agricultural soil parameters in India. Computers and electronics in agriculture, 135, 269-79.

Stanišić, S., Ignjatović, L., Manojlović, D. and Dojčinović, B. (2011). The comparison of sample extraction procedures for the determination of cations in soil by IC and ICP-AES. Open Chemistry, 9(3), 481-491.

Sungur A., Soylak M., Ozcan H. (2014). Investigation of heavy metal mobility and availability by the BCR sequential extraction procedure: Relationship between soil properties and heavy metals availability. Chemical Speciation and Bioavailability, 26, 219–230.

Tessier A., Campbell P. G. C., Bisson M. (1979). Sequential extraction procedure for the speciation of particulate trace metals. Analytical Chemistry, 51, 844–851.

Väisänen, A., Suontamo, R., Silvonen, J. and Rintala, J., 2002. Ultrasound-assisted extraction in the determination of arsenic, cadmium, copper, lead, and silver in contaminated soil samples by inductively coupled plasma atomic emission spectrometry. Analytical and bioanalytical chemistry, 373(1), 93-97.

## Summary/Sažetak

U ovoj studiji analizirani su uzorci tla s dva odabrana mjesta: “A” (aluvijalno tlo) i “B” (glinena ilovača). Hemijska analiza uzoraka tla uključivala je: određivanje pH vrijednosti tla i provodljivosti tla. Dvije različite metode ekstrakcije: metoda treskanja i metoda ultrazvuka primijenjene su za ekstrakciju natrijevih iona iz tla s tri otapala (aqua regia, 5% $CH_3COOH$ i destilirana voda). Vrijednosti pseudo-ukupnog (ekstrahovano sa aqua regia) i bioraspoloživog sadržaja Na (ekstrahovanog sa 5% $CH_3COOH$ i destilovanom vodom) u uzorku tla "A" su u intervalu od 46,35-66,55 mg Na/kg; 14,77-18,59 mg Na/kg i 12,58-15,20 mg Na/kg tla, primjenom metode treskanja. Istom metodom, u slučaju uzorka tla „B“, intervali su 17,15-75,66 mg Na/kg; 20,87-32,80 mg Na/kg i 4,62-20,33 mg Na/kg tla, za ekstrakciju aqua regiom, 5% $CH_3COOH$, odnosno destiliranom vodom. Ekstrakcija ultrazvukom u svim slučajevima dala je bolje rezultate u odnosu na metodu treskanja. Općenito, primjena ultrazvuka pokazuje pozitivan efekat na ekstrakciju iona $Na^+$ iz uzoraka tla pomoću spomenutih otapala.

Glasnik hemičara i tehnologa Bosne i Hercegovine

Bulletin of the Chemists and Technologists of Bosnia and Herzegovina

2022

58

Print ISSN: 0367-4444
Online ISSN: 2232-7266

Original Scientific Article
DOI: https://doi.org/10.35666/2232-7266.2022.58.06
UDC: 542.943'78:577.112.34

19-32

# Synthesis, IR characterization and antioxidant capacity of Cu(II) complexes with amino acids and melatonin

**Ljubijankić, S.[a*], Galijaševic, S.[b], Davidović-Plavšić, B.[c], Balaban, M.[c], Ljubijankić, N.[d]**

[a]*Faculty of Health Studies, University of Bihać, Nositelja hrvatskog trolista 4, Bihać, Bosnia and Herzegovina*

[b]*Sarajevo School of Science and Technology, Sarajevo Medical School, Department of Medical Chemistry and Biochemistry, Hrasnička cesta 3b, Sarajevo, Bosnia and Herzegovina*

[c]*Faculty of Natural Sciences and Mathematics, University of Banja Luka, Mladena Stojanovića 2, Banja Luka, B&H*

[d]*Faculty of Science, Department of Chemistry, Zmaja od Bosne 33-35, Sarajevo, Bosnia and Herzegovina*

**Article info**
Received: 17/02/2022
Accepted: 12/04/2022

**Keywords:**
Copper(II) Chloride
Cu(II) Complexes
Amino Acid
Melatonin
FT-IR

*Corresponding author:
**Sead Ljubijankić**
E-mail: seadlj@gmail.com
Phone: +387 037 316 701

**Abstract:** In this paper, the reactions of anhydrous copper(II) chloride in methanolic solution with alanine, glycine, histidine, L-tryptophan, and melatonin were investigated and the resulting products were characterized by FTIR spectroscopy. Based on FTIR characterization, it was shown that these reaction conditions result in the formation of Cu(II) complexes with glycine and alanine, which are more complex structures than bis(glycinato) - and bis(alaninato) copper(II) complexes. Analysis of the FTIR spectrum of the histidine complex shows the participation of several groups in coordination at the Cu(II) center. The complex prepared with melatonin shows unusual changes in the spectral region of the amidic nitrogen bonds. The latter observation is very significant for very few known metal complexes of melatonin, while the synthesis of most of them is an experimentally demanding process with simultaneous control of several parameters. The antioxidant capacity of the synthesized complexes was examined, with the CEAC range from 121.6 to 734.4 μM. The lowest values of antioxidant capacity were recorded for the copper complex with tryptophan, while the highest values were recorded for the copper complex with alanine. A high antioxidant capacity of the copper complex with melatonin (673.8 μM) was also observed.

## INTRODUCTION

Due to the fact that copper is a biogenic element that performs most of its biological functions within coordination compounds with biomolecules in which, as donors of heteroatoms in the coordination sphere of the metal center, amino acids and their prosthetic groups often occur, there is a need to evaluate coordination behavior $Cu^{+}/Cu^{2+}$ according to individual, proteinogenic amino acids. Many reports were devoted to understanding the coordination characteristics of such complexes (Colaneri *et al*, 2009) especially copper(II) complexes with amino acids. Copper is an essential trace element used by both eukaryotic and prokaryotic cells in anabolic and catabolic processes with fine control of the same, given the fact that an excess of this element is associated with toxic effects. Roughly speaking, the essence of copper activity in biochemical processes is reflected in its redox behavior, especially because it can easily donate electrons to oxygen. This fact makes a certain element a potential generator of free radicals, which requires the establishment of a number of control mechanisms by the cell in order to use its reactivity to its advantage, while suppressing potential harmful effects. Therefore, the human body has established a number of biochemical processes that maintain copper homeostasis, along with homeostasis of iron, normal tissue proliferation and oxidative metabolism (Vest *et al*., 2012). Its sudden availability in the biosphere and biologically acceptable redox potential have made

copper an essential component of oxidative metabolism (Scheiber, Dringen & Mercer, 2013). Rigorous control of copper metabolism takes place in order to prevent undesirable, copper-mediated redox processes that would ultimately create reactive oxygen species given the ease of Cu (I) / (II) conversion. Since metabolic processes involving copper have many unresolved metabolites and metabolic pathways (as well as their control), it was useful to study the coordination behavior of this biometal towards selected biomolecules under controlled conditions by the preparation and characterization of appropriate complexes. The most simple biomolecules normally present in the cell cytoplasm, i.e. the environment where copper is metabolized, are amino acids, which made them a logical starting point for studying the behavior and coordination preferences of copper in biological systems. Given the structure of proteins as important building blocks and functional components of living cells, it is certain that the potential binding of copperin one of its two oxidative states will depend on all levels of protein structure with which it interacts and on physicochemical characteristics of the cellular environment. in which the interactions take place and the product is created (Dos Santos Carvalho & Fernandes, 2019). Copper(II) complexes with amino acids have long been known, and represent a special area of interest in the coordination chemistry of this element precisely because they serve as models for the study of copper metalloproteins. In this context, the behavior of Cu(II) in aquatic systems towards histidine is particularly interesting. It has been observed that most copper binding domains of proteins are rich in this amino acid, which is consistent with the coordination preferences of copper in the +2 oxidation side towards N donor ligands. The copper(II) complex with the simplest amino acid, glycine, was prepared in 1841. by Boussingault (Delf, *et al*). It was later shown that this type of complex does not belong to conventional copper complexes precisely because of the properties of the given ligands, i.e. amino acids. Since amino acids have a larger number of potential donor atoms, the structure of the final complex certainly depends on the reaction conditions, i.e. the nature of the solvent, temperature, pH and counterion, as is the case in a living cell. Oxidative stress occurs due to an imbalance between oxidants and antioxidants in biological systems, and is caused by excessive formation of reactive oxygen species or improper functioning of the antioxidant system (Chiurchiu *et al*., 2016). Reactive oxygen species (ROS), although possessing physiological functions, have been implicated in the pathogenesis of a number of diseases including cardiovascular and neurogenerative diseases, muscular dysfunction, and cancer (Zuo *et al*., 2015; He and Zuo, 2015). In addition to the many physiological effects of melatonin, melatonin has been shown to have strong anti-oxidant properties, due to the fact that it reacts with free radicals giving other metabolites that also have a neutralizing effect on free radicals. In this way, the product of one reaction, becomes a reactant of the other in both cases consuming free radicals. Melatonin, as well as its reaction products with hydroxyl radicals, are not extremely effective in neutralizing hydroperoxyl radicals, but still suppress lipid peroxidation in vivo, most likely by eliminating the initial hydroxyl radicals (Galano *et al*., 2014). In the last two decades, complexes of platinum, ruthenium, copper, cobalt and other metals have been used to modify and / or detect Aβ aggregation. The results of these studies suggest that metal complexes have promising potential in the treatment and diagnosis of Alzheimer's disease (Liu and Wang, 2018). Copper plays a significant role in the pathology of many neurodegenerative diseases, from Wilson and Menkes disease, through amyotrophic lateral sclerosis and Alzheimer's disease, to prion-associated diseases (Waggoner *et al,* 1999*).* Most of these diseases, directly or indirectly, lead to changes in copper metabolism. Changes in copper metabolism can lead to its accumulation in certain regions of the body or change its bioavailability in the cellular environment. Both are associated with increased oxidative stress and the formation of ROS, of course, due to the well-known redox behavior of copper, which the body significantly utilizes under homeostatic conditions (Waggoner *et al*., 1999). Given the nature of melatonin as a scavenger of destructive radicals and the consequent formation of metabolites of good chelating power for Cu (Galano *et al*., 2014) through the *scavenger cascade* of melatonin, it was interesting to examine the effect of melatonin as a potential inhibitor of Cu-protein complex species formation. Research conducted to determine the role of melatonin as a Cu(II) chelator in preventing its degrading effect on DNA (Wang *et al.*, 2019) has concluded that the copper-detoxifying and antioxidant abilities of melatonin are not based solely on scavenger abilities against hydroxyl radicals which occur in Cu(II)/Cu(I) mediated reactions, but strongly suggest the role of melatonin or its metabolites (formed by the scavenger cascade) as chelators. The final evidence lacking for unequivocal confirmation of these assumptions is the synthesis, isolation, and structural characterization of such complex types of melatonin, its metabolites, and copper.

## EXPERIMENTAL

### *Materials and methods*

All chemicals used were commercially available with analytical grade of purity and used without further purification. Infrared spectra were recorded as KBr pellets on a Perkin Elmer spectrum BX FTIR System in

region 4000 – 400 $cm^{-1}$, resolution 2$cm^{-1}$, 8 scenes. The antioxidant activity was determined using the e-BioQuChem (e-BCQ) lab device, following the manufacturer's instruction manual. The results are expressed in μC or in the charge of the electrons released by the antioxidant to neutralize free radicals. This device makes it possible to distinguish fast-acting antioxidants such as ascorbic acid and coenzyme Q10 from co-producing antioxidants such as polyphenols, astaxanthin or α-lipoic acid. Fast-acting antioxidants are the first to be oxidized and are considered to be more potent antioxidants than general antioxidants even though they are present in lower concentrations. Total antioxidant capacity (QT) is obtained as the sum of the antioxidant capacity of the fast-acting (Q1) and co-producing antioxidants (Q2). The results of antioxidant capacity were also expressed in ascorbic acid equivalents (CEAC), for which it was necessary to construct a calibration curve. For this purpose, a dilution series of a solution of ascorbic acid standard in 0.1 M PBS buffer (pH = 7) was prepared in the concentration range 0 - 1000 μM.

***Synthesis of complexes***

All complexes were synthesized by heating the reaction mixture to 65ºC on a magnetic stirrer, under reflux for 5 to 9 hours. Immediately before the syntheses, anhydrous copper(II) chloride ($CuCl_2$) was prepared by drying copper(II) chloride dihydrate ($CuCl_2 \times 2H_2O$) at 120ºC for 2 hours. This drying gave anhydrous $CuCl_2$, which was observed by changing the color from blue, copper(II) chloride dihydrate to brown colored, anhydrous copper(II) chloride. For the synthesis of each complex, solutions of copper(II) chloride in methanol were prepared by dissolving 268.9 mg (0.002 mol) of anhydrous $CuCl_2$ in 40 mL of methanol preheated to 50ºC.

***Synthesis of Cu(II) complex with alanine***

In 40 mL of methanol previously heated to 50ºC, 356.36 mg (0.004 mol) of alanine were dissolved and a previously prepared solution of copper(II) chloride was added to the solution. After mixing, the solution was stirred a magnetic stirrer at 65ºC under reflux for about 5 hours. Immediately after mixing the solution, the reaction mixture showed light green color. After three hours of heating, the color of the mixture turned dark green and did not change until the end of the synthesis. After cooling, the reaction mixture was filtered and the crystals of the complex were washed with water and ether. Finally, the complex was recrystallized from dimethylsufoxide/water and dried in a vacuum desiccator.

***Synthesis of Cu(II) complex with glycine***

The amount of 303.30 mg (0.004 mol) of glycine was dissolved in 40 mL of methanol preheated to 50ºC, and the previously prepared copper(II) chloride solution was added to the solution. The reaction mixture was heated with a magnetic stirrer at 65ºC under reflux for about 5 hours. Immediately after mixing the solution, the reaction mixture had a light blue color which eventually turned a slightly darker shade of blue. The mixture was cooled and left at room temperature for 24 hours. The blue crystals of the resulting complex were then filtered and washed with water and ether, recrystallized from dimethylsufoxide/water and dried in a vacuum desiccator.

***Synthesis of Cu(II) complex with histidine***

To 620.62 mg (0.004 mol) of histidine was added 40 mL of methanol preheated to 50ºC. To the resulting solution was then added a previously prepared solution of copper(II) chloride. During the reaction, the color of the reaction mixture changed from light green-blue at the beginning to dark purple-blue at the end of the synthesis. After cooling and filtering the mixture, the crystals of the complex were washed with water and ether, recrystallized from dimethylsulfoxide/water and dried in a vacuum desiccator.

***Synthesis of Cu(II) complex with L-tryptophan***

For synthesis, 816.92 mg (0.004 mol) of L-tryptophan were weighed and dissolved in 50 mL of methanol heated to about 50ºC. $CuCl_2$ solution was added dropwise to the resulting solution with continuous stirring. The mixture was heated at 65ºC on a magnetic stirrer under reflux for 5 hours. After the end of the synthesis, the copper(II) complex with L-tryptophan was deposited in the form of a powdery substance of dark brown-blue color. The reaction mixture was filtered and the complex washed with hot water to eliminate chlorides, recrystallized from dimethylsulfoxide/water and dried on filter paper in a vacuum desiccator.

***Synthesis of Cu(II) complex with melatonin***

For the synthesis, 929.11 mg (0.004 mol) of melatonin was dissolved in 40 mL of methanol heated to 50°C. A previously prepared solution of copper(II) chloride was added to the resulting solution. Immediately after mixing, the reaction mixture turned greenish brown. The mixture was heated to 65°C while stirring with a magnetic stirrer under reflux for 9 hours. During the synthesis, the color of the mixture changed, to eventually become dark brown, which did not change until the end of the synthesis. After cooling and filtering the mixture, the crystals of the complex were washed with water and petroleum ether, recrystallized from dimethylsufoxide/water and dried in a vacuum desiccator.

## RESULTS AND DISCUSSION

All complexes were synthesized by the reaction of methanolic solutions of $CuCl_2$ and the corresponding amino acids (alanine, glycine, histidine and tryptophan), and melatonin, at 65°C under reflux for 5 to 9 hours.

***FTIR spectra of amino acids and melatonin***

The FTIR spectra of all amino acids show vibrations typical of the carboxyl group, whose displacements in different amino acids are attributed to its protonated or deprotonated form. The asymmetric stretching of the carboxyl group in the given amino acids occurs at about 1600 $cm^{-1}$ and is extremely important for determining the performance and type of coordination in Cu-complexes. The area above 3000 $cm^{-1}$ is not of special importance for free amino acids, but it becomes more important for their Cu-complexes. Vibrations in the amino acid and melatonin spectra in the range of 2000 to 2800 $cm^{-1}$ are not of particular importance in determining subsequent coordination at the metal center. Extremely significant vibrations in the spectra of amino acids, but also the metal complexes is that attributed to the amino group in either protonated or deprotonated form. These bands are found in alanine at about 1590, 1520 and 1230 $cm^{-1}$. Indispensable are the vibrations of the hydrocarbon skeleton that occur at about 1000 $cm^{-1}$ depending on the type of amino acid, as well as those attributed to the aromatic fragment of the molecule in the case of histidine, tryptophan and melatonin. Vibrations of C-H bonds for the aliphatic part of the molecule occur below 3000 to 2900 $cm^{-1}$, while for the aromatic part of the molecule they occur above 3000 $cm^{-1}$ to 3100 $cm^{-1}$ and are clearly visible in the spectra of histidine, tryptophane and melatonin. The expected deviations in spectral characteristics in relation to amino acids show melatonin as a typical amine where this functionality is shown at about 3280 $cm^{-1}$ and at 1490 $cm^{-1}$, while the indole functionality is found at 3305 $cm^{-1}$ and 1270 $cm^{-1}$, respectively. Other bands in the ligand spectra have a more specific character.

***FTIR spectra of Cu(II) complexes***

Copper spectra with amino acids and melatonin show typical low-band bands attributed to metal-ligand vibrations and are of great importance for determining the coordination type and potential geometry of the complex. As copper(II) chloride was used as the starting substance, the retention of chloride in the coordination sphere in the final complex is not excluded. The previously mentioned typical vibrations of amino acids and melatonin, which now play the role of ligands, show typical shifts that indicate a model of coordination at the Cu(II) center. A typical phenomenon after coordination is the abolition of individual bands or the abolition of degenerate vibrational modes. A typical, spectrally noticeable change shown by a coordinated carboxyl group is the appearance of a band corresponding to the C=O bond as well as a band corresponding to the C-O bond, which indicates the abolition of resonance in the uncoordinated carboxyl group, i.e. its participation in coordination to the metal center. An additional change in relation to the spectra of free ligands is often the deprotonation of the amino group due to its coordination, which is observed by the abolition of bands typical of the - $NH_3$ group and the appearance of bands typical of the - $NH_2$ group. Skeletal vibrations do not suffer significant displacements or their bands are canceled if a certain vibration mode becomes impossible after coordination with the metal center, which is also important data. Other bands in the spectra of the complex have a more specific character and are described in detail for each individual complex.

***FTIR characterization of Cu - alanine complex***

It is known that the reaction of copper(II) acetate, as a salt of a weak organic acid, with alanine in adequate solvents and with good pH control creates bis(alaninato) copper(II) complex which occurs in two geometric isomers, ie *trans*-bis alaninate) copper(II) monohydrate and *cis*-bis(alaninato) copper(II) monohydrate. The difference between these two isomers can be easily determined by IR spectroscopy, with vibrations in the spectral range of 750 to 200 $cm^{-1}$ bei considered relevant. The *trans* isomer generally shows fewer bands in said region as well as *trans*-bis(glycinato) copper(II). In essence, metal-ligand vibrations may be sufficient to perform this distinction (Herlinger, Wenhold, & Long, 1970) where vas (Cu-N) vibration occurs as a weak band at 484 $cm^{-1}$ in the case of the trans isomer, while the cis isomer shows vas (Cu-N) at 483 $cm^{-1}$ and *v*s (Cu-N) at 411 $cm^{-1}$. In the case of the prepared Cu complex with alanine *v* (Cu-N) vibration is observed at 472 $cm^{-1}$, which is not correlated with typical bis(alaninato) copper(II) complexes. A wide band in the spectrum of the complex at about 3429 $cm^{-1}$ as well as an intense band at 1637 $cm^{-1}$ are used to detect crystal bound water, the former being attributed to vibrations of O-H bond stretching water molecules and the latter to their symmetric deformation (Nakamoto, 2009). Bands in the range 3297 - 3140 $cm^{-1}$ were attributed to the (N-H) vibrations of the coordinated amino group. These bands are more visible in the complex in relation to the vibrations of the same bond of the protonated amino group in the ligand. The deformation vibration of this group is in the vicinity of the band for C=O bonding and deformation of water molecules, and has a peak at 1598 $cm^{-1}$ (Han, 2010). Vibration of the protonated amino group, i.e. $v_r$ ($NH_3^+$), is not present in the spectrum of the complex, and has been replaced by "*rocking*" and "*wagging*" vibrations of the coordinated amino group at 1150 $cm^{-1}$ and 1022 $cm^{-1}$ (Nakamoto, 2009) the intense band at 666 $cm^{-1}$ also attributes the "*rocking*" vibration

to this group. The band at 1578 $cm^{-1}$ corresponds to the vibration of the *v*(C=O) coordinated carboxyl group, while the *v*(C-O) vibration occurs at 1396 $cm^{-1}$. Resonance of the carboxyl group is reflected in the alanine spectrum by the $\nu_{as}$ ($COO^-$) vibration at 1624 $cm^{-1}$. This band is not present in the spectrum of the complex, which confirms coordination through the carboxyl group. The bands corresponding to the in-pane or "*out-of-plane*" vibrations of the carboxyl group at 850 $cm^{-1}$ and 650 $cm^{-1}$, as well as the deformation at 772 $cm^{-1}$ disappear in the spectrum of the complex and are replaced by "*rocking*" or wagging by vibrations of a coordinated carboxyl group at 530 $cm^{-1}$ and 624 $cm^{-1}$ as much less intense bands (Herlinger, Wenhold and Long, 1970). Bands whose positions and intensities have little or no change in the spectrum of alanine and the respective complex originate mostly from C-H vibrations and deformations of alkyl groups. Namely, the bands at 2927 $cm^{-1}$ and 2856 $cm^{-1}$ in the spectrum of the complex were attributed to the (C-H) vibrations of the methyl and (CH) groups (Garcia *et al.*, 2008). The band at 1113 $cm^{-1}$ attributed to $\nu_{as}$ (C-C) $^+$ ρ ($NH_3$ $^+$), which is in a complex of lower intensity and occurs 1116 $cm^{-1}$, reflects a higher proportion of C-C vibration. Bands of symmetrical and asymmetric deformation of the methyl group in the prepared complex 1366 cm-1 and 1460 cm-1 occur, almost unchanged, relative to the ligand. Bands corresponding to free vibrations of the C-C-N skeleton do not appear in the spectrum of the complex, which is a consequence of coordination through N atoms (Nakamoto, 2009).

**Table 1:** Characteristic vibrations of Cu(II) alanine complex

| Characteristic vibrations of Cu-glycine | Wave number of vibration, ν ($cm^{-1}$) |
|---|---|
| $\nu(O–H)H_2O$ | 3464 b |
| $\delta_s(H_2O)$ | 1640 s |
| $\nu(N–H)NH_2$ | 3356 – 3250 m, b |
| $\nu(C–H)$ | 2984 – 2924 w – m |
| $\delta(NH_2)$ | 1602 s |
| $\nu(C=O)$ | 1578 s |
| $\delta_s(NH_3^+)$ | – |
| $\delta_s(CH_2)$ | 1444 s |
| $\nu(C – O)$ | 1408 s |
| $\rho_w(CH_2)$ | 1338 m |
| $\nu_r(NH_3^+)$ | – |
| $\rho_r(NH_2)$ | 1101 m-s |
| $\rho_w(NH_2)$ | 1060 m |
| $\nu_{as}(C–C–N)$ | – |
| $\rho_r(CH_2)$ | 916 w |
| $\nu_s(C–C–N)$ | – |
| $\rho_w(COO^-)$ | – |
| $\delta(C=O)$ | 742 w |
| $\pi(C=O)$ | 608 m |
| $\nu(Cu–N)$ | 486 m |

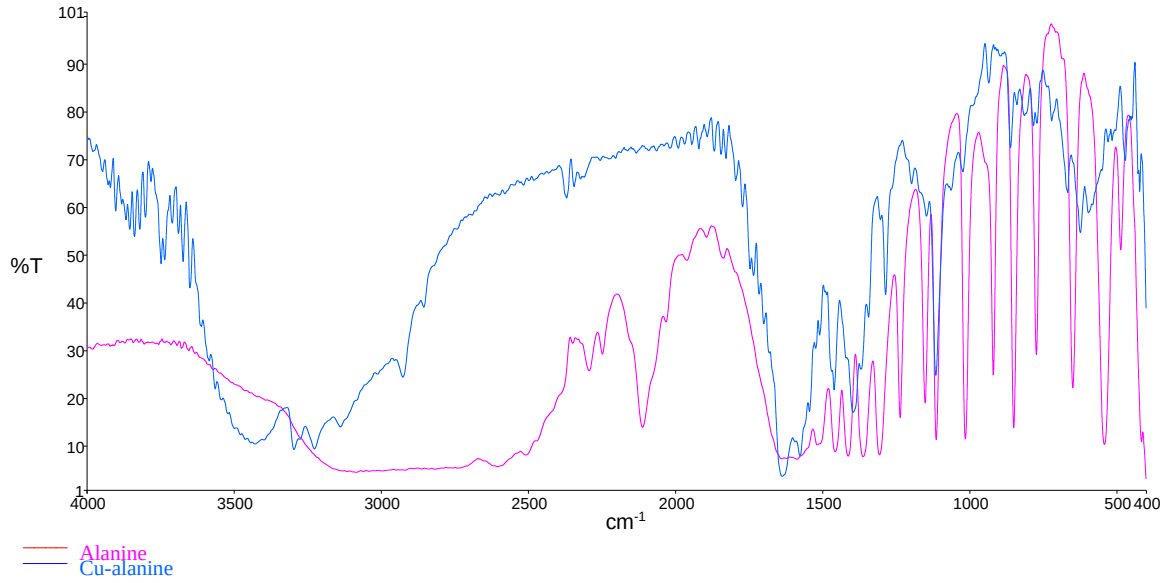


**Figure 1**: Comparative FT-IR spectra of alanine and Cu- alanine complex

***FTIR characterization of Cu - glycine complex***

It is known that the reaction of copper(II) acetate, as a salt of a weak organic acid, with glycine in adequate solvents and with good pH control creates bis (glycinato) copper(II) complex which occurs in two geometric isomers, ie trans-bis glycinato) copper(II) dihydrate and cis-bis (glycinato) copper(II) monohydrate. IR spectroscopy can easily determine the true difference between these two isomers, with vibrations in the spectral range of 750 to 200 $cm^{-1}$ being considered relevant. Having greater symmetry, the trans isomer generally shows fewer bands in said region. In essence, metal-ligand vibrations may be sufficient to perform this distinction (Herlinger, Wenhold and Long, 1970) where *v*(Cu-N) vibration occurs as a weak band at 477 $cm^{-1}$ in the case of the trans isomer, while the cis isomer shows vas (Cu-N) at 471 $cm^{-1}$ and vs (Cu-N) at 454 $cm^{-1}$. In the case of the prepared Cu complex with glycine *v*(Cu-N) vibration is observed at 486 $cm^{-1}$, which is not correlated with typical bis (glycinato) copper(II) complexes. A wide band in the spectrum of the complex at about 3464 $cm^{-1}$ with an intense band at 1640 $cm^{-1}$ is used to prove crystal bound water where the former is attributed to vibrations of stretching O-H bonds of water molecules and the latter to their symmetric deformation (Nakamoto, 2009) . The bands at 3169 $cm^{-1}$ in the glycine spectrum attributed to the (N-H) protonated amino group were replaced by bands in the range of 3356 - 3250 $cm^{-1}$, which are attributed to the (N-H) vibrations of the coordinated amino group. These vibrations for *trans*-bis (glycinato) copper(II) dihydrate occur in the range of 3320 - 3260 $cm^{-1}$, which does not correlate with the bands of the synthesized Cu-glycine complex, which is therefore more complex than simple bis (glycinato) copper (II) complex. The band at 1578 $cm^{-1}$ corresponds to the *v*(C = O) coordinated carboxyl group, while the *v*(C - O) vibration occurs at 1408 $cm^{-1}$, which confirms the coordination of the carboxyl group, as well as the resonance that occurs in the glycine spectrum by vibration at 1612 $cm^{-1}$ which is not present in the spectrum of the complex. The bands corresponding to the "rocking" or "wagging" vibrations of the carboxyl group at 508 $cm^{-1}$ and 698 $cm^{-1}$, as well as the deformation at 610 $cm^{-1}$, disappear in the spectrum of the complex and are replaced by much less intense vibration bands of the coordinated carboxyl group, at 742 $cm^{-1}$ and 608 $cm^{-1}$ (Inomata *et al*., 1988). Bands whose positions and intensities have little or no change in the spectrum of glycine and its complex originate mostly from C - H vibrations and deformations of the $CH_2$ group.

Namely, bands in the range of 3000 to 2900 $cm^{-1}$ appear in both the ligand and the complex, and are attributed to *v*(C-H) vibrations. There is a band "wagging" vibrations of the $CH_2$ group at about 1337 $cm^{-1}$ practically unchanged position in both substances, but much lower intensity in the complex. This change in intensity can be related to electronic changes due to coordination on the charged metal center. The same can be concluded for the "wagging" vibration of the $CH_2$ group, which was shifted from 910 $cm^{-1}$ in the ligand to 916 $cm^{-1}$ in the complex, and significantly reduced in intensity. It is clear that coordination limits the ease of development of certain types of vibrations (especially deformation vibrations and torsional vibrations), which is combined with electrostatic interactions in the crystal lattice of a complex joint and may justify small changes in band positions reflecting vibrations. such as the $CH_2$ group of glycine (Nakamoto, 2009).

**Table 2**. Characteristic vibrations of Cu(II)-glycine complex

| **Characteristic vibrations of Cu-alanine** | **Wave number of vibration, *v* ($cm^{-1}$)** |
|---|---|
| $v(O–H)H_2O$ | *3429 b* |
| $\delta_s(H_2O)$ | *1637 s* |
| $v(N–H)NH_2$ | *3297 – 3140 m, b* |
| $v(C–H)$ | *2927, 2856 w – m* |
| $\delta(NH_2)$ | *1598 m* |
| $v(C=O)$ | *1578 s* |
| $\delta_{as}(CH_3)$ | *1460 s* |
| $\delta_s(NH_3^+)$ | – |
| $\delta_s(CH_3)$ | *1366 s* |
| $v(C–O)$ | *1396 s* |
| $v_{as}(C–C)$ | *1116 m* |
| $v_r(NH_3^+)$ | – |
| $\rho_r(NH_2)$ | *1150 w* |
| $\rho_w(NH_2)$ | *1022 w* |
| $\delta(COO^-)$ | *784, 722 w* |
| $\rho_r(NH_2)$ | *666 m* |
| $\rho_w(COO^-)$ | *624 m* |
| $\rho_r(COO^-)$ | *530 w* |
| $v(Cu – N)$ | *472 m* |

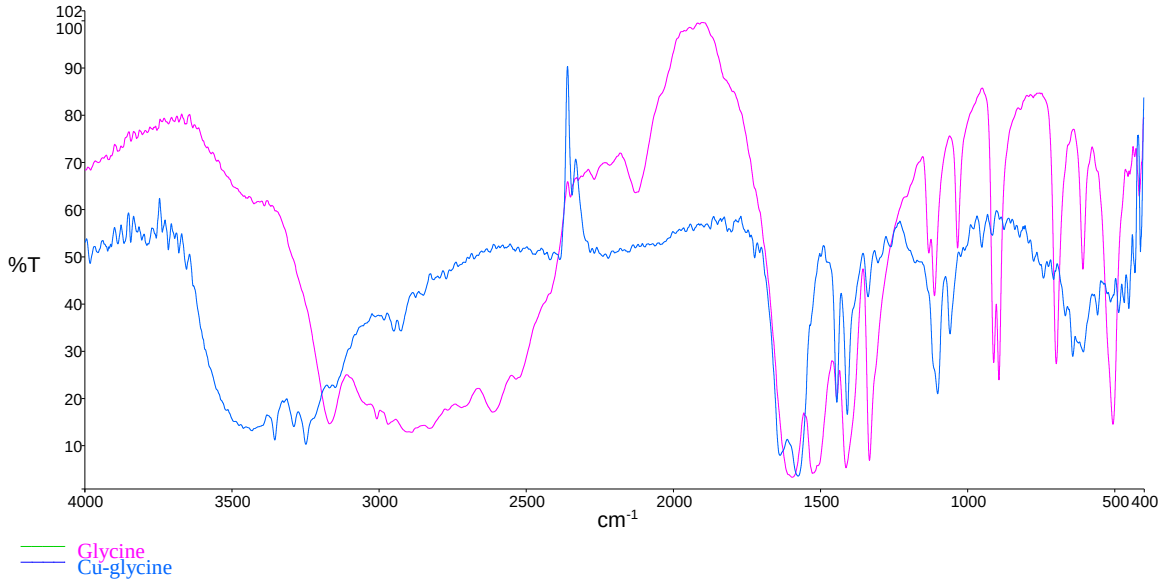


**Figure 2**: Comparative FT-IR spectra of glycine and Cu- glycine complex

**FTIR characterization of Cu - histidine complex**

In terms of coordination chemistry, histidine has been described as a rather complex ligand. Due to the large number of adequately positioned donor atoms, histidine as a ligand can build various complicated complexes with metals that prefer N donor ligands, such as Cu(II). Kruck and Sarkar (1973) described at least six different coordination forms in the Cu(II) histidine system where histidine always occurs as an O, N donor. The N donor atom may come from the amino group of the aliphatic chain or the N atom of the imidazole ring carrying a free electron pair. In the spectrum of the complex at 418 $cm^{-1}$, the band attributed by Drodżewski and Kordon (2000) to *ν*(Cu-N) occurs when the N atom originates from the amino ($NH_2$) group and the assumption was confirmed by isotopic derivatization. This, however, does not exclude the occurrence of histidine as a Nimidazole donor, but only confirms that histidine also acts as an N ($NH_2$) donor in the prepared complex. Coordination to the Cu(II) center via the amino group is supported by changes in other bands, fully or partially attributed to the vibrations of this group in free histidine. Namely, the band attributed to the "scissoring" vibration of the amino group at about 1632 $cm^{-1}$ was moved to 1625 $cm^{-1}$, while the band attributed to *ρw*($NH_2$) at 925 $cm^{-1}$ in the spectrum of the complex disappears. The amino group vibration "rocking" band combined with other histidine vibrations is present at 827 $cm^{-1}$, but expanded and drastically less intense, which also suggests coordination across the amino group (Nakamoto, 2009). The intense band attributed to the combined deformation of the N-H and C-H bonds of the imidazole fragment of the molecule in the histidine spectrum disappears in the spectrum of the complex, which may indicate the participation of the imidazole fragment in coordination with the Cu(II) center. More definite evidence would be found in Cu-Nimidaz. which occurs at about 280 $cm^{-1}$ (Drożdżewski and Kordon, 2000) which is beyond the scope of the performed recordings. The band carrying the highest proportion of carboxyl group vibrations, with a smaller proportion of other histidine vibration modes, was shifted from 1796 $cm^{-1}$ from the ligand spectrum to 1740 $cm^{-1}$ in the complex spectrum (Kruck and Sarkar, 1973), the most significant indicator of histidine coordination over carboxyl groups (Dunbar *et al*., 2018). It should be noted that the Cu(II) complex that two histidine molecules can have multiple forms, one of which contains Cu(II) in the tetragonal distortion of O, N, N donor histidine molecules. The intense band at 625 $cm^{-1}$ attributed to the out-of-plane bending of the N-H bond of the imidazole ring (combined with other vibrations) occurs virtually unchanged in the spectra of both ligands and complexes, which is expected given that this bond remains preserved in complex. Significant is the behavior of the band at 1453 $cm^{-1}$, which is partly attributed to the deformation of the $CH_2$ group, and in the complex occurs at approximately 1400 $cm^{-1}$. This decline is atypical for the group not directly involved in coordination, however the band of this vibration strongly depends on the spatial arrangement of parts of the histidine molecule, so it occurs in different conformations ranging from 1477 to 1424 $cm^{-1}$ (Kumar *et al*., 2010). This band shift in the spectrum of the complex relative to the ligand can be interpreted as

additional evidence of histidine coordination at the Cu(II) center, given that the coordination process almost always causes changes in the conformation of more complex ligands (Nakamoto, 2009). the position of the "*scissoring*" band of the vibration of the $CH_2$ group of histidine.

**Table 3**. Characteristic vibrations of Cu- histidine complex

| Characteristic vibrations of Cu-histidine | Wave number of vibration, ν ($cm^{-1}$) |
|---|---|
| $\nu(C=O) + \delta(O–H) + \delta(C–H)$ | 1740 m |
| $\delta_s(NH_2)$ | 1625 s |
| $\delta_s(CH_2)$ | 1398 s |
| $\delta(C–H) + \delta(N–H)$ | - |
| $\nu(C–NH_2) + \delta(C–H)$ | 1084 m |
| $\rho_w(NH_2)$ | - |
| $\rho_r(NH_2)$ | 827 m, b |
| $\gamma(N_{imidaz.}–H)$ | 625 s |
| $\nu(Cu – N)$ | 418 s |

***FTIR characterization of Cu - tryptophan complex***

The spectrum of the prepared complex shows significant differences in the bands attributed to vibrations in which nitrogen atoms participate, which leads to the first conclusion about its coordination engagement in the complex. The vibration-corresponding bands ($NH_3^+$) of the group completely disappear in the spectrum of the complex and are replaced by vibrations characteristic of the $NH_2$ group. Thus, wild very intense bands appear at 3338 $cm^{-1}$ and 3254 $cm^{-1}$, which correspond to asymmetric and symmetric stretching of the amino group, while at 1627 $cm^{-1}$ there is an intense band of strain deformation in the mentioned group. Vibrations involving the indole nitrogen atom have no significant change in position or intensity. In the vibrations of the nitrogen atom that is directly related to the aliphatic carbon atom, a small shift towards higher wave numbers was observed. Vibration at 3420 $cm^{-1}$ indicates that the nitrogen atom in the indole ring is not deprotonated, and therefore probably not coordinated (Wagner & Baran, 2004). Equally significant changes are observed in the vibration bands of the carboxyl group where symmetrical and asymmetric stretching is not present in the molecule of the complex, thus pointing to the violation of the symmetry of the group and the abolition of resonance between bonds to a single C-O bond and a double C=O bond. Proof of this is the very intense band at 1562 $cm^{-1}$ corresponding to the carbonyl bond from the carboxyl group while at 1382 $cm^{-1}$ the rest of the group occurs in the form of C-O vibration. The intense deformation vibration of this group was shifted toward lower wave numbers at 740 $cm^{-1}$ (Wagner & Baran, 2004). Vibrations corresponding to the hydrocarbon skeleton do not change significantly in position or are eliminated due to differences in the symmetry of the coordinated and free molecules of tryptophan. Metal ligand vibrations are the most convenient form of confirmation of coordination both in terms of the nature and identity of coordinated atoms. Thus, in the spectrum of the complex, typical stretching vibrations of the Cu-N bond occur, which copper forms with the deprotonated amino group of tryptophan, at 475 $cm^{-1}$ as a medium intensity band. Vibrations of Cu-O usually fall below 400 $cm^{-1}$ (about 350 - 310 $cm^{-1}$) so that they are not visible in the given spectrum, but their existence is indicated by changes in the carboxyl group in terms of resonance cancellation due to binding of one oxygen atom from the given group to the Cu center and the accompanying formation of the C=O bond (Nakamoto, 2009; Wagner & Baran, 2004).

**Table 4:** Characteristic vibrations of Cu- tryptophan complex

| Characteristic vibrations of Cu- tryptophan | Wave number of vibration, ν ($cm^{-1}$) |
|---|---|
| $\nu(N–H)_{indole}$ | 3420 vs |
| $\nu_{as}(NH_2)$ | 3338 vs |
| $\nu_s(NH_2)$ | 3254 vs |
| $\nu(NH_3^+) + \nu(C–H)$ | – |
| $\nu(C–H)$ | 2895 w |
| $\delta_{as}(NH_3^+)$ | – |
| $\delta(NH_2)$ | 1627 vs |
| $\nu_{as}(COO^-)$ | – |
| $\nu(C=O)$ | 1562 vs |
| $\delta_s(NH_3^+)$ | – |
| $\delta(CH_2)$ | 1458 s |
| $\nu_s(COO^-)$ | – |
| $\nu(C–O)$ | 1382 m |
| $\tau(CH_2)$ | 1228 m |
| $\nu(C–N)_{aliph.}$ | 1100 m |
| $\delta(COO^-)$ | 740 s |
| $\nu(Cu–N)$ | 475 m |

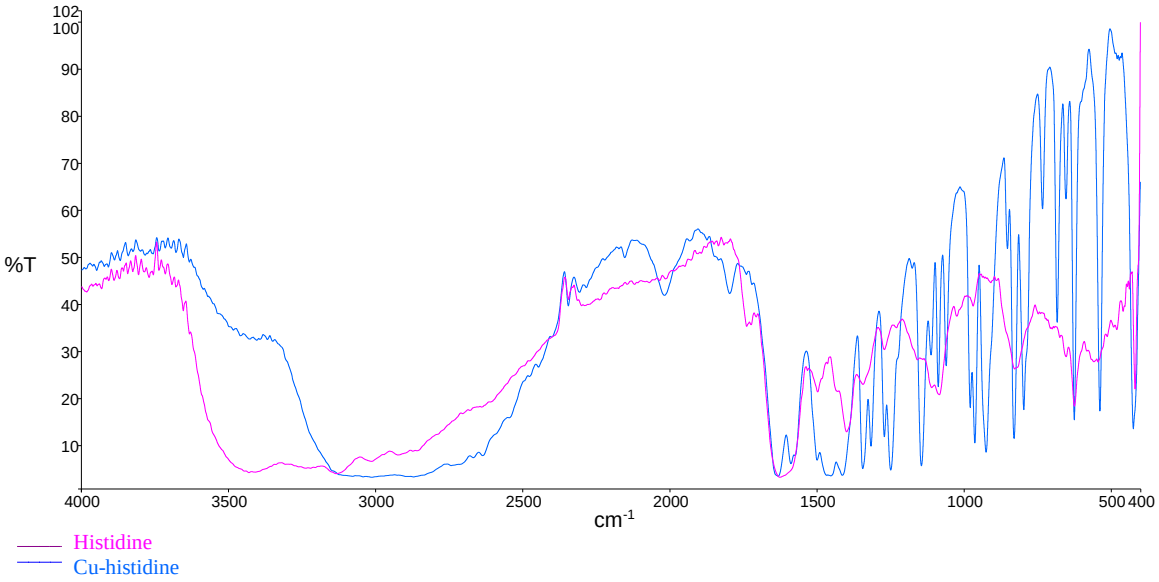


**Figure 3**: Comparative FT-IR spectra of histidine and Cu- histidine complex

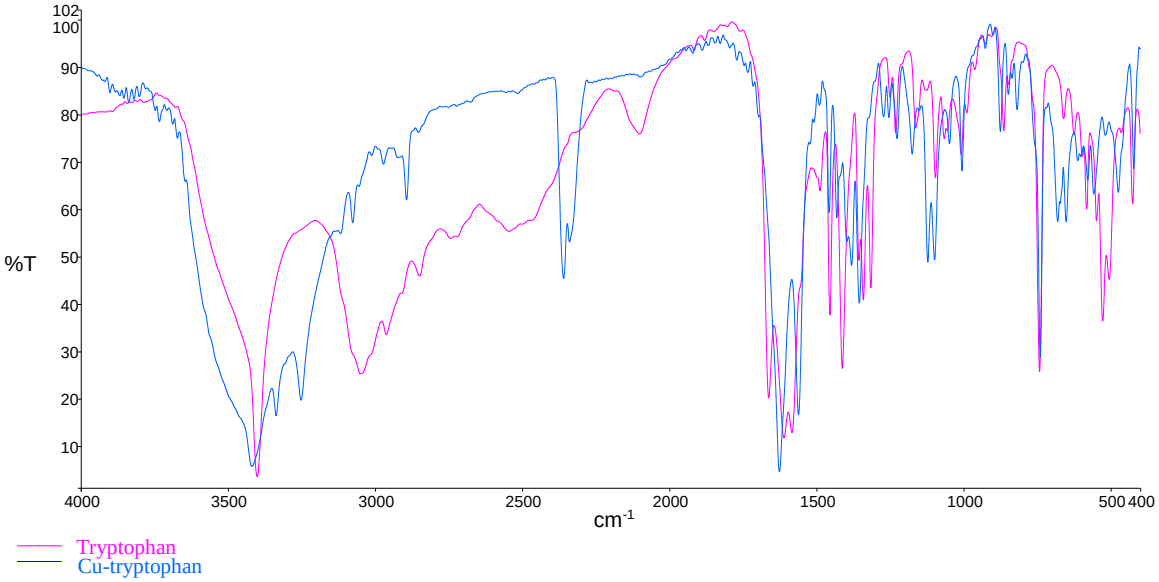


**Figure 4**: Comparative FT IR spectra of of tryptophan and Cu- tryptophan complex

***FTIR characterization of Cu-melatonin complex***

The spectrum of the Cu-melatonin complex shows a band at 3308 $cm^{-1}$ which corresponds to the vibration of the N-H bond of the indole. The appearance of this band, with small changes in symmetric and asymmetric stretching of the C - N bond within the indole ring, leads to the conclusion that this group is intact in the final complex and rejects the possibility of melatonin coordination at the Cu(II) center via N indole atoms (Shimazaki *et al*., 2009). The band carrying the largest share of C=O vibration of the amide group occurs 1632 $cm^{-1}$, is lower in intensity than in the melatonin spectrum, but certainly means that the oxygen atom does not participate in the coordination sphere of the Cu(II) center. This is supported by the sensitivity of this vibration to coordination via the amide oxygen atom, where a shift to higher wave numbers of up to 20 $cm^{-1}$ is expected (Ashok, *et al*., 2006). In contrast to the aforementioned groups, significant changes occur in bands involving vibrations of the amide N atom in the spectra of the melatonin and Cu-melatonin complexes. To evaluate coordination across an amide N atom, $\nu_{as}$ (C-N) amide. + δ (C-N-H) amide, is the most significant band corresponding to the vibration of the amide group and occurs in the spectrum of melatonin at 1490 $cm^{-1}$.

This band is lost in the spectrum of the complex from this spectral region. The band at 954 $cm^{-1}$ in the melatonin spectrum, corresponding to the , *ν*(C-N) amide vibration also disappears in the spectrum of the complex. Vibration γ(N - H) amide + τ(HCCO) amide, which carries a higher proportion of torsional vibrations, changes position and intensity in the spectrum of the complex. These observations suggest the possibility of coordination of melatonin at the Cu(II) center via the N atom of the amide group, which is a common tendency of amide ligands (Marti *et al*., 2012) in the context of Cu(II) coordination chemistry. In the spectrum of the complex, the I-band appears at 480 $cm^{-1}$, which is the area of the IR spectrum where the stretching of the Cu-N bond is expected (Nakamoto, 2009). An extremely interesting phenomenon is the band at 1714 $cm^{-1}$ which is not a common vibrational region of the carbonyl group attached to the N atom as is the case in amides. Ji et al. (2020) provided an interesting overview of the theoretically predicted spectra for simple amide (*N*-methylacetamide) for each individual resonant form. A resonant form that represents said molecule as acetimic acid (where the H atom of the amide group is attached to oxygen while carbon and oxygen form an imine bond (C=N)) shows a stretching vibration of the C=N bond at about 1700 $cm^{-1}$. Coordination at the metal center significantly affects the balance of individual resonant forms, in the direction that favors better coordination with the metal center through the heteroatom that participates in the resonance (Nakamoto, 2009). It can be assumed that the Cu(II) center can coordinate to the N atom of the amide part of the melatonin molecule to induce the formation of (C=N) bonds by stabilizing such a resonant form, which would be manifested by a band at 1714 $cm^{-1}$. Many other experimental data are needed to finally confirm this assumption. Bands of groups that do not participate in coordination occur virtually unchanged in the spectrum of the complex relative to the spectrum of the ligand. Asymmetric and symmetric stretching of the C–H group of the aliphatic part of the molecule occurs in the complex at 2926 $cm^{-1}$ and 2866 $cm^{-1}$, while the "rocking" vibration band of the mentioned bond is also practically unchanged in the complex at 1045 $cm^{-1}$. The band at 1555 $cm^{-1}$ corresponding to the asymmetric stretching of the C=C bond of the indole ring at 2C - 3C is of lower intensity but of the same position, at 1556 $cm^{-1}$ in the spectrum of the complex (Singh *et al*.,2014).

**Table 5:** Characteristic vibrations of Cu - melatonin

| **Characteristic vibrations of Cu-melatonin complex** | **Wave number of vibration, ν ($cm^{-1}$)** |
|---|---|
| $\nu(N–H)_{indole}$ | 3308 s |
| $\nu(N–H)_{amide}$ | - |
| $\nu_{as}(C–H)_{aliph.}$ | 2926 m |
| $\nu_{s}(C–H)_{aliph.}$ | 2866 m |
| $\nu(C=O) + \delta(C–N–H)_{amide}$ | 1632 s |
| $\nu_{as}(C=C)_{2\text{-}3C\text{-}indole}$ | 1556 m |
| $\nu_{as}(C–N)_{amide} + \delta(C–N–H)_{amide}$ | - |
| $\nu_{s}(C–N)_{indole}$ | 1264 w |
| $\nu_{as}(C–N)_{indole}$ | 1206 s |
| $\nu(C–O)_{methoxy}$ | 1174 m |
| $\rho_{r}(C–H)_{aliph.}$ | 1045 ms |
| $\nu(C–N)_{amide}$ | - |
| $\gamma(C–H)_{indole} + \tau(HCCC)_{2\text{-}3C\text{-}indole}$ | 803 m |
| $\tau(HCCO)_{amide}$ | 604 m |
| $\gamma(N–H)_{amide} + \tau(HCCO)_{amide}$ | 538 w |
| $\nu(Cu–N)$ | 480 w |

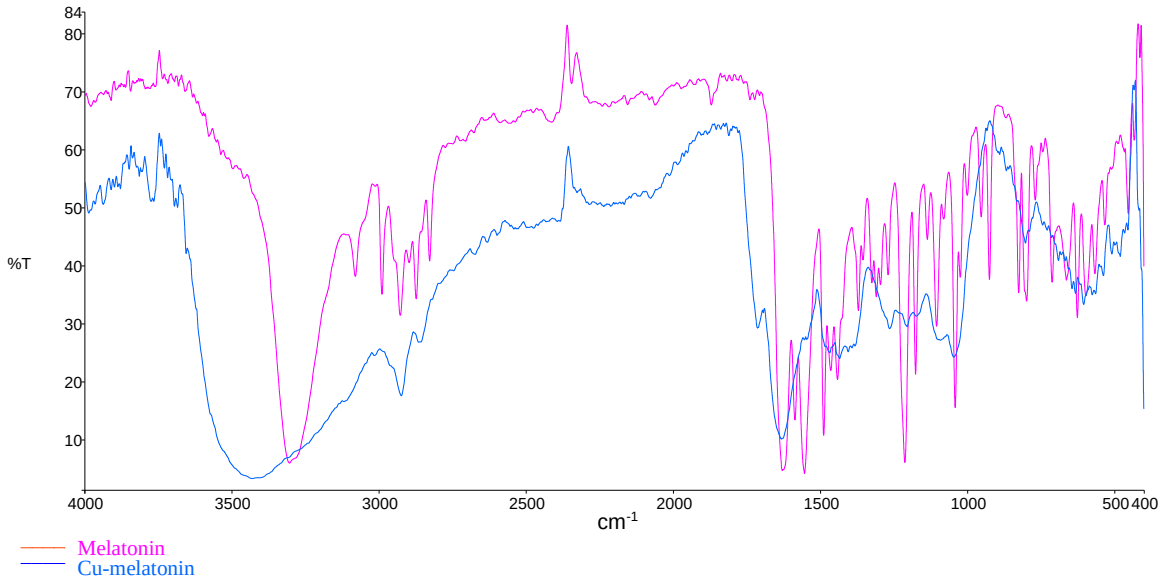


**Figure 5:** Comparative FT IR spectra of melatonin and Cu- melatonin complex

***Determination of antioxidant capacity***

By examining the antioxidant capacity of the synthesized copper complexes, CEAC values in the range of 121.6 - 734.4 μM were obtained. The lowest values of antioxidant capacity were recorded in the copper complex with tryptophan, while the highest values were recorded in the copper complex with alanine. A high antioxidant capacity of the copper complex with melatonin (673.8 μM) was also observed. Melatonin is known to be a good scavenger of hydroxyl radicals, superoxide anion radicals and nitric oxide and is one of the most effective lipophilic antioxidants (Simunkova *et al*., 2019).

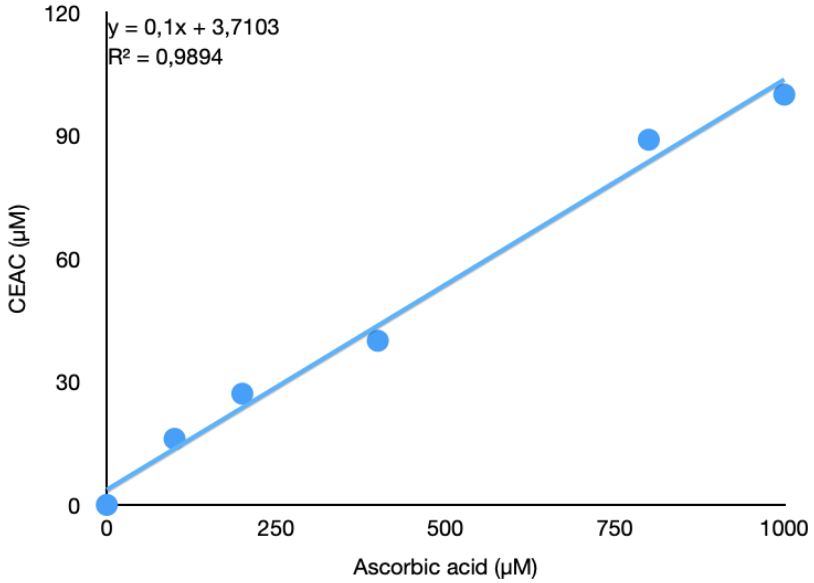


**Figure 6**: Calibration curve with standard ascorbic acid solution

Ascorbic acid is the strongest natural antioxidant and is commonly used in determining antioxidant capacity. To present the results as ascorbic acid equivalents (CEAC), a calibration curve was constructed as shown in Figure 6. The values of Q1 and Q2, as well as QT of the analyzed complexes are shown in Table 6.

**Table 6:** Antioxidant capacity of synthesized complexes expressed in µC

| Complex | Q1 (µC) | Q2 (µC) | QT (µC) |
|---|---|---|---|
| **Cu-Gly** | 3.6 | 20.1 | 23.7 |
| **Cu-Ala** | 24.3 | 50.2 | 74.5 |
| **Cu-His** | 3.9 | 47.2 | 51.1 |
| **Cu-Mel** | 36.2 | 32.6 | 68.8 |
| **Cu-Trp** | 3.9 | 13 | 16.9 |

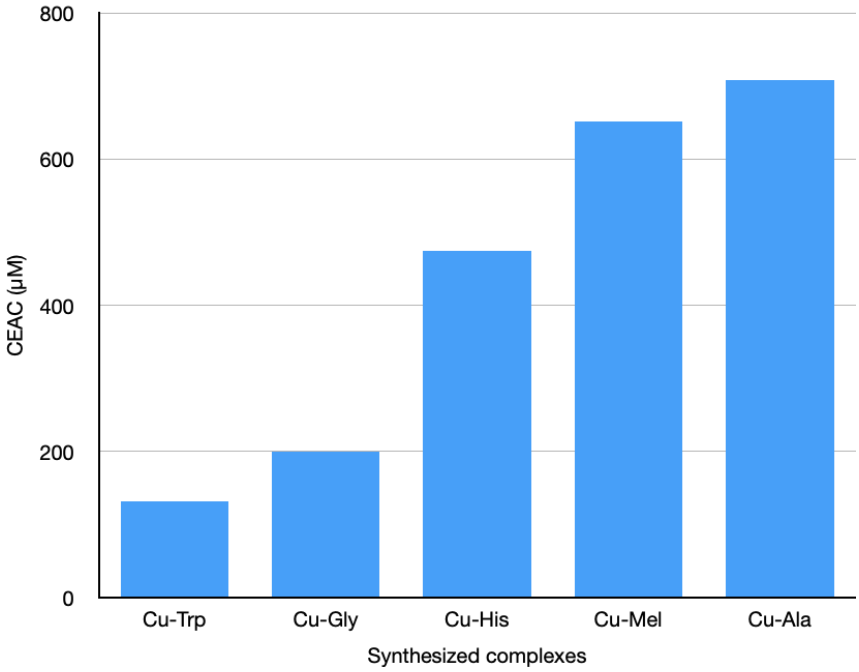


**Figure 7:** Total antioxidant capacity (CEAC) of synthesized complexes

## CONCLUSION

Five complex compounds of copper(II) were prepared following an identical procedure. Four amino acids (glycine, alanine, tryptophan and histidine) and melatonin as a bioactive tryptophan derivative were used as ligands. It was found that this preparative approach in the case of alanine and glycine does not result in the isolation of well-known cis / trans-bis (glycinato) copper(II) or cis / trans-bis (alaninato) copper(II) complexes implying the importance of starting copper(II) salt as well as pH control of the solution, given that said complexes are obtained using copper(II) acetate in approximately neutral aqueous solutions. FTIR characterization of the isolated complexes with glycine and alanine showed deviations from the IR spectral characteristics of the isomeric amino acid carboxylates of copper(II), especially in the region from 800 to 400 cm-1 where isomer-specific vibrations are common. Analysis of the FTIR spectra of prepared complexes of these amino acids provides data on the coordination of both oxygen atoms from the carboxyl group and nitrogen atoms from the amino group of the same, but does not dispute the participation of chlorides and water molecules in the coordination sphere of Cu(II). The histidine complex also shows the participation of oxygen and nitrogen atoms from the aliphatic part of this amino acid, but based on changes in skeletal ring vibrations, potential coordination of nitrogen atoms from the imidazole residue of this amino acid is assumed, which could be concluded based on Cu(II) center coordination preference. In the case of the melatonin complexes, the FTIR spectrum disputes coordination via oxygen atoms either from the amide group of the aliphatic moiety or from the methoxyl substituent on the indole ring, the potential deprotonation of the indole ring and coordination via the nitrogen atom from the same is also challenged. In contrast, the FTIR spectrum of the

complex clearly indicates the coordination of nitrogen atoms from the amide group as well as the potential stabilization of one of the resonant forms of this group based on theoretical considerations. It is important to note that the assumed structures contain coordinated chlorides based on theoretical knowledge and practical data on the behavior of such systems, and that the final judgment on their coordination participation is made by considering the spectral range from 400 to 200 cm-1 not examined in this work. Finally, it can be said that this simple preparative approach results in complex compounds of amino acids and their selected derivatives with copper(II) chloride that are different from the literature described, relatively simple complexes and that additional characterization is needed to establish the final structure of the complex and possible conclusions about mechanistic processes that are ongoing in the given reaction system. The obtained results of the antioxidant capacity of the complexes indicate a possible good antioxidant effect of the copper complex with melatonin and alanine, which indicates the need of further research in terms of the use of other methods to determine antioxidant capacity (Romero-Canelon and Sadler, 2013; Van Rijt and Sadler, 2009; Leung et al., 2015).

## REFERENCES


Ashok, M., Ravinder, V., Prasad, A. V. S. S. (2006) Synthesis, spectral characterization and catalytic applications of Ru(II) complexes with amide ligands. *Transition Metal Chemistry*, 32(1): 23–30. DOI:10.1007/s11243-006-0123-0.

Colaneri M. J., Vitali J., and Peisach J. (2009). Aspects of Structure and Bonding in Copper−Amino Acid Complexes Revealed by Single-Crystal EPR/ENDOR Spectroscopy and Density Functional Calculations, *The Journal of Physical Chemistry*, 113 (19), 5700-5709 DOI: 10.1021/jp811249s

Chiurchiù, V., Orlacchio, A., & Maccarrone, M. (2016). Is modulation of oxidative stress an answer? The state of the art of redox therapeutic actions in neurodegenerative diseases. *Oxidative medicine and cellular longevity*, *2016*. DOI: 10.1155/2016/7909380

Delf, B. W., Gillard, R. D., & O'Brien, P. (1979). The isomers of α-amino-acids with copper(II). Part 5. The cis and trans isomers of bis(glycinato)copper(II), and their novel thermal isomerization. *J. Chem. Soc., Dalton Trans., (8)*, 1301–1305. DOI:10.1039/dt9790001301

Dos Santos Carvalho, C., Fernandes, M. N. (2019) Effects of copper toxicity at different pH and temperatures on the in vitro enzyme activity in blood and liver of fish, Prochilodus lineatus. *Molecular Biology Reports*, 46(5): 4933–4942 DOI:10.1007/s11033-019-04944-y.

Drożdżewski, P., Kordon, E. (2000) Isotopic studies of the metal–ligand vibrations in histamine complexes with Copper(II). *Spectrochimica Acta Part A: Molecular and Biomolecular Spectroscopy*, 56(7): 1299–1304. DOI:10.1016/s1386-1425(99)00232-2.

Dunbar, R. C., Martens, J., Berden, G., Oomens, J. (2018) Transition metal(II) complexes of histidine-containing tripeptides: Structures, and infrared spectroscopy by IRMPD. *International Journal of Mass Spectrometry*, 429: 198–205. DOI:10.1016/j.ijms.2017.10.004.

Galano, A., Medina, M. E., Tan, D. X., Reiter, R. J. (2014) Melatonin and its metabolites as copper chelating agents and their role in inhibiting oxidative stress: a physicochemical analysis. *Journal of Pineal Research*, 58(1): 107–116. DOI:10.1111/jpi.12196.

Galano, A., Tan, D. X., Reiter, R. J. (2014) Cyclic 3-hydroxymelatonin, a key metabolite enhancing the peroxyl radical scavenging activity of melatonin. *RSC Advances*, 4(10): 5220. DOI:10.1039/c3ra44604b.

Herlinger, A. W., Wenhold, S. L., Long, T. V. (1970) Infrared spectra of amino acids and their metal complexes. II. Geometrical isomerism in bis(amino acidato)copper(II) complexes. *Journal of theAmerican Chemical Society*, 92(22): 6474–6481. DOI:10.1021/ja00725a015.

Inomata, Y., Shibata, A., Yukawa, Y., Takeuchi, T., Moriwaki, T. (1988) The metal complexes of aminoacids and their N-substituted derivatives—VII. The i.r. spectra and normal coordinate analyses ofbivalent metal complexes with N-methylglycine and N-phenylglycine. *Spectrochimica Acta Part A: Molecular Spectroscopy*, 44(1): 97–107. DOI:10.1016/0584-8539(88)80265-4.

Kruck, T. P. A., Sarkar, B. (1973) Structure of the Species in the Copper (II)–L-Histidine System. *Canadian Journal of Chemistry*, 51(21): 3563–3571. DOI:10.1139/v73-531.

Kumar, S., Rai, A. K., Rai, S. B., Rai, D. K. (2010) Infrared and Raman spectra of Histidine: an ab initio DFT calculations of Histidine molecule and its different protonated forms. *Indian Journal of Physics*,84(5): 563–573 DOI:10.1007/s12648-010-0039-6.

Liu, H., Qu, Y., & Wang, X. (2018). Amyloid β-targeted metal complexes for potential applications in Alzheimer's disease. *Future medicinal chemistry*, *10*(6), 679-701. DOI: 10.4155/fmc-2017-0248

Martí, I., Ferrer, A., Escorihuela, J., Burguete, M. I., Luis, S. V. (2012) Copper(II) complexes of bis(amino amide) ligands: effect of changes in the amino acid residue. *Dalton Transactions*, 41(22):6764. DOI:10.1039/c2dt12459a.

Nakamoto, K. (2009) *Infrared and Raman Spectra of Inorganic and Coordination Compaunds: Part A,Theory and Applications in Inorganic Chemistry.* 6th ed. New Jersey: John Wiley and Sons, Inc.

Nakamoto, K. (2009) *Infrared and Raman Spectra of Inorganic and Coordination Compaunds:Part B, Applications in Coordination, Organometallic and Bioinorganic Chemistry.* 6th ed. New Jersey: John Wiley and Sons, Inc.

Romero-Canelon, I., & Sadler, P. J. (2013). Next-generation metal anticancer complexes: multitargeting via redox modulation. *Inorganic chemistry*, *52*(21), 12276-12291. DOI: 10.1021/ic400835n

Scheiber, I., Dringen, R., Mercer, J. F. B. (2013) *Copper: Effects of Deficiency and Overload.* In: Interrelations Between Essential Metal Ions and Human Diseases, Dordrecht: Springer Netherlands, pp: *359–387*. DOI:10.1007/978-94-007-7500-8_11.

Shimazaki, Y., Yajima, T., Takani, M., Yamauchi, O. (2009) Metal complexes involving indole rings: Structures and effects of metal–indole interactions. *Coordination Chemistry Reviews*, 253(3-4): 479 492. DOI:10.1016/j.ccr.2008.04.012.

Simunkova, M., Alwasel, S. H., Alhazza, I. M., Jomova, K., Kollar, V., Rusko, M., & Valko, M. (2019). Management of oxidative stress and other pathologies in Alzheimer's disease. *Archives of toxicology*, *93*(9), 2491-2513. DOI: 10.1007/s00204-019-02538-y

Van Rijt, S. H., & Sadler, P. J. (2009). Current applications and future potential for bioinorganic chemistry in the development of anticancer drugs. *Drug discovery today*, 14(23-24), 1089-1097. DOI: 10.1016/j.drudis.2009.09.003

Vest, K. E., Hashemi, H. F., Cobine, P. A. (2012) The Copper Metallome in Eukaryotic Cells. Met Ions Life Sci., 12: 451–478 DOI:10.1007/978-94-007-5561-1_13.

Waggoner, D. J., Bartnikas, T. B., Gitlin J. D. (1999), The Role of Copper in Neurodegenerative Disease. *Neurobiology of Disease*, 6(4): 221-230. DOI: 10.1006/nbdi.1999.0250

Wagner C. C., Baran E. J. (2004) Spectroscopic and magnetic behavior of the Copper(II) complexs of L-tryptophan. *Acta Farm. Bonaerense*, 23(3): 339-42. ISSN 0326-2383

Wang, J., Wang, X., He, Y., Jia, L., Yang, C. S., Reiter, R. J., Zhang, J. (2019) Antioxidant and Pro Oxidant Activities of Melatonin in the Presence of Copper and Polyphenols In Vitro and In Vivo. *Cells*, 8(8):903. DOI:10.3390/cells8080903.

Zuo, L., Zhou, T., Pannell, B. K., Ziegler, A. C., & Best, T. M. (2015). Biological and physiological role of reactive oxygen species–the good, the bad and the ugly. *Acta physiologica*, *214*(3), 329-348. DOI: 10.1111/apha.12515

## Summary/Sažetak

Ispitana je reakcija bezvodnog bakar(II) hlorida u metanolnom rastvoru sa alaninom, glicinom, histidinom, triptofanom kao i reakcija s melatoninom. Produkti reakcija ispitani su FTIR spektroskopijom kako bi se izvršila distinkcija produkata reakcije u odnosu na, u literaturi, prethodno opisane komplekse istih aminokiselina sa Cu(II) kao što su *cis*- i *trans*-bis(glicinato)bakar(II). Od velikog interesa bila je reakcija $CuCl_2$ s melatoninom u ovim uvjetima. FTIR karakterizacija sintetiziranih kompleksa pokazala je da ovi reakcioni uslovi rezultiraju nastankom kompleksa Cu(II) s glicinom i s alaninom koji su složenije građe od bis(glicinato)- i bis(alaninato)bakar(II) kompleksa. Kompleks priređen s melatoninom pokazuje interesantne trake u spektralnom području za koje je odgovoran atom azota iz amido grupe melatonina. Posljednje opažanje je vrlo značajno jer je poznat vrlo mali broj metalnih kompleksa melatonina koji su dobro okarakterizirani, dok je sinteza većine njih eksperimentalno zahtjevan proces uz simultanu kontrolu više faktora. Ispitivanjem antioksidativnog kapaciteta sintetiziranih kompleksa bakra dobijene su vrijednosti CEAC u rasponu od 121.6 - 734.4 μM. Najniže vrijednosti antioksidativog kapaciteta su zabilježene kod kompleksa bakra sa triptofanom, dok su najviše vrijednosti zabilježene kod kompleksa bakra sa alaninom. Uočen je i visok antioksidativni kapacitet kompleksa bakra sa melatoninom (673.8 μM).

Glasnik hemičara i tehnologa Bosne i Hercegovine

Bulletin of the Chemists and Technologists of Bosnia and Herzegovina

2022

58

Original Scientific Article

Print ISSN: 0367-4444
Online ISSN: 2232-7266

DOI: https://doi.org/10.35666/2232-7266.2022.58.04

UDC: 538.9:537.311.6"71"

33-38

# Temporal evolution of electrical resistance through the granular packing of Ni beads

**Dujak, D.[a,*], Đekić, M.[b], Ćubela, D.[c]**

[a] *Faculty of Electrical Engineering, Zmaja od Bosne, University campus, 71 000 Sarajevo, Bosnia and Herzegovina*

[b] *Faculty of Science, Zmaja od Bosne 33-35, 71 000 Sarajevo, Bosnia and Herzegovina*

[c] *Faculty of Metallurgy and Technology, Travnička cesta 1, 72 000 Zenica, Bosnia and Herzegovina*

**Article info**
Received: 12/04/2022
Accepted: 22/06/2022

**Keywords:**
Ni beads
Electrical resistance
Weak contacts
Granular metallic packing
Mittag-Leffler function

***Corresponding author:**
**Dijana Dujak**
E-mail: ddujak@etf.unsa.ba
Phone: +387 33 250 700

**Abstract:** In this paper we investigate the temporal evolution of the electrical resistance through different two-dimensional (2D) packings of Ni beads when 1 mA current is injected in them. In the first stages of measurements, resistance decreases towards a saturation value and it can be fitted with Mittag-Leffler function. Fitting parameters show that the relaxation dynamics does not depend on the type of the packing. Different packings show differences in the initial values of the resistance which is attributed to the formation of new microcontacts during the formation of the new packing. Pauses in the flow of the current cause the resistance either to decrease, increase or remain the same, depending on the packing. Longer measurements show, that after the initial drop, the resistance starts to rise which can probably be attributed to the deterioration of microcontacts between the beads. Small variations in temperature do not affect the temporal evolution of the resistance.

## INTRODUCTION

The electrical properties of metallic granular packings differ from the properties of the bulk samples of the same material. When an electric current is imposed on such a system, its voltage is not unambiguously determined by the current flow through the packing, i.e. the current-voltage dependence is not linear, but shows hysteresis properties and memory effects (Falcon & Castaing, 2005; Falcon & Castaing, 2005; Vandembroucq et al., 1997; Dorbolo et al., 2002; Falcon et al., 2004).

Previous research has identified several important factors causing this phenomenon: grain to grain contact is imperfect because of the surface roughness, electrical paths are created in the conducting states and geometrical variables such as the system dimensionality are to be taken into account (Dorbolo et al., 2002).

Tests of the change in electrical resistance over time have shown the resistance drop, which is initially more intense and later it slows down. Temporal evolution of resistance R(t) in metallic granular packings when a stable current through the system is established can be found only in a few papers (Yoon et a., 1999; Dorbolo et al., 2003; Lee et al., 2007; Jakšić et al. 2017). The decrease in resistance is considered to be the result of improved micro contacts (Toler et al., 2013) between the granules due to their local welding. Therefore, the electrical conductivity of granular packing is sensitive to mechanical and temperature perturbations (Vandewalle et nal., 2001; Bonamy et. al., 2000). Examining the temporal evolution of resistance in metallic granular packings of different materials can help to better understand the mechanisms behind it.

## EXPERIMENTAL

Temporal evolution of electrical resistance R(t) was recorded for 2D granular packings of 52 Ni beads with radii $10.3 \pm 0.02$ mm. Surface roughness of the beads varied between 1.6-6.3 μm corresponding to N7-N9 roughness classes. Ni beads were placed in a rectangular

box with dimensions 13.5 cm x 3.3 cm made out of plastic and wood. Brass electrodes were mounted along the lateral sides of the box, as presented in Figure 1.

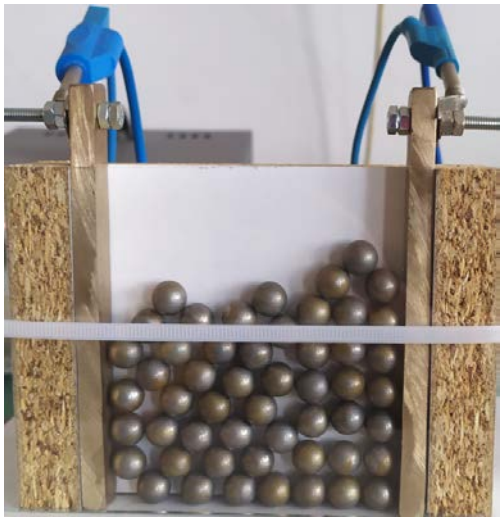

**Figure 1.** Experimental set-up for 2D packing of Ni beads.

The measurements were conducted for different 2D packings of the beads. The packing of the beads was established by the following procedure: the metallic grains were poured into the box which was initially placed in the horizontal position thus enabling all the beads to separate from each other (terminating contacts between all the beads). After that the box was straightened and then tilted under $8^{\circ}$ inclination angle in respect to the horizontal position thus enabling us to visually control 2D ordering.
The box was placed on an anti-vibrational surface and the temperature in the room was measured using digital thermometer with recorded variations of 1.7 ℃ during measurements. The temporal evolution of the resistance was recorded by allowing a steady flow of current I = 1 mA from the current source Keithley 228 through the granular packing. The voltage was measured using Multimetar GDM 8621A (GW – Instek). The acquisition of data was carried out and controlled by a home-made computer program recording voltage with a 10 s step and calculating resistance using Ohms law. The resistance of each granular packing was measured for different time intervals.
Very strong contacts between all the components in the system were formed and any change in the voltage value recorded during measurements was caused exclusively because of the changes within the granular packing. This was checked by measuring the values of voltage between the electrodes and the measuring devices (the voltage was constant between the current source and the electrode and between the multimeter and the electrode).

## RESULTS AND DISCUSSION

Resistance measurements were carried out on a number of different 2D packings of Ni beads through which a constant current I = 1 mA was injected. The measurements were performed right after the formation of a particular packing which lasted for a few seconds.

Figure 2 shows five representative measurements of the temporal evolution of the resistance for different packings during 1200 s. It can be concluded that the initial values of the resistance differ from each other regardless of the fact that we always used the same beads. This means that the initial resistance depends on the type of packing which can be attributed to creation of new contacts during the formation of a new packing (Jakšić et al., 2017). Also, the resistance decreases with time, faster in the first stages of relaxation and later on it slows down with a tendency of saturation.

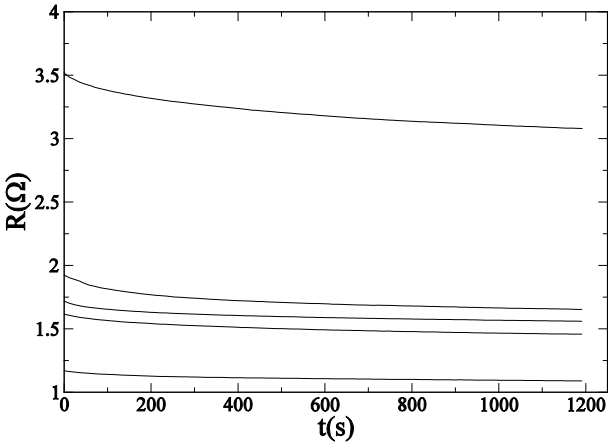


**Figure 2**: Temporal evolution of resistance for five different packings of Ni beads.

Our experimental data presented in Figure 2 can be fitted with Mittag-Leffler (ML) function of the form:

$$R(t) = R(\infty) - [R(\infty) - R_0]E_\alpha\left[-\left(\frac{t}{\tau}\right)^\alpha\right] \quad (1)$$

where $R(\infty)$ is asymptomatic value of resistance R(t) with $t \to \infty$, $R_0$ is the initial value of resistance, and $E_\alpha$ is ML function of order $\alpha$, $0 < \alpha < 1$ (Haubold et al., 2011). ML function is defined through the inverse Laplace transform:

$$E_\alpha\left[-\left(\frac{t}{\tau}\right)^\alpha\right] = \lambda[(u + \tau^{-\alpha}u^{1-\alpha})^{-1}] \quad (2)$$

From which the series expansion can be obtained:

$$E_\alpha\left[-\left(\frac{t}{\tau}\right)^\alpha\right] = \sum_{n=0}^{\infty}\frac{(-(t/\tau)^\alpha)^n}{\Gamma(1+\alpha n)} \quad (3)$$

ML function interpolates between the initial stretched exponential form:

$$E_\alpha\left[-\left(\frac{t}{\tau}\right)^\alpha\right] \sim \phi_1 = \exp\left[-\frac{1}{\Gamma(1+\alpha)}(t/\tau)^\alpha\right], t \ll \tau \quad (4)$$

and the power behavior for later times:

$$E_\alpha\left[-\left(\frac{t}{\tau}\right)^\alpha\right] \sim \phi_2 = \frac{1}{\Gamma(1-\alpha)}(t/\tau)^{-\alpha}, \quad t \gg \tau \quad (5)$$

The same function was used in (Jakšić et al., 2017) for fitting the electrical conductivity for a constant flow of 1 mA current through a metallic cylinder packing.
Experimental results of R(t) (red line) fitted with ML function (equation (1), blue line) for three different packings of the beads, represented in Figure 3a-c show excellent agreement. The fitting parameters are as follows:

$a)\ \tau_1 = 1.5421 \cdot 10^3 \text{s},\ \alpha_1 = 0.57583,$ b) $\tau_2 = 1.5410 \cdot 10^3 \text{s},\ \alpha_2 = 0.6255$ and c) $\tau_3 = 9.2724 \cdot 10^3 \text{s},\ \alpha_3 = 0.3535$. It can be concluded that the relaxation dynamics does not depend on the way in which the beads are arranged in the packing. For instance, two different packings can have the same relaxation dynamics ($\tau_1 \approx \tau_2$) and the evolution of the resistance toward the saturation value ($\alpha_1 \approx \alpha_2$), but on the other hand these processes can take place on a much different time scales ($\tau_3 \neq \tau_2,\ \alpha_3 \neq \alpha_2$) for different packings.

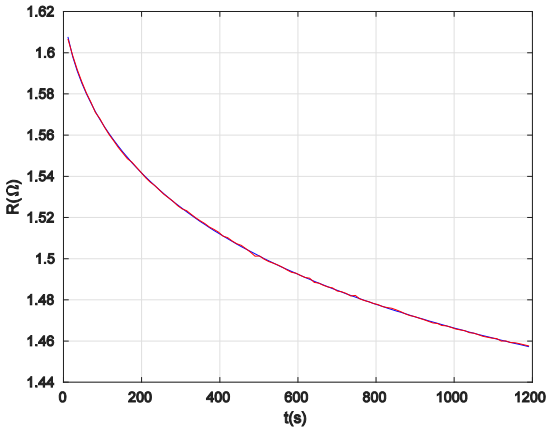


(a)

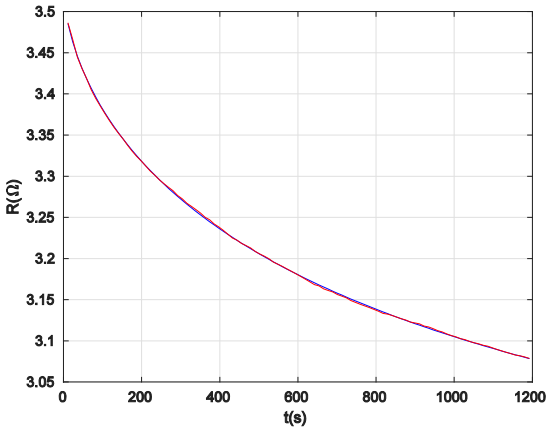


(b)

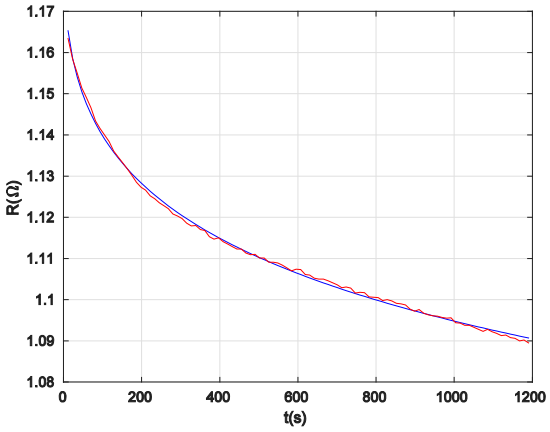


(c)

**Figure 3**: Temporal evolution of resistance for three different packings of Ni beads (red line), and Mittag-Leffler function fit of equation (1) (blue line).

In order to compare the rate of the lowering of the resistance for different packings, the time evolution of the normalized resistance $R/R_0$ (where $R_0$ is the initial resistance) was examined (Figure 4). It can be concluded that the change in the resistance can be the same for different packings but that is not a rule. Depending on the microcontacts that were established between the beads, the rate of the lowering of the resistance can either be faster or slower in different packings, which is in accordance with the results of M-L fitting.

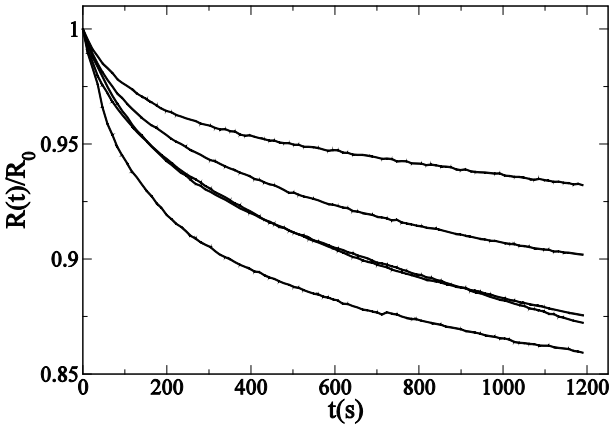


**Figure 4**: Normalized resistance versus time for different packings of the Ni beads.

Because every packing of the beads had different initial resistance, the measurements were conducted when the current was turned off for 10 s. These measurements were repeated for a number of different packings.

The typical results, presented in Figure 5, indicate that every break in the flow of the current can lead either to decreasing or increasing of the resistance, whereas in some cases the resistance remains unchanged. This means that in some cases the contacts between the beads were improved but in other cases they were weakened. The same breaks in the current flow were done consecutively on the same packing during longer measurements, which is presented in Figure 7a-d, where all three previously mentioned cases were also observed.

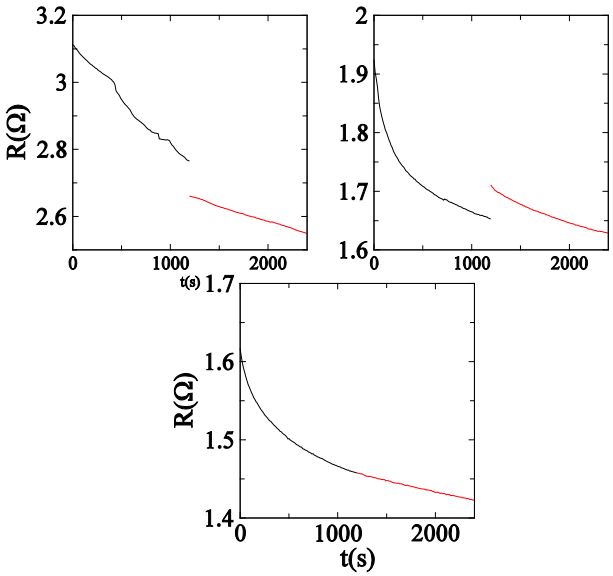


**Figure 5**: Temporal evolution of resistance during 2400 s, with the pause of 10 s after first 1200 s.

The same step changes in the resistance can be acquired if the current is turned off for longer periods of time. During

these breaks, the conditions in the laboratory as well as the packing were not altered in any way. Figure 6 represents cases where the current was switched off for 30 minutes and 20 h respectively. The value of the resistance is either decreased or increased after the current is switched on again. The order of change in the value of the resistance is the same as in the case of the short breaks in the current flow.

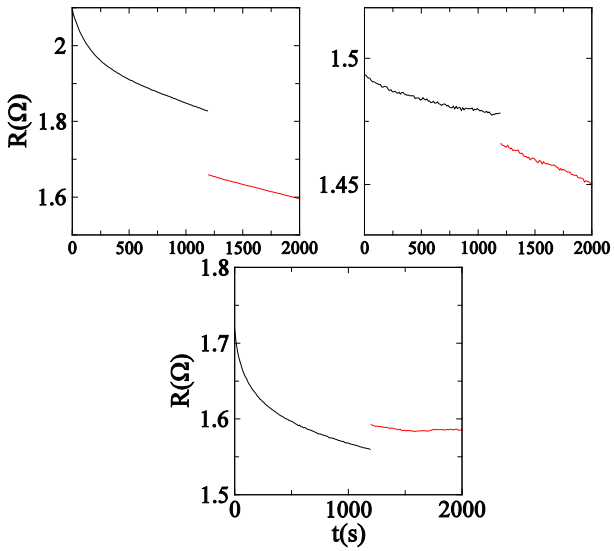


**Figure 6:** Temporal evolution of resistance during 2400 s, with 30 min pause (graph above) and 20 h pause (graph below) after the first 1200 s.

Figure 7a-d shows the typical resistance variations for four different packings. The measurements for the individual packing were performed during 7000 s, where after every 1200 s the current was switched off for 10 s. The slight temperature changes during the measurements were also recorded. Regardless of the fact that small temperature variations were recorded, resistance kept decreasing following every break in the current flow, which is in accordance with the results of the previous authors who kept the temperature constant throughout the measurements.

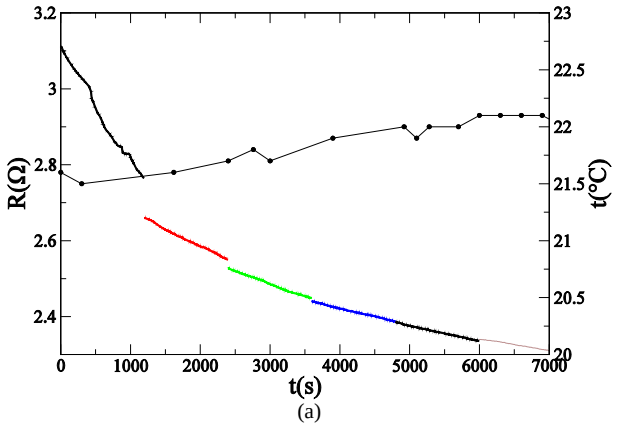


(a)

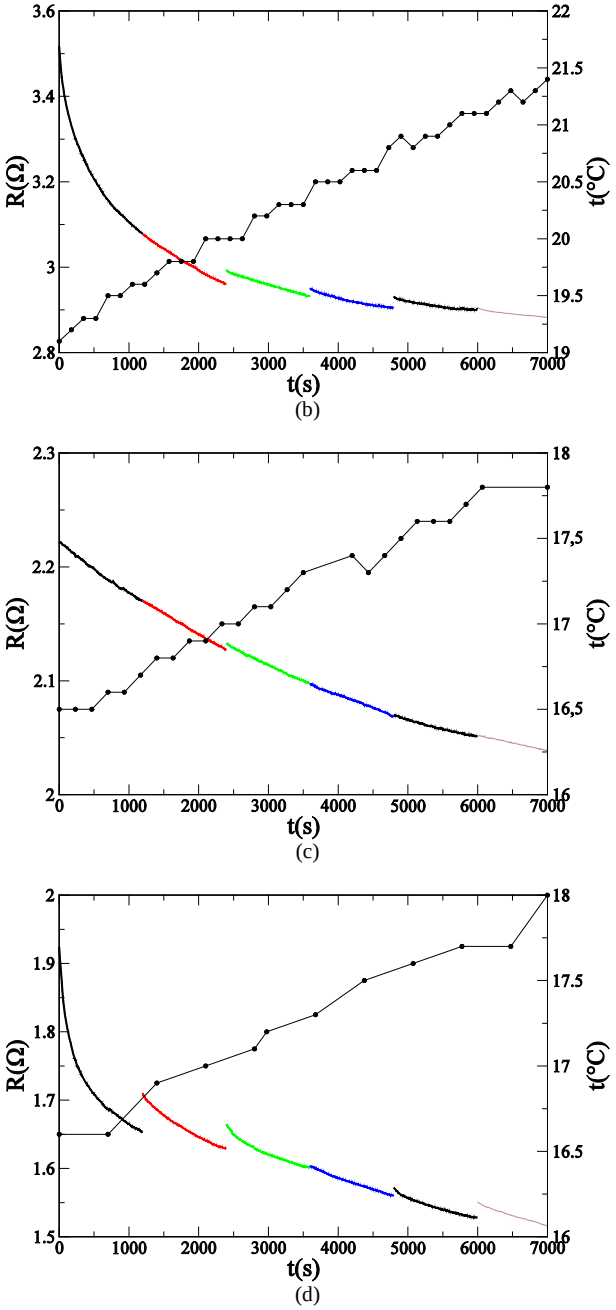


(b)

(c)

(d)

**Figure 7:** Temporal evolution of resistance with 10 s pauses after every 1200 s (left axis). Temperature variations during measurements (right axis).

A number of longer measurements that lasted up to 12000 s was also conducted and the typical results are presented in Figure 8. It can be seen that following the initial drop, the resistance starts to rise in the later phases of the experiments. We stipulate that this rise in resistance is caused because of the deterioration of contacts between the beads, but what causes this deterioration needs to be further examined.

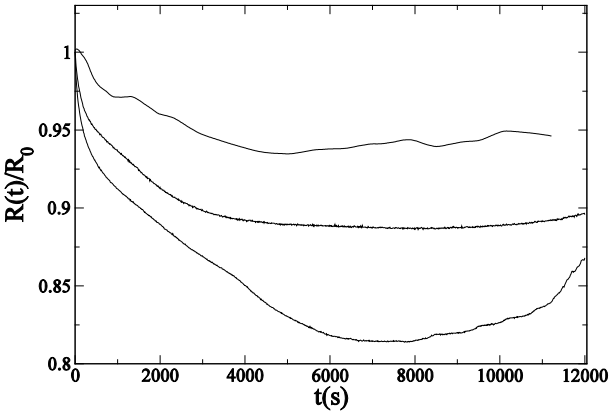


**Figure 8**: Temporal evolution of normalized resistance up to 12000 s long measurements

## CONCLUSION

According to our results, the electrical resistance of a granular packing of Ni beads with 1 mA injected current drops in the first phases of relaxation towards a saturation value but later on it begins to rise which can be concluded from the longer measurements. This increase is not caused by external vibrations since it is well known that this kind of influence is recorded as an abrupt and step change in resistance during experiments. The decrease in the resistance in the first stages of measurements can be approximated with Mittag-Leffler function.

Pauses in the flow of the current through the packing can cause changes in the resistance, namely it can either increase or decrease.

Small increases of temperature do not affect the decrease of the resistance during relaxation.

**Acknowledgements**

We thank Benjamin Fetić for the realization of the experimental set-up and Senad Hatibović for making the box with electrodes that was used during the measurements.

## REFERENCES

Bonamy D., Laurent L., Claudin Ph., Bouchaud J.-Ph. and Daviaud F., (2000). Electrical conductance of a 2D packing of metallic beads under thermal perturbation, Europhys. Lett. 51, 614.

Dorbolo S., Ausloos M., and Vandewalle N., (2002). Hysteretic behavior in metallic granular matter, Appl. Phys. Lett. 81, 936.

Dorbolo S., Ausloos M., Vandewalle N., Houssa M., (2003). Aging process of electrical contacts in granular matter, J. Appl. Phys. 94, 7835.

Falcon E., Castaing B., Creyssels M., (2004). Nonlinear electrical conductivity in a 1D granular medium, Eur. Phys. J. B 38, 475–483.

Falcon E., Castaing B. (2005). Electrical conductivity in granular media and Branly's coherer: A simple experiment, American Journal of Physics 73, 302.

Falcon E., Castaing B. (2005). Electrical properties of granular matter: From "Branly effect" to intermittency, eBook Powders and Grains, ISBN 9780429107733

Haubold H. J., Mathai A. M., Saxena R. K., (2011). Mittag-Leffler Functions and Their Applications, Journal of Applied Mathematics, Article ID 298628, doi:10.1155/2011/298628

Jakšić Z. M., Cvetković M., Šćepanović J. R., Lončarević I., Budinski-Petković Lj. and Vrhovac S. B., (2017). The electrical conductance growth of a metallic granular packing, Eur. Phys. J. B 90: 108.

Lee J. J., Lee C. W., Yu I., Jung Y. K., Lee J., (2007). Slow relaxation of randomly packed hard spheres, J. Phys.: Condens. Matter 19, 356202.

Toler B. F., Coutu Jr 1 R. A., McBride J. W. (2013). A review of micro-contact physics for microelectromechanical systems (MEMS) metal contact switches, J. Micromech. Microeng. 23, 103001.

Vandembroucq D., Boccara A.C., and Roux S., (1997). Breakdown Patterns in Branly's Coheror. Journal de Physique III, EDP Sciences, 7 (2), 303-310.

Vandewalle N., Lenaerts C., Dorbolo S., (2001). Non-Gaussian electrical fluctuations in a quasi-2d packing of metallic beads, Europhys. Lett. 53, 197

Yoon S. S., Lee J. J., Yu I. (1999). Pattern formations in granular systems and their implications to dynamics of ferroelectrics, Journal of the Korean Physical Society, 35.

**Summary/Sažetak**

U ovom radu smo ispitali vremensku evoluciju električnog otpora u različitim dvodimenzionalnim (2D) pakovanjima Ni kuglica kada se kroz njih propusti struja jačine 1 mA. Naši rezultati pokazuju da u prvim fazama mjerenja otpor opada prema nekoj vrijednosti zasićenja. Eksperimentalni rezultati u prvim fazama mjerenja se veoma dobro mogu fitovati Mittag-Leffler funkcijom. Parametri fita pokazuju da dinamika relaksacije ne zavisi od tipa pakovanja tj. različita pakovanja mogu imati iste parameter fita. Pored toga, različita pakovanja pokazuju razlike u početnim vrijednostima otpora što se može pripisati formiranju novih mikrokontakata prilikom formiranja novog pakovanja. Duže ili kraće pauze u protoku struje uzrokuju promjenu otpora za određeno pakovanje. Naime u zavisnosti od tipa pakovanja kuglica, otpor može da poraste, opadne ili čak ostane nepromijenjen. Duža mjerenja pokazuju da nakon početnog pada, otpor počinje da raste, što se vjerovatno može pripisati pogoršanju mikrokontakata između kuglica. Male promjene temperature ne utiču na vremensku evoluciju otpora.

Glasnik hemičara i tehnologa Bosne i Hercegovine

Bulletin of the Chemists and Technologists of Bosnia and Herzegovina

2022

58

Short Communication

Print ISSN: 0367-4444
Online ISSN: 2232-7266

DOI: https://doi.org/10.35666/2232-7266.2022.58.05
UDC: 620.196[546.131:669.35'5]

39-42

# Investigation of the effect of the addition $H_2O_2$ on the general corrosion of brass in hydrochloric acid

**Kasapović, D, Bikić, F.**

*University of Zenica, Faculty of Metallurgy and Technology, Travnička cesta 1, Zenica, Bosnia & Herzegovina*

**Article info**
Received: 02/09/2020
Accepted: 07/06/2022

**Keywords:**
Brass,
Hydrochloric acid
General corrosion,
Taffel extrapolation method
Potentiostat/galvanostat

***Corresponding author:**
**Kazazović Dejana**
E-mail: dejana.kasapovic@mtf.unze.ba

**Abstract:** In this paper, the influence of hydrochloric acid and the addition of oxidizing agents on the rate of general corrosion of brass was investigated. For comparison, the corrosion rate of copper and zinc in hydrochloric acid and in hydrochloric acid with oxidizing agent was also tested. The Taffel extrapolation method was used to examine the general corrosion of brass, copper and zinc. The Taffel extrapolation method involves scanning potential of the working electrode of ±250 mV in relation to its open-circuit otential ($E_{OCP}$), at a speed of 0.5 $mVs^{-1}$. Investigation of corrosion was conducted in a corrosion cell according to the ASTM G5 (ASTM G5-94) standard, on a potentiostat/galvanostat instrument, Princeton Applied Research, model 263A-2, with PowerCORR® software, which is part of the Power Suite softwere package. The tests were performed at room temperature, 20±1°C. The results show that the corrosion rate of brass is higher in hydrochloric acid with oxidizing agent than the corrosion rate of brass in hydrochloric acid. Examining the effect of hydrochloric acid and the addition of oxidizing agent on the rate of general corrosion of brass, it was found that the corrosion of brass has caused the zinc contained in it. Corrosion of zinc is highest in 0.1 M HCl + 0.1 M $H_2O_2$ compared to corrosion of brass and copper in 0.1 M HCl + 0.1 M $H_2O_2$, where corrosion of copper is lowest in 0.1 M HCl + 0.1 M $H_2O_2$.

## INTRODUCTION

Brass is an alloy of copper and zinc containing 5-40% Zn as the main alloying element (Choucri *et al.*, 2019), other elements may be added to modify properties such as strength, machinability, or corrosion resistance (Francis, 2010). It has been used extensively in a variety of corrosive environment for many years (Akabueze *et al.*, 2012). Brass (along with bronze) are the oldest alloys used in marine technology (Feron, 2007).

Copper alloys with zinc can be double, triple and complex, with a copper content of at least 50% and zinc of not more than 44% (ordinary brass), as the main added element (Avramović *et al.*, 2006). Brass is commonly used as a condenser and heat exchanger (Gapsari *et al.*, 2018). Brass has characteristic colors. The color varies depending on the copper content (Avramović *et al.*, 2006).

Brass undergoes an electrochemical process of selective corrosion which zinc dissolves in contact with the electrolyte (the dezincification process), leaving behind a porous layer of copper. The corrosion behavior of brass with respect to dezincification, de-alloying, and stress corrosion has been studied (El-Mahdy *et al.*, 2013). In oxygen-containing hydrochloric acid solutions, the corrosion rate of brass is increased because zinc and copper are dissolved by an oxygen reduction reaction:

$$4Cu_{(Cu\text{-}Zn)} + O_2 + 4H^+ \rightarrow 4Cu^+ + 2H_2O \quad (1)$$

$$2Zn_{(Cu\text{-}Zn)} + O_2 + 4H^+ \rightarrow 2Zn^{2+} + 2H_2O \quad (2)$$

$$O_2 + 4H^+ + 4e^- \leftrightarrow 2H_2O \quad (3)$$

Dissolved oxygen from solution leads to oxidation of Cu(I)-complex to Cu(II):

$$4Cu^+ + O_2 + 4H^+ \rightarrow 4Cu^{2+} + 2H_2O \quad (4)$$

Increasing the concentration of Cu(II)-complex in the solution increases the participation of the following reaction in the corrosion process:

$$Cu^{2+} + Cu \rightarrow 2Cu^+ \quad (5)$$

Copper can be redeposited from the solution on the brass surface:

$$Cu^{2+} + Zn \rightarrow Cu + Zn^{2+} \quad (6)$$

and also:

$$2Cu^{+} + Zn \rightarrow 2Cu + Zn^{2+} \quad (7)$$

Regardless of the type of corrosion reaction, autocatalytic dissolution and dissolution with the oxygen reduction reaction occurs, with repositioning. The process causes a relatively high concentration of zinc and a low concentration of copper in solution. In these investigation the redeposition process is the reason for dezincification (Avramović *et al.*, 2006).

In this paper, the influence of hydrochloric acid and the addition of oxidizing agents on the rate of general corrosion of brass were investigated. For comparison, the corrosion rate of copper and zinc in hydrochloric acid and in hydrochloric acid with oxidizing agent was also tested.

## EXPERIMENTAL

Brass whose chemical composition is given in Table 1 was used for testing. For comparison, the corrosion rate of copper with a purity of 98.1% and zinc with a purity of 99.0% in hydrochloric acid and in hydrochloric acid with oxidizing agent was also tested. Chemical analysis of brass was performed at the Kemal Kapetanović Institute in Zenica. Standards JUS C.AI.185:1979 (Cu, Pb); JUS C.AI.159:1978; Analytical Methods for Atomic Absorption Spectrometry (Zn, Fe) were used to analyze the chemical composition of brass.

**Table 1.** Chemical composition of brass

| Element | Cu | Zn |
|---|---|---|
| Mas. % | 70,0 | 29,8 |

The tests were carried out in the following solutions: 0.1 M HCl; 0.1 M HCl + 0.1 M $H_2O_2$. The following chemicals were used in the preparation solutions: hydrochloric acid 35% (HCl, Lach-Ner, Czech Republic) and hydrogen peroxide 30% (GRAM-MOL, Zagreb, Croatia) all of p.a. purity.

The Taffel extrapolation method was used to examine general corrosion of brass. The Taffel extrapolation method involves scanning the potential of the working electrode of ±250 mV in relation to its open circuit potential ($E_{OCP}$), at a speed of 0.5 $mVs^{-1}$. Investigation of corrosion was conducted in a corrosion cell according to the Standard ASTM G5 (ASTM G5-94), on a potentiostat/galvanostat instrument, Princeton Applied Research, model 263A-2, with PowerCORR® software, which is part of the Power Suite softwere package. The tests were performed at room temperature, 20±1°C.

## RESULTS AND DISCUSSION

Figure 1. and Table 2. show the effect of adding an oxidizing agent to HCl solutions on the general corrosion rate of brass.

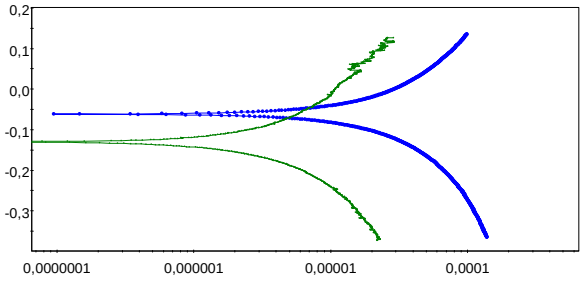


**Figure 1**. Tafel curves samples of brass
1 – sample treated in 0.1 M HCl;
2 – sample treated in 0.1 M HCl + 0.1 M $H_2O_2$

**Table 2**. The values of open circuit potential and corrosion current density of brass samples treated in HCl

| The type of HCl solutions | $E_{ocp}$(mV) | Corrosion current density, $i_{cor.}$ ($\mu Acm^{-2}$) |
|---|---|---|
| 0.1 M HCl | -130,152 | $1,067 \cdot 10^{1}$ |
| 0.1 M HCl + 0.1 M $H_2O_2$ | -61,692 | $9,567 \cdot 10^{2}$ |

The results shown in Figure 1 and Table 2 show that the general corrosion rate of brass generally increases with the addition of $H_2O_2$. Table 2 shows that the addition of $H_2O_2$ increases the corrosion current density, a key parameter for estimating corrosion rate.

For comparison, the corrosion rate of zinc in hydrochloric acid and in hydrochloric acid with oxidizing agent was also tested. Figure 2. and Table 3. also show the corrosion rate of zinc in hydrochloric acid and in hydrochloric acid with oxidizing agent. The corrosion rate of zinc is higher in hydrochloric acid and in hydrochloric acid with oxidizing agent than the corrosion rate of brass in hydrochloric acid and hydrochloric acid with oxidant, as can be seen from the results of corrosion current density shown in Table 2 and Table 3.

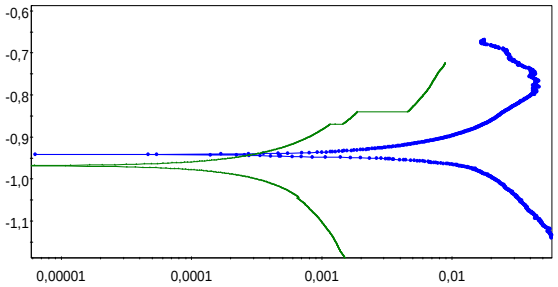


**Figure 2.** Tafel curves samples of zinc
1 – sample treated in 0.1 M HCl;
2 – sample treated in 0.1 M HCl + 0.1 M $H_2O_2$

Table 3. The values of open circuit potential and corrosion current density of zinc samples treated in HCl

| The type of HCl solutions | $E_{ocp}$(mV) | Corrosion current density, $i_{cor.}$ ($\mu Acm^{-2}$) |
|---|---|---|
| 0.1 M HCl | -968.025 | $1.447 \cdot 10^{3}$ |
| 0.1 M HCl + 0.1 M $H_2O_2$ | -941.531 | $1.463 \cdot 10^{4}$ |

For comparison, Figure 3 and Figure 4 shows the corrosion rate of brass and zinc in hydrochloric acid and in hydrochloric acid with oxidizing agent.

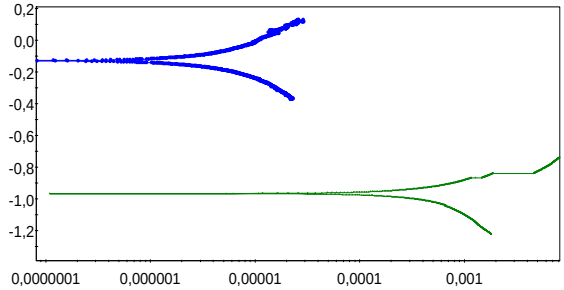


**Figure 3**. Tafel curves samples of brass and zinc
1 – sample of brass treated in 0.1 M HCl;
2 – sample of zinc treated in 0.1 M HCl

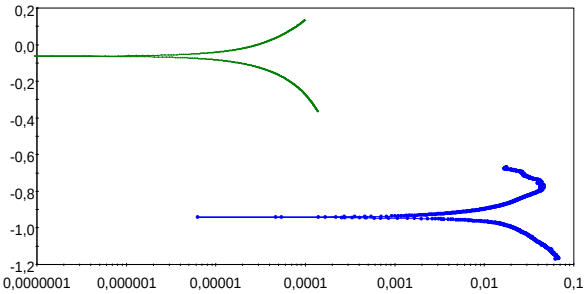


**Figure 4**. Tafel curves samples of brass and zinc
1 – sample of brass treated in 0.1 M HCl + 0.1 M $H_2O_2$;
2 – sample of zinc treated in 0.1 M HCl + 0.1 M $H_2O_2$

Figure 3 and Figure 4 show that the main cause of corrosion of the brass is zinc contained in it, and this is confirmed by the following Figure 5 corrosion of copper in hydrochloric acid and in hydrochloric acid with oxidizing agent.

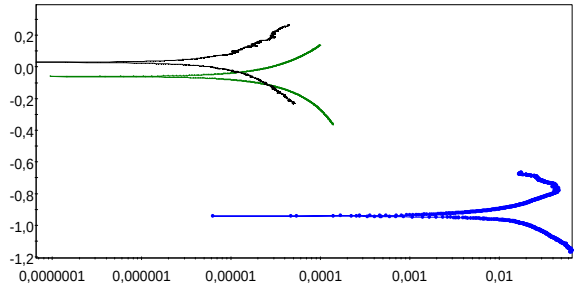


**Figure 5.** Tafel curves samples of brass, zinc and copper
1 – sample of brass treated in 0.1 M HCl + 0.1 M $H_2O_2$;
2 – sample of zinc treated in 0.1 M HCl + 0.1 M $H_2O_2$;
3 – sample of copper treated in 0.1 M HCl + 0.1 M $H_2O_2$

Figure 5. shows that the rate of general corrosion of copper is the lowest in 0.1 M HCl + 0.1 M $H_2O_2$. Since the standard electrode potential for zinc is at more negative potentials than that for copper, it is expected that zinc dissolution will occur before copper dissolution according to the following equation (Radovanovic *et al.*, 2018):

$$Zn \rightarrow Zn^{2+} + 2e^- \qquad (8)$$

Furthermore, in chloride solutions there is also a reaction between zinc and $Cl^-$ ions according to the following equation (Radovanovic *et al.*, 2018):

$$Zn + 4Cl^- \rightarrow ZnCl^{2-}{}_4 + 2e^- \qquad (9)$$

Moreover, copper dissolution occurs in acidic solution as shown by the following equations (Radovanovic *et al.*, 2018):

$$Cu \rightarrow Cu^+ + e^-$$
$$Cu^+ \rightarrow Cu^{2+} + e^- \qquad (10)$$

CuCl occurs in the reaction between $Cu^+$ and $Cl^-$ ions according to the following equation:

$$Cu^+ + Cl^- \rightarrow CuCl \qquad (11)$$

However, in the presence of atmospheric oxygen, oxidation of $Cu^+$ to $Cu^{2+}$ occurs according to the following equation (Radovanovic *et al.*, 2018):

$$4Cu^+ + O_2 + 4H^+ \rightarrow 4Cu^{2+} + 2H_2O \qquad (12)$$

The CuCl layer reacts with $Cl^-$ and forms a soluble $CuCl^-{}_2$ complex according to the following equation (Radovanovic *et al.*, 2018):

$$CuCl + Cl^- \rightarrow CuCl^-{}_2 \qquad (13)$$

Based on the literature data, which refer to the conditions in the examined system, the formed $CuCl_2$ complex can be dissolved into the bulk solution. Also, in an acidic solution, $CuCl_2$ is oxidized to $Cu^{2+}$ ions according to the following equations (Radovanovic *et al.*, 2018):

$$CuCl^-{}_{2(ads)} \rightarrow CuCl^-{}_{2(sol)}$$
$$CuCl^-{}_{2(ads)} \rightarrow Cu^{2+} + 2Cl^- + 2e \qquad (14)$$

## CONCLUSION

The alloy dissolution process begins with the simultaneous dissolution of both components of the alloy (Cu and Zn). The dissolution reaction occurs according to (Al Kharafi *et al.*, 2010):

$$Brass(Cu+Zn) \rightarrow xCu^{2+} + yZn^{2+} + 2(x+y)\,e \qquad (15)$$

where x and y are the fractions of dissolved copper and zinc, respectively. At the free corrosion potential, the electrons resulting from equation (15) are consumed in the cathodic reduction of hydrogen peroxide. A mechanism involving decomposition (or disproportionation) of $H_2O_2$ leading to $O_2$ formation, followed by electrochemical reduction of $O_2$, may be suggested.

$$2H_2O_2 \rightarrow 2H_2O + O_2 \qquad (16)$$
$$O_2 + 4H^+ + 4e^- = H_2O \qquad (17)$$

Another mechanism that depends on the direct reduction of $H_2O_2$ in an acidic medium is possible, i.e.

$$H_2O_2 + 2H^+ + 2e^- \rightarrow 2H_2O \qquad (18)$$

Electroreduction of $H_2O_2$ can be considered to occur by generating adsorbed $OH_{ad}$ species that receive an electron to give $OH^-$ and finally combine with $H^+$ to give $H_2O$ (Al Kharafi *et al.*, 2010).

Thus, the results show that the corrosion rate of brass is higher in hydrochloric acid with oxidizing agent than the corrosion rate of brass in hydrochloric acid.

Examining the effect of hydrochloric acid and the addition of oxidizing agent on the rate of general corrosion of brass, it was found that the corrosion of brass has caused the zinc contained in it. Corrosion of zinc is highest in 0.1 M HCl + 0.1 M $H_2O_2$ compared to corrosion of brass and copper in 0.1 M HCl + 0.1 M $H_2O_2$, with copper corrosion lowest in 0.1 M HCl + 0.1 M $H_2O_2$.

**REFERENCES**

Akabueze, C. I., & Itodo A. U. (2012). Inhibitory Action of 1–phenyl–3–methylpyrazol–5–one (HPMP) and 1–phenyl–3–methyl–4–(*p*–nitrobenzoyl)–pyrazol–5–one (HPMNP) on the Corrosion of Alpha and Beta Brass in HCl Solution, *American Journal of Chemistry*, *2*(3), 142-149.

Al Kharafi F. M., Ghayad I. M., & Abdullah, R. M. (2010) Effect of hydrogen peroxide on the dezincification of brass in acidified sodium sulfate solution under free corrosion conditions, *J. Mater. Environ. Sci.*, *1*(1) (2010) 58-69

ASTM G5-94, Standard Reference Test Method for Making Potentiostatic and Potentiodynamic Anodic Polarization Measurements.

Avramović, Z., & Antonijević, M. (2006). Korozija mesinga. *Zaštita materijala*, *47*(3), 49-60.

Choucri, J., Zanotto, F., Grassi, V, Balbo, A., Ebn Touhami, M., Mansouri, I., & Monticelli, C. (2019). Corrosion Behavior of Different Brass Alloys for Drinking Water Distribution Systems. *Metals*, *9*(6), 649.

El-Mahdy, G. A., Dyab, A. K., Atta, A. M., & Al-Lohedan, H. A. (2013). Brass Corrosion under a single droplet of NaCl. *International Journal of Electrochemical Science*, *8*, 9858-67.

Féron, D. (2007). *Corrosion behaviour and protection of copper and aluminium alloys in seawater*, Cambridge, Woodhead Publishing and CRC Press. ISSN 1354-5116

Francis R. (2010). The Corrosion of Copper and Its Alloys, NACE International, ISBN: 978-1-57590-225-8

Gapsari, F., Andoko, H., & Wijaya, H. (2018). Corrosion behavior of brass in nitric acid. *Metalurgija*, *57*(4), 333-336.

Radovanovic, M. B., Tasic, Z. Z., Petrovic Mihajlovic, M. B., & Antonijevic, M. M. (2018). Protection of Brass in HCl Solution by L-Cysteine and Cationic Surfactant. *Advances in Materials Science and Engineering*, Volume 2018, Article ID 9152183

**Summary/Sažetak**

U ovom radu ispitivan je uticaj hlorovodične kiseline i oksidacionog sredstva na brzinu opšte korozije mesinga. Poređenja radi, ispitivana je i brzina korozije bakra i cinka u hlorovodičnoj kiselini i hlorovodičnoj kiselini s dodatkom oksidansa. Za ispitivanje opšte korozije uzoraka mesinga, bakra i cinka upotrijebljena je Tafelova ekstrapolacijska tehnika. Navedena metoda podrazumijeva skeniranje potencijala radne elektrode ±250 mV u odnosu na potencijal otvorenog kruga ($E_{OCP}$), brzinom od 0,5 $mVs^{-1}$. Istraživanja korozije provedena su u korozionoj ćeliji prema standardu ASTM G5, na instrumentu potenciostat/galvanostat, Princeton Applied Research, model 263A-2, koristeći softver PowerCORR®. Ispitivanja su provedena na sobnoj temperaturi, 20±1°C. Rezultati pokazuju da je brzina korozije mesinga veća u hlorovodičnoj kiselini s dodatkom oksidansa od brzine korozije u hlorovodičnoj kiselini. Ispitivanjem uticaja hlorovodične kiseline i dodatka oksidacionog sredstva na brzinu opšte korozije mesinga, ustanovljeno je da je koroziju mesinga uzrokovao cink koji se nalazi u njemu. Korozija zinka je najveća u 0.1 M HCl + 0.1 M $H_2O_2$ u odnosu na korziju mesinga i bakra u 0.1 M HCl + 0.1 M $H_2O_2$, gdje je korozija bakra najmanja u 0.1 M HCl + 0.1 M $H_2O_2$.

# INSTRUCTIONS FOR AUTHORS

## GENERAL INFORMATION

*Bulletin of the Chemists and Technologists of Bosnia and Herzegovina (Glasnik hemičara i tehnologa Bosne i Hercegovine)* is a semiannual international journal publishing papers from all fields of chemistry and related disciplines.

### Categories of Contributions

1. *Original Scientific Papers* – (about 10 typewritten pages) report original research which has not been published previously, except in a preliminary form. The paper should contain all the necessary information to enable reproducibility of the described work.
2. *Short Communications* – (about 5 typewritten pages) describing work that may be of a preliminary nature but which merits immediate publication.
3. *Notes* – (about 3 typewritten pages) report unpublished results of short, but complete, original research or describe original laboratory techniques.
4. *Reviews* – (about 30 typewritten pages) present a concise and critical survey of a specific research area. Generally, these are prepared by the invitation of the Editor.
5. *Book and Web Site Reviews* – (about 2 typewritten pages).
6. *Extended Abstracts* – (about 2 typewritten pages) of Lectures given at international meetings.

### Reviewing the Manuscript

All contributors are evaluated according to the criteria of originality and quality of their scientific content, and only those deemed worthy will be accepted for publication. To facilitate the reviewing process, authors are encouraged to suggest three persons competent to review their manuscript. Such suggestions will be taken into consideration but not always accepted.

The Editor-In-Chief and Editors have the right to decline formal review of a manuscript when it is deemed that the manuscript is:

1. on a topic outside the scope of the Journal;
2. lacking technical merit;
3. of insufficient novelty for a wide international readership;
4. fragmentary and providing marginally incremental results; or
5. is poorly written.

**Proofs**

When a manuscript is ready for printing, the corresponding author will receive a PDF-formatted manuscript for proof reading, which should be returned to the journal within one week. Failure to do so will be taken as the authors are in agreement with any alteration which may have occurred during the preparation of the manuscript.

**Copyright**

Subscribers may reproduce tables of contents or prepare lists of articles including abstracts for internal circulation within their institutions. Permission of the Publisher is required for resale or distribution outside the institution and for all other derivative works, including compilations and translations.

**Professional Ethics and Publication Policy**

The journal expects the Editors, Referees and authors to adhere to the well-known standards of professional ethics. Authors are responsible for the factual accuracy of their contributions. Submission of the paper commits the author not to submit the same material elsewhere. Referees should act promptly. If certain circumstances preclude prompt attention to the manuscript at the time it is received, the non-received manuscript should be returned immediately to the Editor or the Referee should contact the Editor for possible delay of the report submission date. The Editor accepts full responsibility for his decisions on the manuscripts.

**PREPARATION AND SUBMISSION OF MANUSCRIPT**

**Cover Letter**

Manuscripts must be accompanied by a cover letter in which the type of the submitted manuscript. It should contain:

1. full name(s) of the author(s),
2. mailing address (address, phone and fax numbers, e-mail) of the author to whom correspondence should be addressed,
3. title of the paper (concise, without any abbreviations),
4. type of contribution,
5. a statement that the article is original and is currently not under consideration by any other journal or any other medium, including preprints, electronic journals and computer databases in the public domain, and
6. the names, full affiliation (department, institution, city and country), and
7. e-mail addresses of three potential Referees.

Contributors from Bosnia and Herzegovina should provide the name and full affiliation of at least one Referee from abroad.

Authors are fully encouraged to use ***Cover Letter Template.***

**Manuscript preparation**

The submitted articles must be prepared with Word for Windows. Manuscripts should be typed in English (either standard British or American English, but consistent throughout) with 1.5 spacing (12 points Times New Roman; Greek letters in the character font Symbol) in A4 format leaving 2.5 cm for margins. Authors are fully encouraged to use ***Manuscript Template***.

All contributions should be written in a style that addresses a wider audience than papers in more specialized journals. Manuscripts with grammar or vocabulary deficiencies are disadvantaged during the scientific review process and, even if accepted, may be returned to the author to be rewritten in idiomatic English. The authors are requested to seek the assistance of competent English language expert, if necessary, to ensure their English is of a reasonable standard. The journal maintains its policy and takes the liberty of correcting the English of manuscripts scientifically accepted for publication.

Tables and figures and/or schemes should not be embedded in the manuscript but their position in the text indicated. In electronic version (Word.doc document) tables and figures and/or schemes should follow the text, each on a separate page. Please number all pages of the manuscript including separate lists of references, tables and figures with their captions.

IUPAC and International Union of Biochemistry and Molecular Biology recommendations for the naming of compounds should be followed.

SI units, or other permissible units, should be employed. The designation of physical quantities should be in Times New Roman font. In text, graphs, and tables, brackets should be used to separate the designation of a physical quantity from the unit. Please do not use the axes of graphs for additional explanations; these should be mentioned in the figure captions and/or the manuscript (example: “pressure at the inlet of the system, kPa” should be avoided).

*Percents* and *per mills*, although not being units in the same sense as the units of dimensioned quantities, can be treated as such. Unit symbols should never be modified (for instance: w/w %, vol.%, mol.% ) but the quantity measured has to be named, *e.g.* mass fraction, $w$=95 %; amount (mole) fraction, $x$=20 %.

Latin words, as well as the names of species, should be in *italic*, as for example: *i.e., e.g., in vivo, ibid, Artemisia annua* L., *etc*. The branching of organic compound should also be indicated in *italic*, for example, *n*-butanol, *tert*-butanol, *etc*.

Decimal numbers must have decimal points and not commas in the text (except in the Bosnian/Croatian/Serbian abstract), tables and axis labels in graphical presentations of results. Thousands are separated, if at all, by a comma and not a point.

**Structure of the Manuscript**

The manuscript must contain, each on a separate page, the title page, abstract in English, (abstract in Bosnian/Croatian/Serbian), graphical abstract (optional), main text, list of references, tables (each table separately), illustrations (each separately), and legends to illustrations (all on the same page).

1. ***Title page*** must contain: the title of the paper (bold letters), full name(s) of the author(s), full mailing addresses of all authors (italic), keywords (up to 6), the phone and fax numbers and the e-mail address of the corresponding author.
2. A one-paragraph ***abstract*** written of 150–200 words in an impersonal form indicating the aims of the work, the main results and conclusions should be given and clearly set off from the text. Domestic authors should also submit, on a separate page, a Summary/Sažetak. For authors outside Bosnia and Herzegovina, the Editorial Board will provide a Bosnian/Croatian/Serbian translation of their English abstract.
3. Authors are encouraged to submit a ***graphical abstract*** that describes the subject matter of the paper. It should contain the title of the paper, full name(s) of the author(s), and graphic that should be no larger than 11 cm wide by 5 cm tall. Authors are fully encouraged to use ***Graphical Abstract Template.***
4. ***Main text*** should have the following form:
   - ***Introduction***should include the aim of the research and a concise description of background information and related studies directly connected to the paper.
   - ***Experimental*** section should give the purity and source of all employed materials, as well as details of the instruments used. The employed methods should be described in sufficient detail to enable experienced persons to repeat them. Standard procedures should be referenced and only modifications described in detail.
   - ***Results and Discussion***should include concisely presented results and their significance discussed and compared to relevant literature data. The results and discussion may be combined or kept separate.
   - The inclusion of a ***Conclusion***section, which briefly summarizes the principal conclusions, is highly recommended.
   - ***Acknowledgement*** (optional).
   - Please ensure that every ***reference*** cited in the text is also present in the reference list (and *vice versa*). Unpublished results and personal communications are not recommended in the reference list, but may be mentioned in the text. If these references are included in the reference list they should follow the standard reference style of the journal and should include a substitution of the publication date with either "Unpublished results" or "Personal communication" Citation of a reference as "in press" implies that the item has been accepted for publication. As a minimum, the full URL should be given and the date when the reference was last accessed. Any further information, if known (DOI, author names, dates, reference to a source publication, etc.), should also be given. No more than 30 references should be cited in your manuscript.

     In the text refer to the author's name (without initials) and year of publication (e.g. "Steventon, Donald and Gladden (1994) studied the effects..." or "...similar to values reported by others (Anderson, Douglas, Morrison, *et al.*, 1990)..."). Type the names of the first three authors at first citation. At subsequent citations use first author *et al.* The list of references should be arranged alphabetically by

authors' names and should be as full as possible, listing all authors, the full title of articles and journals, publisher and year.

Examples of ***reference style***:

a) Reference to a journal publication:
   Warren, J. J., Tronic, T. A., Mayer, J. M. (2010). Termochemistry of proton-coupled electron transfer reagents and its implications. *Chemical Reviews*, *110 (12)*, 6961-7001.
b) Reference to a book:
   Corey, E. J., Kurti, L. (2010). *Enantioselective chemical synthesis*. (1st Ed.) Direct Book Publishing, LLC.
c) Reference to a chapter in an edited book:
   Moody, J. R., Beck II, C. M. (1997). Sample preparation in analytical chemistry. In Setlle, F. A. (Ed.), *Handbook of instrumental techniques for analytical chemistry*. (p.p. 55-72). Prentice Hall.
d) Reference to a proceeding:
   Seliskar, C. J., Heineman, W.R., Shi, Y., Slaterbeck, A.F., Aryal, S., Ridgway, T.H., Nevin, J.H. (1997). *New spectroelectrochemical sensor*, in Proceedings of 37th Conference of Analytical Chemistry in Energy and Technology, Gatlinburg, Tenesee, USA, p.p. 8-11.
e) Patents:
   Healey, P.J., Wright, S.M., Viltro, L.J., (2004).*Method and apparatus for the selection of oral care chemistry*, The Procter & Gamble Company Intellectual Property Division, (No.US 2004/0018475 A1).
f) Chemical Abstracts:
   Habeger, C. F., Linhart, R. V., Adair, J. H. (1995). Adhesion to model surfaces in a flow through system. *Chemical Abstracts,* CA 124:25135.
g) Standards:
   ISO 4790:1992. (2008). *Glass-to-glass sealings - Determination of stresses*.
h) Websites:
   Chemical Abstract Service, www.cas.org, (18/12/2010).

- ***Tables*** are part of the text but must be given on separate pages, together with their captions. The tables should be numbered consequently in Latin numbers. Quantities should be separated from units by brackets. Footnotes to tables, in size 10 font, are to be indicated consequently (line-by-line) in superscript letters. Tables should be prepared with the aid of the Word table function, without vertical lines. Table columns must not be formatted using multiple spaces. Table rows must not be formatted using Carriage returns (enter key; ↵ key). Tables should not be incorporated as graphical objects.
- ***Figures and/or Schemes*** (in high resolution) should follow the captions, each on a separate page of the manuscript. High resolution illustrations in TIF or EPS format (JPG format is acceptable for colour and greyscale photos, only) must be uploaded as a separate archived (.zip or .rar) file.

Figures and/or Schemes should be prepared according to the artwork instructions.

- ***Mathematical and chemical equations*** must be numbered, Arabic numbers, consecutively in parenthesis at the end of the line. All equations should be embedded in the text except when they contain graphical elements (tables, figures, schemes and formulae). Complex equations (fractions, inegrals, matrix…) should be prepared with the aid of the Word Equation editor.

**Artwork Instructions**

Journal accepts only TIF or EPS formats, as well as JPEG format (only for colour and greyscale photographs) for electronic artwork and graphic files. MS files (Word, PowerPoint, Excel, Visio) are NOT acceptable. Generally, scanned instrument data sheets should be avoided. Authors are responsible for the quality of their submitted artwork.

Image quality: keep figures as simple as possible for clarity - avoid unnecessary complexity, colouring and excessive detail. Images should be of sufficient quality for the printed version, i.e. 300 dpi minimum.

Image size: illustrations should be submitted at its *final size* (8 cm for single column width or 17 cm for double column width) so that neither reduction nor enlargement is required.

Photographs: please provide either high quality digital images (250 dpi resolution) or original prints. Computer print-outs or photocopies will not reproduce well enough for publication. Colour photographs rarely reproduce satisfactorily in black and white.

The facility exist for color reproduction, however the inclusion of color photographs in a paper must be agreed with Editor in advance.

**Reporting analytical and spectral data**

The following is the recommended style for analytical and spectral data presentation:

1. ***Melting and boiling points***:
   mp 163–165°C (lit. 166°C)
   mp 180°C dec.
   bp 98°C
   Abbreviations: mp, melting point; bp, boiling point; lit., literature value; dec, decomposition.
2. ***Specific Rotation***:
   $[a]^{23}_{D}$ –222 (*c* 0.35, MeOH).
   Abbreviations: a, specific rotation; D, the sodium D line or wavelength of light used for determination; the superscript number, temperature (°C) at which the determination was made; In parentheses: *c* stands for concentration; the number following *c* is the concentration in grams per 100 mL; followed by the solvent name or formula.

3. ***NMR Spectroscopy***:
   $^{1}$H NMR (500 MHz, DMSO-$d_6$) d 0.85 (s, 3H, $CH_3$), 1.28–1.65 (m, 8H, 4´$CH_2$), 4.36–4.55 (m, 2H, H-1 and H-2), 7.41 (d, *J* 8.2 Hz, 1H, ArH), 7.76 (dd, *J* 6.0, 8.2 Hz, 1H, H-1'), 8.09 (br s, 1H, NH).
   $^{13}$C NMR (125 MHz, $CDCl_3$) d 12.0, 14.4, 23.7, 26.0, 30.2, 32.5, 40.6 (C-3), 47.4 (C-2'), 79.9, 82.1, 120.0 (C-7), 123.7 (C-5), 126.2 (C-4).
   Abbreviations: d, chemical shift in parts per million (ppm) downfield from the standard; *J*, coupling constant in hertz; multiplicities s, singlet; d, doublet; t, triplet; q, quartet; and br, broadened. Detailed peak assignments should not be made unless these are supported by definitive experiments such as isotopic labelling, DEPT, or two-dimensional NMR experiments.
4. ***IR Spectroscopy***:
   IR (KBr) n 3236, 2957, 2924, 1666, 1528, 1348, 1097, 743 $cm^{-1}$.
   Abbreviation: n, wavenumber of maximum absorption peaks in reciprocal centimetres.
5. ***Mass Spectrometry***:
   MS *m/z* (relative intensity): 305 ($M^+H$, 100), 128 (25).
   HRMS–FAB (*m/z*): $[M+H]^+$calcd for $C_{21}H_{38}N_4O_6$, 442.2791; found, 442.2782.
   Abbreviations: *m/z*, mass-to-charge ratio; M, molecular weight of the molecule itself; $M^+$, molecular ion; HRMS, high-resolution mass spectrometry; FAB, fast atom bombardment.
6. ***UV–Visible Spectroscopy***:
   UV ($CH_3OH$) $l_{max}$ (log e) 220 (3.10), 425 nm (3.26).
   Abbreviations: $l_{max}$, wavelength of maximum absorption in nanometres; e, extinction coefficient.
7. ***Quantitative analysis***:
   Anal.calcd for $C_{17}H_{24}N_2O_3$: C 67.08, H 7.95, N 9.20. Found: C 66.82, H 7.83, N 9.16.All values are given in percentages.
8. ***Enzymes and catalytic proteins relevant data:***
   Papers reporting enzymes and catalytic proteins relevant data should include the identity of the enzymes/proteins, preparation and criteria of purity, assay conditions, methodology, activity, and any other information relevant to judging the reproducibility of the results[1]. For more details check Beilstein Institut/STRENDA (standards for reporting enzymology data) commission Web site (http://www.strenda.org/documents.html).

**Submission Checklist**

The following list will be useful during the final checking of an article prior to sending it to the journal
for review:

- E-mail address for corresponding author,

[1] For all other data presentation not mentioned above please contact Editor for instructions.

- Full postal address,
- Telephone and fax numbers,
- All figure captions,
- All tables (including title, description, footnotes),
- Manuscript has been "spellchecked" and "grammar-checked",
- References are in the correct format for the journal,
- All references mentioned in the Reference list are cited in the text, and *vice versa*.

**Submissions**

Submissions should be directed to the Editor by e-mail: ***glasnik@pmf.unsa.ba***, or ***glasnikhtbh@gmail.com***. All manuscripts will be acknowledged on receipt (by e-mail) and given a reference number, which should be quoted in all subsequent correspondence.

Glasnik hemičara i tehnologa Bosne i Hercegovine

*Bulletin of the Chemists and Technologists of Bosnia and Herzegovina*

Print ISSN: 0367-4444
Online ISSN: 2232-7266

Zmaja od Bosne 33-35, BA-Sarajevo
Bosnia and Herzegovina
Phone: +387-33-279-918
Fax: +387-33-649-359
E-mail: glasnik@pmf.unsa.ba
glasnikhtbh@gmail.com

# Sponsors

Glasnik hemičara i tehnologa Bosne i Hercegovine

*Bulletin of the Chemists and Technologists of Bosnia and Herzegovina*

Print ISSN: 0367-4444
Online ISSN: 2232-7266

Zmaja od Bosne 33-35, BA-Sarajevo
Bosnia and Herzegovina
Phone: +387-33-279-918
Fax: +387-33-649-359
E-mail: glasnik@pmf.unsa.ba
glasnikhtbh@gmail.com


**www.elektroprivreda.ba/stranica/te-kakanj**

FMON
Federalno ministarstvo obrazovanja i nauke

**www.fmon.gov.ba**

Ministarstvo za obrazovanje, nauku i mlade Kantona Sarajevo

**https://mon.ks.gov.ba**